UNIVERSIDAD NACIONAL AUTÓNOMA DE MÉXICO

POSGRADO EN CIENCIAS BIOLÓGICAS

INSTITUTO DE BIOLOGÍA

SISTEMÁTICA

(PROYECTO)

TAXONOMÍA INTEGRATIVA DE LAS ESPECIES DEL GÉNERO *Phloeosinus* (Curculionidae: Scolytinae) DISTRIBUIDAS EN MÉXICO

TESIS

(**POR ARTÍCULO CIENTÍFICO**)

TESTING THE CLASSICAL TYPOLOGICAL TAXONOMY: AN APPROACH TO EVALUATE THE SPECIES HYPOTHESES IN *Phloeosinus* spp., FROM MEXICAN TRANSITION ZONE BASED ON PHYLOGENOMIC DATA AND MULTIPLE CHARACTER SOURCES

QUE PARA OPTAR POR EL GRADO DE:

MAESTRA EN CIENCIAS BIOLÓGICAS

PRESENTA:

ALICE NELLY FERNÁNDEZ CAMPOS

TUTOR PRINCIPAL DE TESIS: **Dr. FRANCISCO ARMENDÁRIZ TOLEDANO**
Instituto de Biología, UNAM

COMITÉ TUTOR: **Dr. JUAN JOSÉ MORRONE**
Facultad de Ciencias, UNAM

Dr. ALEJANDRO ZALDÍVAR RIVERÓN
Instituto de Biología, UNAM

CIUDAD UNIVERSITARIA, CD. MX. **MARZO, 2024**

UNIVERSIDAD NACIONAL AUTÓNOMA DE MÉXICO

POSGRADO EN CIENCIAS BIOLÓGICAS

INSTITUTO DE BIOLOGÍA

SISTEMÁTICA

(PROYECTO)

TAXONOMÍA INTEGRATIVA DE LAS ESPECIES DEL GÉNERO *Phloeosinus* (Curculionidae: Scolytinae) DISTRIBUIDAS EN MÉXICO

TESIS

(**POR ARTÍCULO CIENTÍFICO**)

TESTING THE CLASSICAL TYPOLOGICAL TAXONOMY: AN APPROACH TO EVALUATE THE SPECIES HYPOTHESES IN *Phloeosinus* spp., FROM MEXICAN TRANSITION ZONE BASED ON PHYLOGENOMIC DATA AND MULTIPLE CHARACTER SOURCES

QUE PARA OPTAR POR EL GRADO DE:

MAESTRA EN CIENCIAS BIOLÓGICAS

PRESENTA:

ALICE NELLY FERNÁNDEZ CAMPOS

TUTOR PRINCIPAL DE TESIS: **Dr. FRANCISCO ARMENDÁRIZ TOLEDANO**
Instituto de Biología, UNAM

COMITÉ TUTOR: **Dr. JUAN JOSÉ MORRONE**
Facultad de Ciencias, UNAM

Dr. ALEJANDRO ZALDÍVAR RIVERÓN
Instituto de Biología, UNAM

CIUDAD UNIVERSITARIA, CD. MX. **MARZO, 2024**

COORDINACIÓN GENERAL DE ESTUDIOS DE POSGRADO
COORDINACIÓN DEL POSGRADO EN CIENCIAS BIOLÓGICAS
INSTITUTO DE BIOLOGÍA
OFICIO: CGEP/CPCB/IB/0210/2024
ASUNTO: Oficio de Jurado

M. en C Ivonne Ramírez Wence
Directora General de Administración Escolar, UNAM
P r e s e n t e

Me permito informar a usted que en la reunión ordinaria del Comité Académico del Posgrado en Ciencias Biológicas, celebrada el día **22 de enero de 2024** se aprobó el siguiente jurado para el examen de grado de **MAESTRA EN CIENCIAS BIOLÓGICAS** en el campo de conocimiento de **Sistemática** de la alumna **FERNÁNDEZ CAMPOS ALICE NELLY** con número de cuenta **522003886** por la modalidad de graduación de **tesis por artículo científico** titulado: **"Testing the classical typological taxonomy: an approach to evaluate the species hypotheses in *Phloeosinus* spp., from Mexican Transition Zone based on phylogenomic data and multiple character sources",** que es producto del proyecto realizado en la maestría que lleva por título: **"Taxonomía integrativa de las especies del género *Phloeosinus* (Curculionidae: Scolytinae) distribuidas en México",** ambos realizados bajo la dirección del **DR. FRANCISCO ARMENDÁRIZ TOLEDANO,** quedando integrado de la siguiente manera:

Presidente:	DR. ISMAEL ALEJANDRO HINOJOSA DÍAZ
Vocal:	M. EN C. GRISELDA MONTIEL PARRA
Vocal:	DRA. ROXANA ACOSTA GUTIÉRREZ
Vocal:	DR. TONATIUH RAMÍREZ REYES
Secretario:	DR. JUAN JOSÉ MORRONE

Sin otro particular, me es grato enviarle un cordial saludo.

A T E N T A M E N T E
"POR MI RAZA HABLARÁ EL ESPÍRITU"
Ciudad Universitaria, Cd. Mx., a 26 de febrero de 2024

COORDINADOR DEL PROGRAMA

POSGRADO EN CIENCIAS BIOLOGICAS
COORDINACIÓN

DR. ADOLFO GERARDO NAVARRO SIGÜENZA

c. c. p. Expediente del alumno

AGNS/RGA/EARR/rga

AGRADECIMIENTOS INSTITUCIONALES

En primer lugar, al Posgrado en Ciencias Biológicas de la UNAM por el apoyo brindado durante el desarrollo y termino de este proyecto de investigación.

Al Consejo Nacional de Humanidades, Ciencias y Tecnologías (CONAHCYT) por la beca de maestría con número de CVU 1146407 durante agosto de 2021 a julio de 2023. Así como al financiamiento otorgado por PAPIIT 2020.

A los miembros de mi comité tutor, Dr. Francisco Armendáriz Toledano (Tutor principal), Dr. Juan José Morrone Lupi y Dr. Alejandro Zaldívar Riverón, por el interés y apoyo demostrado en este proyecto.

AGRADECIMIENTOS A TÍTULO PERSONAL

Al Dr. Francisco Armendáriz Toledano, por su apoyo, asesoría y paciencia para finalizar este trabajo.

Al Instituto de Biología, UNAM, por el apoyo brindado durante el desarrollo y termino de este proyecto de investigación.

A María Berenit Mendoza Garfías del Laboratorio de Microscopía y Fotografía de la Biodiversidad 1 (LANABIO) por su apoyo para la obtención de imágenes.

A los miembros del jurado: M. en C. Griselda Montiel Parra, Dra. Roxana Acosta Gutiérrez, Dr. Ismael Alejandro Hinojosa Díaz, Dr. Juan José Morrone y Dr. Tonatiuh Ramírez Reyes por tomarse el tiempo de revisar este trabajo.

A mis amigas y compañeras de laboratorio, Montserrat Cervantes Espinoza, Valeria Guzmán Robles, Raquel Cid Muñoz y Jazmín García Román por su apoyo, motivación y sobre todo su amistad y buenos momentos compartidos a lo largo de todo este tiempo.

A Carlitos, por tu amistad y por siempre motivarme y apoyarme a dar este paso hacia la investigación.

A todas las personas que alguna vez me escucharon hablar respecto a este tema.

A ti que ahora estás, gracias por acompañarme.

A mi familia.

ÍNDICE

RESUMEN

El género *Phloeosinus* consta de más de 80 especies en el mundo, de las cuales nueve de ellas se distribuyen en México y para las cuales no se cuenta con estudios taxonómicos recientes desde su descripción hace más de 50 años. Asimismo, algunos taxones presentan problemas taxonómicos, debido a similitudes morfológicas. Además de que, el estatus taxonómico de varias de ellas está basado en el árbol huésped del que fueron recolectadas y en atributos morfológicos cualitativos externos, principalmente del declive elitral, la cabeza y el pronoto, dejando de lado características de la morfología interna como los correspondientes a los genitales. Por lo anterior, en este trabajo bajo un contexto de taxonomía integrativa se implementó el uso de diferentes métodos de observación y de análisis de variación como morfometría tradicional y geométrica para estudiar características morfológicas externas e internas de las especies de *Phloeosinus* distribuidas en México, y también a través de la implementación de análisis filogenómicos utilizando datos de RAD-seq, se evaluó la monofilia de algunas de estas especies y si la estructura de los linajes reconocidos es congruente con su estatus de especie. Los análisis morfométricos con datos cualitativos y cuantitativos mostraron diferencias entre los grupos de especies estudiadas, principalmente en características asociadas al declive elitral. Los análisis de morfometría geométrica mostraron que existe variación en la forma del pronoto y los élitros de estas especies. El estudio del esternito IX de las hembras de *Phloeosinus* fue el que mostró mayores diferencias entre las especies. Finalmente se observó congruencia entre los árboles filogenéticos obtenidos y los resultados de los análisis morfológicos.

ABSTRACT

The genus *Phloeosinus* consists of more than 80 species in the world, nine of which are distributed in Mexico and for which there are no recent taxonomic studies since their description more than 50 years ago. Also, some taxa present taxonomic problems due to morphological similarities. In addition, the taxonomic status of several of them is based on the host tree from which they were collected and on external qualitative morphological attributes, mainly of the elytral declivity, head and pronotum, leaving aside internal morphological characteristics such as those corresponding to the genitalia and terminalia. Therefore, in this work, under the context of integrative taxonomy, we implemented the use of different methods of observation and analysis of variation such as traditional and geometric morphometry to study external and internal morphological characteristics of *Phloeosinus* species distributed in Mexico, and also through the implementation of phylogenomic analysis using RAD-seq data, we evaluated the monophyly of some of these species and whether the structure of the recognized lineages is congruent with their species status. Morphometric analyses with qualitative and quantitative data showed differences between the groups of species studied, mainly in characteristics associated with elytral declivity. Geometric morphometric analyses showed that there is variation in the shape of the pronotum and elytra of these species. The study of the sternite IX of Phloeosinus females showed the greatest differences between species. Finally, congruence was observed between the phylogenetic trees obtained and the results of the morphological analyses.

INTRODUCCIÓN GENERAL

El género *Phloeosinus* de escarabajos descortezadores corresponde a un grupo de especies fleófagas que se alimentan y reproducen dentro de coníferas de la familia Cupressaceae (Wood, 1982; Cervantes-Espinoza *et al.,* 2022). Este género comprende más de 80 especies a nivel mundial, cuya distribución abarca principalmente las regiones Neártica y Paleártica (Faccoli y Sidoti 2013; Kirkendall *et al*. 2015). Son especies monógamas y durante el periodo de reproducción las hembras construyen sus sistemas de galerías sobre árboles moribundos o debilitados fisiológicamente por lo que se las considera saprobias tardías. Sin embargo, pueden colonizar y matar árboles aparentemente sanos por lo que también se las considera plagas (Blackman, 1942; Wood, 1982; Faccoli y Sidoti, 2013).

En México habitan nueve especies del género: *P. arizonicus* Blackman, 1942; *P. baumanni* Hopkins, 1905; *P. cristatus* Leconte, 1868; *P. deleoni* Blackman, 1942; *P. palearis* Wood, 1969; *P. serratus* Leconte, 1942; *P. spinosus* Blackman, 1942, *P. tacubayae* Hopkins, 1905 y *P. taxodii taxodiicolens* Wood, 1956. Sin embargo, el conocimiento que se tiene sobre ellas es escaso e incipiente, su distribución actual no es clara y el grado de especificidad y las preferencias hacia los huéspedes, así como el impacto que tienen sobre las comunidades forestales naturales y urbanas están pobremente estudiados. A pesar de ello algunas especies se consideran plagas forestales y se incluyen en la norma oficial Mexicana NOM-019-SEMARTNAT-2017, para su control y manejo. Aunado a esto, la información taxonómica que se tiene de ellas está soportada por eventos de recolecta esporádicos y registros escasos, con especies que sólo se han colectado una o dos veces en la región. Además de lo anterior, algunos pares de especies presentan problemas de identificación debido a su gran similitud morfológica, ejemplo de ello son *P. taxodii taxodiicolens- P. tacubayae*, *P. palearis- P. serratus* y *P. baumanni- P. variaolatus* (Wood, 1982). Asimismo, el estatus taxonómico de estas especies está soportado por su distribución geográfica y por haber sido colectadas en diferentes plantas huéspedes y desde su descripción no se ha hecho una revisión del mismo. También, las diferencias morfológicas entre las especies que se reproducen en *Juniperus* spp., son muy leves y difíciles de interpretar, por lo que los registros de distribución, especialmente en el norte de México, se basan en identificaciones erróneas. En el norte de la Zona de Transición Mexicana (ZTM), en Coahuila y Nuevo León, las poblaciones de todas las especies de *Juniperus* y en consecuencia de los escarabajos descortezadores, están compuestas por parches que varían extremadamente en tamaño

(Estrada-Castillón *et al*., 2014, Hernández-García *et al*., 2020), lo cual podría estar promoviendo el aislamiento de las poblaciones y una variación genotípica y fenotípica considerable. Desde un punto de vista taxonómico, en conjunto, estas circunstancias conducen a la necesidad de evaluar la diversidad de las especies del género en esta área.

En *Phloeosinus*, como en la mayoría de los escarabajos descortezadores, comúnmente la taxonomía se realiza utilizando atributos morfológicos cualitativos externos, principalmente del declive elitral, la cabeza y el pronoto (Hopkins, 1905; Blackman, 1982; Wood, 1982; López-Buenfil *et al*., 2001; Pérez-Silva *et al.*, 2021; Burgos-Solorio y Atkinson 2022; Atkinson 2023; Atkinson *et al*., 2023). Aunque estos caracteres han sido importantes en la taxonomía alfa de los escarabajos descortezadores, en algunos casos son de poca utilidad en especies crípticas (Armendáriz Toledano *et al.,* 2014, 2017), debido a que los hábitos del grupo han homogeneizado su morfología, ocultando su verdadera diversidad (Hulcr *et al.,* 2015). Por lo tanto, otros sistemas de caracteres como la microescultura, los terminalia, las estructuras internas y las piezas bucales, así como diferentes métodos de observación y análisis de variación, como la morfometría tradicional y la morfometría geométrica han mejorado el reconocimiento de los límites de las especies (Armendáriz-Toledano *et al.,* 2014; García-Román *et al.,* 2019; Valerio-Mendoza *et al.,* 2019). Asimismo, el uso de las antenas, el proventrículo, segmentos abdominales, del aparato estridulador, la varilla seminal, el ancla y la espermateca ha sido reconocido como una fuente rica de caracteres taxonómicos y como una herramienta útil para la delimitación en especies cripticas (Armendáriz et al. 2017, García Román *et al*., 2022; Johnson *et al.,* 2020; McNichol *et al.,* 2021; Ospina-Garcés *et al.,* 2021; Mandelshtam *et al.* 2022).

Por otro lado, los estudios genéticos que abordan la sistemática de Scolytinae se han realizado mayoritariamente utilizando datos moleculares de Sanger (principalmente mitocondriales) (Stauffer *et al*., 1997; Cognato y Sperling, 2000; Jordal, 2007; Dole *et al.,* 2010; Victor y Zuñiga, 2016; Pistone *et al.,* 2018; Jordal, 2023). Sin embargo, el uso de un solo tipo de marcador molecular (mitocondrial o nuclear) no ha sido suficiente para dilucidar las relaciones filogenéticas entre géneros y especies (Cognato y Sperling, 2000; Pistone *et al*., 2018). Múltiples marcadores obtenidos a través de técnicas de secuenciación de nueva generación (NGS), como la secuenciación de ADN asociada al sitio de restricción (RAD-Seq), que, en escarabajos descortezadores, ha demostrado ser una herramienta poderosa para la inferencia de relaciones filogenéticas y evolutivas, estudios biogeográficos y

diversificación en el género *Dendroctonus* (Godefroid *et al.,* 2019; Ramírez-Reyes *et al.,* 2023).

Por lo anterior, el objetivo de este trabajo fue abordar las hipótesis de especies de *Phloesinus* spp., reconocidas en la ZTM mediante un enfoque de taxonomía integrativa utilizando datos morfológicos y moleculares. A través de análisis filogenómicos con datos de RAD-seq, se evaluó la monofilia de las especies y si la estructura de los linajes reconocidos es congruente con su estatus de especie.

Manuscripts submitted to Insect Systematics and Diversity

OXFORD UNIVERSITY PRESS | Insect Systematics and Diversity

Testing the classical typological taxonomy: an approach to evaluate the species hypotheses in Phloeosinus spp., from Mexican Transition Zone based on phylogenomic data and multiple character sources.

Journal:	*Insect Systematics and Diversity*
Manuscript ID	ISD-2023-0071
Manuscript Type:	Research
Date Submitted by the Author:	13-Dec-2023
Complete List of Authors:	Fernández-Campos, Alice Nelly; Universidad Nacional Autónoma de México, Posgrado en Ciencias Biológicas Ramírez-Reyes, Tonatiuh; Universidad Autónoma de Nuevo León, Facultad de Ciencias Forestales Atkinson, Thomas; University of Texas at Austin, Insect Collection Cuellar-Rodríguez, Gerardo; Universidad Autonoma de Nuevo León, Facultad de Ciencias Forestales Armendariz - Toledano, Francisco ; Universidad Nacional Autonoma de Mexico, Instituto de Biología- CNIN
Please choose a section from the list:	Taxonomy
Organism Keywords:	Scolytidae
Field Keywords:	Forest Entomology, Molecular Systematics, Morphology, Taxonomy

Francisco Armendáriz-Toledano
Instituto de Biología, Departamento de Zoología, Colección Nacional de Insectos. Universidad Nacional Autónoma de México, Circuito Zona Deportiva S/N, C.U. Coyoacán, 4510 Ciudad de México, México.
Email: farmendariztoledano@ib.unam.mx

Testing the classical typological taxonomy: an approach to evaluate the species hypotheses in *Phloeosinus* spp., from the Mexican Transition Zone based on phylogenomic data and multiple character sources

Alice Nelly Fernández-Campos[1,2], Tonatiuh Ramírez-Reyes[2,3], Gerardo Cuellar-Rodríguez[3] Thomas H. Atkinson[4], Francisco Armendáriz-Toledano[2]

[1]Posgrado en Ciencias Biológicas, Universidad Nacional Autónoma de México. Unidad de Posgrado, Edificio D, 1° Piso, Circuito de Posgrados, Ciudad Universitaria, Coyoacán, C.P. 04510, CDMX, México

[2]Instituto de Biología, Departamento de Zoología, Colección Nacional de Insectos, Universidad Nacional Autónoma de México, Circuito Zona Deportiva S/N, C.U. Coyoacán, 04510 Ciudad de México, México.

[3]Facultad de Ciencias Forestales, Universidad Autónoma de Nuevo León, Carretera Nacional 85, Km. 145, 67700 Linares, Nuevo León, México.

[4]University of Texas Insect Collection, 3001 Lake Austin Blvd., Suite 1.314 Austin, Texas 78702, U.S.A.

Abstract

Phloeosinus species from the Mexican Transition Zone have remained for more than 50 years without taxonomic studies. Some taxa present taxonomic problems due to morphological similarities, also, differences between species that breed in *Juniperus* spp., are very slight and difficult to interpret, thus distribution records, especially in the north of Mexico, are based on misidentifications. In this study, based on the principles of integrative taxonomy, we test the species hypotheses of eight of the nine

Phloeosinus spp., recognized in the MTZ using molecular and morphological data. From a wide phenotype representation, studying multiple character sources (body measurements and traits, body shape and morphology of female sternite IX) and with different multivariate methods of analysis, we evaluate the degree of morphological variation in the recognized species. Also, through phylogenomic analyses using RAD-seq data, we evaluated the monophyly of the species and whether the structure of the recognized lineages is congruent with their species' status. Collectively the analyses performed supported that at least seven species are consistent with their previous hypotheses. Although, *P. serratus* was the only taxon one in which there was evidence that its taxonomic label masks a greater diversity, and at least three putative species can be recognized corresponding to different populations isolated from three different host species with patchy distributions.

Key words: Morphometrics, integrative taxonomy, cryptic species

Introduction

Phloeosinus bark beetles are monogamous and phloeophagous species that feed and reproduce in conifers of Cupressaceae (Blackman 1942, Wood 1982). Most members are late saprophytes with a good capacity for adult aggregation and low tolerance to host defenses; few members are aggressive opportunists, with a high capacity for adult aggregation, a moderate tolerance to host defenses, and a capacity to kill physiologically stressed trees, causing considerable tree mortality, thus, can be pests in natural and urban settings (Craighead and George 1930, Fettig 2016, Cervantes-Espinoza et al. 2022).

The genus consists of 80 described species, of which more than 66 are taxonomically valid, whose distribution is Holarctic (Schedl 1956, Wood 1986, Wood and Bright 1992, Knížek, 2011, Faccoli and Sidoti 2013). Blackman (1942) recognized 45 species in North America. These were reduced through synonymy to 27 by Wood (1982) who also added two additional taxa bringing the total to 29, whose distribution ranges from Alaska to El Salvador in Central America. Eight species and a subspecies are found in the Mexican transition zone (MTZ) (Cervantes et al. 2022): *Phloeosinus arizonicus* Blackman, 1942; *Phloeosinus baumanni* Hopkins, 1905; *Phloeosinus cristatus* Leconte, 1868; *Phloeosinus deleoni*

Blackman, 1942; *Phloeosinus palearis* Wood, 1969; *Phloeosinus serratus* Leconte, 1942; *Phloeosinus spinosus* Blackman, 1942, *Phloeosinus tacubayae* Hopkins, 1905 and *Phloeosinus taxodii taxodiicolens* Wood, 1956. These species have remained for more than 50 years without taxonomic studies, a situation that, beyond being a product of their stability as a hypothesis, reflects the lack of studies and revisions in the group. Two species were described in the late 19th and early 20th centuries, while the rest between 1940-1970, epochs that correspond to the period of classical typological taxonomy in Scolytinae and the most prolific for the taxonomy of the subfamily, respectively (Hulcr et al. 2015).

Consequently, biological, and ecological information is available for a few *Phloeosinus* spp. and the current distribution of the species in the MTZ is supported by punctual, scarce, scattered, and old collection records (Hopkins 1905, Blackman 1942, Wood 1982, Atkinson et al. 1986). Furthermore, these taxa present some taxonomic problems. Morphological differences between species that breed in *Juniperus* spp., are very slight and difficult to interpret, thus distribution records, especially in the north of Mexico, are based on misidentifications. In the north of MTZ, in Coahuila, and Nuevo Leon populations of all *Juniperus* host species, and consequently of the beetles, are composed of extreme patches of varying size (Estrada-Castillón et al. 2014, Hernández-García et al. 2020), that could be promoting populations isolation and considerable genotypic and phenotypic variation. Recent integrative and phylogenomic analyses in *Dendroctonus*, suggest that MTZ harbor more diversity in Scolytinae species because cryptic species are present (Armendáriz-Toledano et al. 2014, 2015, Pureswaran et al. 2016, Valerio-Mendoza et al. 2019, Sullivan et al. 2021, Ramírez-Reyes et al. 2023). From a taxonomic point of view, together, these circumstances lead to the need for an evaluation of the diversity of the species of the genus in the area.

In *Phloeosinus* such as most bark beetles, the taxonomy is commonly done using external qualitative morphological attributes, mainly the elytral declivity, the head, and the pronotum (Hopkins 1905, Blackman 1942, Wood 1982, López-Buenfil et al. 2001, Pérez-Silva et al. 2021, Burgos-Solorio and

Atkinson 2022, Atkinson 2023, Atkinson et al. 2023). Although these traits have been important in the alpha taxonomy of bark beetles, in some cases these are of little use in cryptic species (Armendáriz Toledano et al. 2014, 2017), because the habits of the group have homogenized their morphology, hiding their true diversity (Hulcr et al. 2015). Therefore, other character systems such as microsculpture, terminalia, internal structures, and mouthparts, as well as different methods of observation and variation analysis, such as traditional morphometrics and geometrics morphometrics have improved the recognition of species boundaries (Armendáriz-Toledano et al. 2014, García-Román et al. 2019, Valerio-Mendoza et al. 2019). Instead, the use of antenna, proventriculus, abdominal segments, stridulatory apparatus, seminal rod, anchor, and spermatheca has been recognized as a rich source of systematic traits (Armendáriz et al. 2017, García-Román et al. 2022, Johnson et al. 2020, McNichol et al. 2021, Ospina-Garcés et al. 2021, Mandelshtam et al. 2022).

On the other hand, the genetic studies that address Scolytinae systematics have been made mostly using Sanger´s molecular data (mainly mitochondrial) (Stauffer et al. 1997, Cognato and Sperling 2000, Jordal 2007, Dole et al. 2010, Victor and Zuñiga 2016, Pistone et al. 2018, Jordal 2023). The use of a single type of molecular marker (mitochondrial or nuclear) has not been sufficient to elucidate phylogenetic relationships between genera and species (Cognato and Sperling 2000, Pistone et al. 2018). Multiple markers obtained through next-generation sequencing (NGS) techniques, such as restriction site-associated DNA sequencing (RAD-Seq), in bark beetles, have proven to be a powerful tool for the inference of phylogenetic and evolutionary relationships, biogeographical studies, and diversification in the genus *Dendroctonus.* (Godefroid et al. 2019, Ramírez-Reyes et al. 2023).

Based on the principles of integrative taxonomy, i.e., species delimitation supported by multiple data sources (Dayrat 2005), in this study, we test the species hypotheses of eight of the nine *Phloeosinus* spp., recognized in the MTZ using molecular and morphological data. From a wide phenotype representation, studying multiple character sources (*i.e*., body measurements, body sculpture, body pubescence, body shape, morphology of female sternite IX) and different multivariate methods of

analysis, we evaluate the degree of morphological variation in the recognized species. Through phylogenomic analyses using RAD-seq data, we evaluated the monophyly of the species and whether the structure of the recognized lineages is congruent with their species' status.

Materials and methods

Morphological analyses

Obtaining material. Adults' specimens corresponding to *Phloeosinus* spp., inhabit MTZ were analyzed (*P. baumanni, P. tacubayae, P. deleoni, P. cristatus, P. serratus, P. spinosus, P. arizonicus* and *P. taxodii tacodiicolens*). To represent intraspecific variation, up to three different geographical locations were considered for each species. In each site, between three and eight adults were randomly selected for morphological and three for genetic analyses. The sampling method was like the one established by Hernández-García et al. (2020); the beetles were obtained using freshly cut branches of the targeted host tree, as a lure, from sites without apparently infested trees, or in sites where infested trees were available. Specimens from entomological collections were also reviewed (Table 1). In total 133 specimens from 16 localities were considered. The sex of specimens was determined by the shape and relative size of both the seventh and eighth abdominal tergites (Cervantes-Espinoza et al. 2023) and by dissecting the genitalia. Taxonomic identifications were carried out using the keys proposed by Blackman (1942) and Wood (1982). The assignation of specimens to some taxon was used as a hypothesis to test.

Specimen preparation. Adults were transferred to 1.5 ml microtubes with Tween 20, and ultrasonicated for 3 min in Branson Model B200 Ultrasonic Cleaner, then were rinsed with distilled water and again ultrasonicated with commercial acetone, and one more wash with distilled water was repeated. The cleaned specimens were photographed in lateral, dorsal, and ventral positions, and magnifications (10x and 40x) focusing on dorsal and lateral views of the pronotum and elytra, using a stereo microscope and a compound microscope (Rising Technology, RisingView). The removal and mounting of the morphological structures (sternite IX) were carried out following the protocols reported by

Armendáriz-Toledano et al. (2015). For morphometric purposes mounted structures were measured, quantified, and photographed directly in the slides with an ocular micrometer under a phase contrast microscope (400×). Some specimens and morphological structures were dried at a critical point and coated with gold in the Quorum model Q15OR ES equipment, for their respective observation in a Hitachi Scanning Electron Microscope, model SU1510. The elements of elytral sculpture (punctures, granules, pubescence, etc.) were measured and quantified directly in the SEM photographs. Discrete quantitative and qualitative characters were recorded from stereo microscope observations and specimen photographs.

Character selection. The insects were examined to identify morphological characters in addition to those previously proposed in the taxonomic keys (Blackman 1942, Wood 1982). A total of 44 morphological characters were reviewed, of which 38 were of external morphology (24 quantitative and 14 qualitative) and 6 quantitative characters of internal morphology corresponding to sternite IX of females. All continuous traits were measured with RisingView (vx64, 4.8.16295.20200101) software from photographs. Because the characters related to the color differ among head, pronotum, and elytra, therefore each one was considered as an independent trait.

The characters, their acronym, description, and their respective character states in parenthesis are listed below:

1. Head color (HC). In *Phloeosinus* the head color can be (1) black (Fig. 1A), (2) brown (Fig. 1B), or (3) reddish brown (Fig 1C).

2. Size of head pubescence (SHP). The head is covered by pubescence, these vary in size, and they may be homogeneous in size or present two sizes in the same specimen. These character states were considered: (1) uniformly short, whose length is shorter than the width of the eye notch (Fig. 1D); (2) uniformly long, whose length is longer than the width of the eye notch (Fig. 1E), (3) heterogeneous in size, short and large (Fig. 1F).

3. Frons sculpting pattern (FSP). Frons surface presents different micro-sculpture elements that together form the sculpture patterns. According to the presence of these elements at the center of frons, these character states were considered: (1) granules (Fig. 1G), (2) punctuations (Fig. 1H), or (3) a combination of both (Fig. 1I).

4. Frons vestiture pattern (FVP). The pubescence present on the frons can vary according to their abundance and distribution, giving rise to certain patterns. These may be: (1) abundant distributed heterogeneously (Fig. 2A), (2) sparse distributed heterogeneously (Fig. 2B), (3) sparse distributed homogeneously (Fig. 2C), (4) abundant distributed homogeneously (Fig. 2D).

5. Vestiture pattern of epistomal margin (EMVP). The epistomal surface displays pubescence at the inferior margin, whose abundance varies among species: (1) abundant covering the entirely the epistomal margin (Fig. 3A and B) or (2) sparse, showing some areas without pubescence (Fig. 3C and D).

6. Pubescence size of epistomal margin (SEMP). The pubescence length present in this structure varied among (1) uniformly short, they do not cover the first third of mandibles (Fig. 3A and C), (2) uniformly long, covering more than a half of mandibles (Fig. 3B), (3) heterogeneous in size, a mix of both "short and long" (Fig. 3D).

7. Elevation of the forehead carina (SFC). At the middle of the frons, there is a thin longitudinal cuticular elevation or carina. This cuticular element can be (1) inconspicuous (almost imperceptible under light microscopy) (Fig. 1I) or (2) pronounced concerning the epistomal margin, easily observed under light microscopy (Fig. 1G)

8. Color of pronotum (CP): This character has been considered for phylogenetic analysis in *Dendroctonus.* In *Phloeosinus* this trait varies among the analyzed species. These character states were considered: (1) black (Fig. 4A), (2) brown (Fig. 4B), (3) dark brown (Fig. 4C), (4) reddish brown and (Fig. 4D), (5) yellowish brown (Fig. 4E).

9. Color of elytra (EC): For this structure, the color varied among (1) black (Fig. 4A), (2) brown (Fig. 4B), (3) dark brown (Fig. 4C), (4) reddish brown (Fig. 4D), and (3) yellowish brown (Fig. 4E).

10. Elytral disc vestiture (VD). In the margin of the elytral disc is pubescence and its organization is variable among species: These character states were considered: (1) abundant (Fig. 5A) and (2) sparse (Fig. 5B).

11. Size of the elytral disc pubescence (SEDP): The pubescence length varied among (1) long (Fig. 5C), (2) short (Fig. 5D), or (3) a mix of both "short and long" (Fig. 5E).

12. Vestiture of the elytral declivity (VDE): The elytral declivity is covered with different types of pubescence such as hairs and scales, whose density is variable: (1) abundant (Fig. 5F), (2) sparse (Fig. 5G).

13. Vestiture of the elytral declivity (PVDE): The vestiture is constituted by hairs and scales. Adults display vestiture patterns conformed by: (1) hairs (Fig. 5H), (2) only scales (Fig. 5I) or (3) hairs and scales (Fig. 5J).

14. Pattern of sculpture and vestiture of interstriae II at elytral declivity (PEVI2-DE). Specifically, the vestiture pattern varied among all species, they can be (1) glabrous (Fig. 5K), (2) with hairs (Fig. 5L), (3) scales (Fig. 5M), (4) scales and hairs (Fig. 5N), (5) teeth (Fig. 5O).

Quantitative characters of external morphology include the following: (15) total length in dorsal view (TL-I), (16) total length in lateral view (TL-II), (17) eye length (EL, Fig. 1C), (18) mandible length (LM, Fig. 6C), (19) length of head from vertex to gula (LH, Fig. 6C), (20) length of head-pronotum (HPL, Fig. 6A), (21) pronotum length (PL, Fig. 6A), (22) width of anterior region of pronotum (WPA, Fig. 6A), (23) width of posterior region of pronotum (WPP, Fig. 6A), (24) thorax length (LDT, Fig. 6B), (25) length of pronotum-elytra (LPE, Fig. 6A), (26) elytral length (LE, Fig. 6A), (27) body width at base of elytral disc (AC, Fig. 6A), (28) abdomen length in ventral view (LA, Fig. 6B), (29) abdomen width in ventral view (AA, Fig. 6B), (30) distance between coxae of foreleg (DC-I, Fig. 6B), (31) distance between coxae of midleg (DC-II, Fig. 6B), (32) distance between coxae of hindleg (DC-III,

Fig. 6B), (33, 34) number of crenulations on the right and left elytral disc margin (NCM-DED, NCM-DEI), (35, 36) number of dentitions in interstriae I of right and left elytral declivity (NDI1-DED, NDI1-DEI), (37, 38) number of dentitions in interstriae III of the right and left elytral declivity (NDI3-DED, NDI3-DEI).

Quantitative characters corresponding to sternite IX of females included the following: (1) angle of base (AB), (2) distance between lateral apices of posterior margin (DALMP), (3) distance between the central silks (DSC), (4) distance between the arch (DA), (5) length of the anterior projection (LPA), (6) Length of the posterior to anterior margin (LMPA) (Supplementary Fig. S1).

Multivariate statistics. Each specimen was considered an operational taxonomic unity (OTU). To explore whether character set variation segregated OTU´s into discrete groups corresponding to species, a series of ordination analyses were performed using matrices that included the external morphological characters of females (n= 56) and males (n=77) independently and together (n=133: 56♀ and 77♂). Principal component analyses (PCA´s) were performed using correlation matrices of continuous characters (TL-I, TL-II, EL, LM, LH, HPL, PL, WPA, WPP, LDT, LPE, LE, AC, LA, AA, DC-I, DC-II, DC-III, NCM-DED, NCM-DEI, NDI1-DED, NDI1-DEI, NDI3-DED, NDI3-DEI), and principal coordinate analyses (PCoA´s) were performed from a paired Gower matrices combining quantitative and qualitative characters (CH, SHS, FSP, FVP, EMVP, SEMS, SFC, CP, CE, VD, SEDS, VDE, PVDE, PEVI2-DE). To evaluate the discriminatory power of the character systems and the integrity of the species analyzed, a series of discriminant analyses were carried out using continuous traits; the power of the resulting discriminant functions and character systems to identify species was established as the percentage of individuals correctly classified by the function. Finally, to observe whether there were statistically significant differences among the groups, analyses of similarities (ANOSIM) or multivariate analyses of variance (MANOVA) were performed. The characters corresponding to sternite IX of females (AB, DALMP, DSC, DA, LPA, LMPA) were analyzed in an independent matrix and the same analyses mentioned above were applied.

Geometric morphometrics. Shape variation of the pronotum (♀, ♂), elytra (♀, ♂), and sternite IX of females were analyzed. The contour of the morphological structures was quantified using potential homologous landmarks (lm´s) and semilandmarks (sml´s). The shape of the pronotum, in dorsal view, was defined by three type II lm´s, one type III lm, and 28 sml´s; the elytron in lateral view, by two type II lm's and 28 sml´s; the sternite IX by six type I lm´s and 14 sml´s (Supplementary Fig. S2). The positioning of the semilandmarks was defined using combs on the photographs of each of the structures with the software MakeFan6 from the Integrated Morphometrics Package (Sheets, 2003). Two combs of 10 parallel lines each were placed on the pronotum, the first located between the lateral curvatures of the posterior region and the second located in the mid-dorsal region in the anterior-posterior direction. A comb of 15 parallel lines was placed at the maximum points of the elytra in the dorsal region of the elytral disc and at the ventral end of the elytral declivity. One comb with ten divisions (landmarks 7-16) and two with five divisions each (lamdmarks 2-6 and 2-17) were used to establish the configuration of landmarks and semilandmarks of the sternite IX. Landmark configurations of pronotum, elytra, and IX sternite are presented in Supplementary (Figure S2).

Landmarks and semilandmarks were digitized using tpsDig 1.40 software (Rohlf 2004). To remove variation due to size, scale, and rotation of shape configurations, a generalized Procrustes analysis was applied using PAST software (Hammer and Harper. 2001). To reduce the number of variables associated with the description of the main trends in the shape variation of the structures a relative warp analysis (RWA) was performed and to evaluate the shape patterns of the structures the first three relative deformation components (or relative warps-RW´s) of each analysis were plotted. In each RWA, the positional variation of the landmarks of each structure was described through deformation grids. To explore whether variation in pronotum and elytra shape recovered discrete groups of species, linear discriminant analyses (LDA) were performed. To explore whether the shape variation was statistically significant among species a multivariate analysis of variance (MANOVA) was performed

using the relative warps values obtained from the first ten principal components (PC's) or resulting from the relative warp analyses.

About P. serratus. Since *P. serratus* was the only species for which samples were obtained from three different hosts from different geographic localities, an analysis including three populations from different hosts was performed to observe whether the variation in structures segregated discrete groups. The methodology for each analysis was the same as described above for each structure. The three populations were labeled based on the host from which they were collected.

Genotyping by sequencing (GBS) data analysis. The extraction of genomic DNA, library preparation, and sequencing were carried out using protocols established by LGC genomics (Biosearch Technologies, Berlin, Germany). In total 31 samples belonging to six species of *Phloeosinus* (*P. baumanni, P. cristatus, P. deleoni, P. serratus, P. tacubayae, P. taxodii taxodiicolens*), were sent for DNA extraction, library preparation and sequencing (Supplementary Table S1). Briefly, the representation-reduced genome technique selected was GBS (paired) which belongs to techniques of the Radseq family. The enzyme selected to fragment the genomic DNA was PstI, because these samples were multiplexed with other *Dendroctonus* samples in the same sequencing run (see Ramírez-Reyes et al. 2023 for more information). In total, 100 million paired-end reads (150 bp paired-end read) were sequenced for the 31 samples by using the Illumina NextSeq (500/550 v2). Additionally, we took advantage of joint sequencing with some *Dendroctonus* species and included three samples of two species as an outgroup for phylogenetic analyzes (*D. mesoamericanus* and *D. adjunctus*).

In total 34 samples were analyzed with the ipyrad v.0.9.92 pipeline (Eaton and Overcast 2020). Because there is no reference genome for *Phloeosinus* spp., we selected a reference genome close to both bark beetle genera (*Dendroctonus* and *Phloeosinus*) to map loci and perform the assembly and variant calling, therefore, we used the reference genome of *Ips nitidus* (BioProject PRJNA722788). Initially, we carried out assembly tests only with the genus of interest (*Phloeosinus*). These initial tests allowed us to discard 11 samples that were shown to contain few traces of the beetle genome.

Subsequently, the samples that passed the assembly tests (only four species of *Phloeosinus*: *P. baumanni, P. tacubayae, P. deleoni, P. serrratus*), were incorporated together with the three samples of *Dendroctonus* (outgroup). In total, 46 fastq files were analyzed (23 paired samples), and the samples corresponding to *P. cristatus* and *P. taxodii taxodiicolens* were discarded for the final assemblies due to their low quality. Some of the parameters indicated to ipyrad were: data type (pairgbs), the maximum number of low-quality bases allowed in a read Q < 20 (5 bases), Qscore Phred (33), clustering threshold (85%), adapter filter value (2 the maximum), minimum length of reads after filtering (35 pb), maximum number of alleles in a consensus sequence (2), minimum number of samples per locus (4) and maximum number of heterozygous sites per locus (30%). From the parameters indicated in the first assembly, two more were created, in which only the minimum number of samples was modified to call a locus (8 and 16 samples). These last two assemblies (min_8 and min_16) and their output files were selected to perform the genomic and phylogenomic analyses in the present study (see Results).

Genetic structure and phylogenomic analysis. To explore the genetic structure of the species and subsequently quantify the degree of genetic differentiation, we used the SNPs called during assembly (min16). The genetic structure was visualized through a PCA. The PCA and divergence quantification (Fst) were calculated and performed with the adegenet (Jombart and Ahmed 2011) and VCFR (Knaus and Grünwald 2017) packages in Rstudio.

Once the genetic structure of the populations and their correspondence with the species has been determined, we explored phylogenetic hypotheses with the gene concatenation approach with two models: maximum likelihood (ML) and Bayesian inference (BI). The ML approach was implemented in IQTREE v 2.2.0 (Minh et al. 2020) for both concatenated loci matrices (min8 and min16). First, we determined the most probable evolution model for each matrix based on three criteria AIC, AICc, and BIC. Once the model that best fits has been determined, we performed the ML phylogenies. For these analyses, two metrics were used to assess branch support, the SH-like approximate likelihood ratio test (Guindon et al. 2010), and ultrafast bootstrapping (Hoang et al. 2018).

In the case of the Bayesian model, we implemented the phylogenetic search with Mr. Bayes v.3.3.7 (Huelsenbeck and Ronquist 2001) for both concatenated loci matrices (min8 and min16). First, the best-fit substitution model for BI was selected based on the BIC using JMODELTEST v.2.1.10 (Darriba et al. 2012). Once the model was selected, two independent analyses with started random trees were performed each one with four Markov chains. The Markov Chain Monte Carlo processes were run for 4×10^5 generations with a sampling frequency of every 1,000 generations. The first 25% of the MCMC samples were discarded as burn-in. The Bayesian posterior probability was calculated from a 50% majority rule from the 200,000 trees. A consensus tree was constructed by summarizing the bootstrapping values.

Integration of information

The integration of information was made through a congruence matrix, in which each hypothesis (*i.e*., species) was contrasted with the set of data and analyses to which its morphological or genetic variation was subjected. In total, the variation of each species was evaluated with 14 different analyses, according to the nature of the data analyzed (genetic or morphological), the source of the characters used (external or internal morphology), the nature of the variation of the attributes (discrete or continuous), and the sex of the specimens studied (females, males, or both) (Table 4).

Results

Multivariate analysis. The results of applied analyses to the 24 quantitative and 38 quantitative and qualitative characters from females and males together and alone are presented in Table 2. In all of them, the first three PC´s quantified more than 90% of the variation of traits; and respective scatter plots display the OUT´s, in most cases, segregated according to hypothesis species (Figs. 7A and B). In all analyses, for females and males, the LDA correctly classified 100% of the specimens according to the species hypothesis.

The scatter plots of LDA and PCoA of quantitative attributes showed five phenotypic groups. Although, the groups are different in each one. For the LDA of quantitative attributes, *P. taxodii*

taxodiicolens, P. serratus, P. deleoni were displayed as discrete groups, while *P. arizonicus, P. tacubayae,* and *P. spinosus* appeared overlapped, and *P. baumanni* and *P. cristatus* partially overlapped (Fig. 7A). On the other hand, the scatter plot of PCoA using qualitative and quantitative external attributes recovered one group conformed by *P. baumanni, P. cristatus* and *P. deleoni* and *P. serratus.* While the other species were displayed as independent groups (Fig. 7B). The MANOVA test using quantitative continuous traits supported statistically significant differences (λ_{Wilks}= 0.0003149, F= 9.595, $p \leq 0.0001$) among all groups corresponding to the hypothesis species, the same were for ANOSIM ($R > 0.3904$ and $p= 0.0001$) using quantitative and qualitative attributes. For all analyses, the characters that most influenced the variation were the number of dentitions in the first and third, right and left interspaces (NDI1-DED, NDI1-DEI, NDI3-DED, NDI3-DEI) and the number of crenulations on the elytral disc (NCI1-DED, NCI1-DEI). For the independent analyses for females and males, the scatter plots were similar to those described above and the characters that most influenced the variation were similar (Supplementary Fig. S3).

The PCA applied to the 6 quantitative characters of sternite IX, quantified in the first three PCs 92.75% of the total variation (PC1, 44.68%; PC2, 38.69%; PC3, 9.67%), the scatter plot of the first two components (PC1 vs PC2) showed a total separation of all species (Fig. 7C). The LDA correctly classified 96.77% of the specimens and the scatter plot showed a separation of OUT´s according to hypothesis species (Fig. 7D). The MANOVA test supported significant differences (λ_{Wilks}= 0.001852, F= 10.44, $p \leq 0.0001$) among species. In both analyses, the characters that most influenced the variation were the distance between the lateral apices of the posterior margin, the length from posterior to anterior margin, and the distance of the arch, (DALMP, LPA, DA)

Geometric morphometrics

The results of shape analyses of pronotum and elytra are presented in Table 3. In both structures the results for females and males were similar, so, here only show the scatter plot for males (see Supplementary Fig. S4 for females results).

Pronotum. Superposition of pronotum configurations and the relative deformation grids of two first relative warps display the shape variation of the structure located at the posterior and anterior angles and in the lateral area of the middle and posterior section (Fig. 8A). In females the LDA of the first ten relative warps correctly classified 78.59% of the specimens and for males the 77.92%. The scatter plot showed a large overlap between groups, except in *P. baumanni*. The shape of the pronotum of this species is rounded at the lateral edges concerning the other species and the curvatures of the anterior edge are less marked compared to the other species (Fig. 8B). For females the ANOSIM significance test supported statistically significant differences (R values < 0.35, p=0.0001) except for *P. cristatus* with the rest of species (R values < 0.23, $p \geq 0.12$), *P. serratus* with *P. tacubayae* and *P. taxodii taxodiicolens* (R values < 0.1889, p > 0.05) and *P. taxodii taxodiicolens* with *P. baumanni* (R = 0.1801, p = 0.1153). On the other hand, for males the ANOSIM showed statistically significant differences (R = 0.3507, $p \leq 0.0001$), except for *P. taxodii taxodiicolens* with *P. baumanni, P. cristatus* and *P. deleoni* ($R \leq 0.2$, p > 0.05), *P. cristatus* with *P. serratus* (R = 0.0913, p = 0.1293), and *P. spunosus* with *P. deleoni* and *P. tacubayae* (R < 0.2, p > 0.05)

Elytra. Superposition of elytral configurations and grids of two first relative warps display the shape variation of the structure in the curvature of the lower edge and elytral declivity slope (Fig. 8C). In females the LDA of the first ten relative warps correctly classified 89.29% of the specimens and for males the 89.61%. The scatter plot shows six species forming an overlapping phenotypic group, but *P. baumanni* and *P. deleoni* were discrete groups (Fig. 8D). For *P. deleoni* the elytral slope is very steep, whereas for *P. deleoni* it is very curved. The ANOSIM for females supported statistically significant differences (R = 0.18, p= 0.006), except for *P. cristatus* versus *P. baumanni, P. serratus, P. tacubayae* and *P. taxodii taxodiicolens* (R < 0.6 , p > 0.05), *P. baumanni* versus *P. tacubayae* (R = 0.09, p = 0.0958), and *P. serratus* versus *P. deleoni, P. tacubayae* and *P. taxodii taxodiicolens* (R < 0.1, p > 0.05). For males ANOSIM showed statistically significant differences (R = 0.3, p = 0.0001), *P. baumanni* was the only specie that differentiated from the others (R > 0.5, $p \leq 0.0001$), *P. tacubayae*

versus *P. cristatus, P. serratus, P. spinosus, P. arizonicus* and *P. taxodii taxodiicolens* did not show differences ($R < 0.3$, $p > 0.05$), also *P. serratus* vs. *P. cristatus, P. spinosus, P.taxodii taxodiicolens* ($R < 0.1$, $p < 0.05$) and *P. arizonicus* v.s *P. spinosus* and *P. taxodii taxodiicolens* ($R < 0.2$, $p > 0.05$).

Sternite IX of females. Shape variation observed in superposition configurations and grids of the two first relative warps was related and located in the curvature of the posterior margin (Fig. 8E). The first three relative warps explained almost 97.28% of the total variation (RW1, 72.14; RW2, 17.08; RW3, 8.05). The LDA correctly classified 95% of the specimens and the scatter plot showed the separation of the four species analyzed in discrete groups. And the ANOSIM supported statistically significant differences ($R > 0.5$, $p=0.0001$) among all hypothesis species (Fig. 8F).

Description of shape patterns of both elytra and sternite IX allowing species discrimination are presented in the section "Integrating the information from different sources".

About *P. serratus*

Phloeosinus serratus was the only sampled species obtained from different host species, *Juniperus coahuilensis* (JC), *J. saltillensis* (JS), and *Cupressus arizonica* (CA). Also, in all analyses, this taxon showed high variation among all studied samples (see plots for above analyses). Individual analyses were performed to study the intraspecific variation inside this species. The results obtained from LDA applied for males and females together using the 24 quantitative characters correctly classified the 100% of the individuals according to respective hosts. The scatter plot showed that the three populations from different host were morphologically differentiated and recovered in three well-defined discrete groups (Fig. 9A). Although, the MANOVA did not support statistically significant differences between the populations ($\lambda_{Wilks}= 0.003263$, $F= 2.751$, $p = 0.0654$). For the PCoA using 38 quantitative and qualitative characters, the first three components recovered 59.11% of the variation (Fig. 9B). The scatter plot from this analysis showed the three groups overlapped, but the MANOVA supports statistically significant differences among them ($R \geq 0.3$, $p \leq 0.001$).

For the geometric morphometrics of the body, the LDA of the pronotum shape correctly classified 95% of females and 100% of males. In both cases, the scatter plot showed three discrete groups (Fig. 9C and D). ANOSIM did not show statistically significant differences for females (R= 0.01422, p= 0. 3831), but for the males there were statistically significant differences among *P. serratus*-CA versus *P. serratus-JC* (R = 0.216, p = 0.03), and *P. serratus*-CA versus *P. serratus-JS* (R = 0.268, p = 0.038), while between *P. serratus-JC* versus *P. serratus-JS* did not show differences ($R \leq 0$, p = 0.7782). For the elytra shape the results were similar, thus all populations of *P. serratus* were segregated into discrete groups (Fig. 9E and F). The LDA correctly classified 93.33% of females and the 100% of males. Although females did not support statistical differences ($R \leq 0$, p= 0.7872), males support statistically significant differences among *P. serratus-JC* versus *P. serratus-JS* (R = 0.2, p = 0.0141). The results of shape analysis of sternite IX showed all populations were segregated in non-overlapping groups (Fig. 9G and H) but the ANOSIM showed statistically significant differences only for *P. serratus-JC* versus *P. serratus-JS* (R = 0.578, p = 0.0037).

Genotyping by sequencing (GBS) data analysis

Once the samples with poor coverage and poor quality (*P. cristatus* and *P. taxodii taxodiicolens*) were discarded, three assemblies were created, one basic assembly with the parameters mentioned above and two more modifying the minimum number of samples to call a locus (min8 and min16), which were used for genomic and phylogenomic analyses. The min8 assembly presented 612 loci on average, reflected in a concatenated matrix of 137,897 characters (48% missing data) with 3,768 parsimoniously informative sites and 6,032 SNPs. For its part, the min16 assembly obtained 369 loci on average, forming a concatenated matrix of 69,018 characters (34% missing data) with 2,123 parsimoniously informative sites and 3,031 SNPs. For both assemblies, the sample with the lowest coverage was *D. mesoamericanus* (outgroup sample).

The first three axes of the PCA components explained more than 70% of the variance of the SNP matrix (3,031 SNPs, 25% missing data), showing the existence of four genetic groups within

Phloeosinus, which coincide with the taxa recognized at the date (*P. tacubayae, P. serratus, P. deleoni* and *P. baumanni*; Fig. 10). The Fst values were congruent with the structured genetic groups, with Fst = 0.80 on average for the four taxa and high values of genetic differentiation among them.

Regarding phylogenomic analyses, all ML phylogenomic trees were congruent with each other. First, the largest matrix with 137,897 characters presented the two most probable models of evolution, one congruent for AIC and AICc (TVM+F+I+I+R5) while the BIC found the TVM+F+R4 model. Despite this, both topologies were identical (Fig. 11). The phylogenetic trees recovered *Phloeosinus* as monophyletic clade. Inside the genus *P. baumanni* is monophyletic and is the sister group of *P. tacubayae*. At the same time, *P. deleoni* is also monophyletic and is the sister group of *P. baumanni* and *P. tacubayae.* While *P. serratus* specimens from different host species were not recovered as a monophyletic group. All clades showed high values of branch support (SH-like approximate likelihood ratio test and ultrafast bootstrap). For its part, the smaller matrix of 69,018 characters showed convergence of the GTR+F+R4 model for AIC and AICc, while the BIC showed the TVM+F+I model. Identical to the results obtained from the larger matrix, the topology and phylogenetic relationships were the same as those described above (Supplementary Fig. S6).

All BI phylogenomic trees were congruent with each other and with the ML trees. All clades showed high values of branch support. With JModelTest for both matrices, the best substitution model was TVM+I+G for AIC and BIC. The phylogenetic inferences were implemented using the GTR+I+G model (this model is more like TVM model), because the TVM model is unavailable in MrBayes. Finally, the results obtained from both matrices were identical in topology and phylogenetic relationships (Supplementary Fig. S7).

Integrating the information from different sources

The combination of different data sources and types of analysis of *Phloeosinus* spp. showed that each taxon analyzed as a hypothesis is supported by at least two sets of data, morphological, genetic, or both. (Table 4). Of the species for which genetic and morphological information was available,

Phloeosinus baumanni was the best-supported hypothesis, because both phylogenetic inference analyses supported it as monophyletic, and nine morphological ones as a taxon well differentiated phenotypically (Fig. 7 and 8). *Phloeosinus tacubayae* and *P. deleoni* were also supported as independent lineages in both phylogenetic trees, and by seven morphological analyses each (Fig. 11). Phylogenetic inferences did not support the monophyly of *P. serratus* however in four morphological tests, it was displayed as a discrete group (Fig. 7, 8 and 9). The remaining species were not analyzed using genetic data, however, two of them, *P. taxodii taxodiicolens*, and *P. cristatus* displayed well-differentiated phenotypes, recovering them as discrete groups. The low number of specimens obtained of *P. arizonicus* and *P. spinosus* limited the number of analyses performed to evaluate them, however, the analyses of quantitative and qualitative attributes of external morphology supported these species with discrete phenotypes distinct to other *Phloeosinus* spp. (Fig. 7B).

Concerning the data analyzed, in five species quantitative characters were good for distinguishing them, while for *P. arizonicus, P. tacubayae* and *P. spinosus* not. The combination of quantitative and qualitative characters supported the hypothesis for *P. arizonicus, P. tacubayae, P. taxodii taxodiicolens* and *P. spinosus,* while for the rest of the species, it does not. The analyses applied from the attributes of sternite IX support all five species hypotheses analyzed (*P. baumanni, P. deleoni, P. tacubayae, P. taxodii taxodiicolens* and *P. serratus*). In the body shape analyses, *P. baumanni* was the only species for which the shape of both structures (pronotum and elytra) allows its distinction in a clearer way concerning the other analyzed species. On the other hand, the phylogenetic inferences allow the recognition of three to four analyzed species, *P. serratus* was the only species that cannot be recognized as a monophyletic group (Fig. 11).

The evaluation of phenotypic variation in the recognized species by mean multiple character sources, allows us to recognize a combination of traits of body size (total length), body sculpture (number of crenulations in the elytral disc and number of dentitions on the interstriae of elytral declivity), body

shape (pronotum and elytra), morphology of female sternite IX (size and shape) that together allow a better the species recognition.

Phloeosinus arizonicus. Length 1.57-2.57 mm; 10 crenulations per side on the margin of elytral disc; 6-7 dentitions on the surface of interstriae I of elytral declivity and 5-7 on the surface of interstriae III of elytral declivity. The shape of the pronotum is characterized by rounded lateral and anterior edges, while the posterior edge and the angles that form it are very well-defined. The width and length of this structure is similar. The posterior central angle is pronounced more than the posterior lateral angle. The shape of the elytra is characterized by a rounded elytral declivity with a very steep slope starting in the last third of the elytra.

Phloeosinus baumanni. Length 2.8-3.9 mm; 13 crenulations per side on the margin of the elytral disc; 5 dentitions on the surface of inter striae I and 8 on the surface of inter striae III of elytral declivity. The pronotum is larger than the width, its shape characterized by a narrower anterior edge than the posterior one, the middle section at the lateral edges becomes narrow towards the anterior region, and the posterior angles (lateral and central) are rounded but are not very marked. The shape of the elytra is characterized by a straight elytral slope with a very steep slope. The shape of female sternite IX is characterized by a straight posterior edge in the central section and slightly curved in the laterals. The anterior margins are straight.

Phloeosinus cristatus. Length 2.7-3.5 mm; 12 crenulations per side on the margin of the elytral disc; 3-6 dentitions on the surface of inter striae I and 8-11 on the surface of inter striae III of elytral declivity. The pronotum is rounded on the anterior edge, the lateral edges taper slightly in the anterior middle section, the posterior angles are pointed, but the central angle is more marked than the others. The shape of the elytra is characterized by slightly curved elytral declivity that start in the last third of elytra. the width of this structure (distance between lateral apices of posterior margin) is larger than the length.

Phloeosinus deleoni. Length 2.7-3.3 mm; 13 crenulations per side on the margin of elytral disc; 5 dentitions on the surface of interstriae I and 5 on the surface of interstriae III of elytral declivity. Pronotum is characterized by rounded lateral and anterior edges, while the posterior edge and the angles that form it are very well defined. The shape of the elytra is characterized by slightly curved elytral declivity that start in the second third of elytra. The shape of female sternite IX is characterized by a curved posterior edge, the anterior margins are slightly convex and rounded in the apices and, the width (distance between lateral apices of posterior margin) is larger than the length.

Phloeosinus serratus. Length 2.4-3.2 mm; 12 crenulations per side on the margin of elytral disc; 6-8 dentitions on the surface of interstriae I and 10-13 on the surface of interstriae III of the elytral declivity. Pronotum is characterized by parallel lateral edges in the posterior middle section and narrow in the anterior middle section, the posterior lateral angles are rounded and prominent than the central angle. The shape of the elytra is characterized by very slightly curved elytral declivity that start in the last third of elytra. The shape of female sternite IX is characterized by a curved posterior edge, the anterior margins are slightly convex and the width and length are similar.

After fine analysis of the elytral disc and elytral declivity elements, and shape of IX sternite, differences were found among populations - host of *P. serratus*. These are in the size and number of dentitions on the insterstriae I and III, the number of crenulations on the elytral disc margin, curvature of posterior margin of IX sternite and relative proportions of this segment. Specimens from *C. arizonica* population, length is 2.4 to 3 mm., 11 crenulations per side on the margin of elytral disc, 7 dentitions on the surface of interstriae I, and 10 on the surface of interstriae III, both of elytral declivity are present, and the shape of sternite IX is very curved on the posterior margin and the anterior edges are convex, the width and length are almost proportional. While for *J. coahuilensis* population, specimen´s length is 2.94 to 3.27 mm., 12 crenulations per side on the margin of the elytral disc, 10 dentitions on the surface of interstriae I of elytral declivity, and 11 on the surface of interstriae III of elytral declivity are present, and the shape of sternite IX is less curved on the posterior margin and in

the center are almost straight, the width are larger than the length. Finally, for *J. saltillensis* population, the specimens´s length is 2.67 to 2.96 mm, 11-12 crenulations per side on the margin of elytral disc, 8 dentitions on the surface of interstriae I of elytral declivity and 12 on the surface of interstriae III of elytral declivity are present, and the shape of sternite IX is curved on the posterior margins and the anterior edges are lightly convex, the width is larger than the length.

The shape of body structures was similar in the three populations, with slight variations in the shape of the anterior angles (pronotum), in the curvature of the elytral declivity (elytra), and in the curvature and width of the posterior margin of sternite IX in females. The variation among the external structures (pronotum and elytra) may be derived from the host in which these insects are found or from other factors.

Phloeosinus spinosus. Length 2-2.1 mm; 10 crenulations per side on the margin of the elytral disc; 5 dentitions on the surface of interstriae I and 5 on the surface of interstriae III of elytral declivity. The pronotum is characterized by a lateral edge slightly curved in the posterior middle section and narrow in the anterior middle section, the posterior angles are rounded and all of them are equal (none stands out more than the other), and the width is larger than the length. The shape of the elytra is characterized by very curved elytral declivity that starts in the last third of the elytra.

Phloeosinus tacubayae. Length 2-2.5 mm; 12 crenulations per side on the margin of the elytral disc; 6-7 dentitions on the surface of interstriae I, and 6 on the surface of interstriae III of the elytral declivity. Pronotum is characterized by curved lateral edges in the posterior middle section and narrow in the anterior middle section, the anterior edge is rounded but is not very marked; the posterior central angle is pointed, and the posterior lateral angles are rounded, and the length is larger than the width. The shape of the elytra is characterized by very rounded elytral declivity that starts in the last third of the elytra. The shape of female sternite IX is characterized by a straight posterior edge and rounded anterior margins, the width (distance between lateral apices of posterior margin) is smaller than the length.

Phloeosinus taxodii taxodiicolens. Length 2.2-2.7 mm. 11-14 crenulations per side on the margin of the elytral disc; 8.13 dentitions on the surface of interstriae I and 12-15 on the surface of interstriae III of the elytral declivity. The pronotum is rounded at anterior edge. The lateral edges are curved in the posterior middle section and narrow and the anterior middle section, the posterior central angle is pointed, and the posterior lateral angles are rounded but are not very marked and the length is larger than the width. The shape of the elytra is characterized by curved elytral declivity that start in the last third of the elytra. The shape of female sternite IX is characterized by a curved posterior edge and convex anterior margins and the width (distance between lateral apices of posterior margin) is larger than the length.

Discussion

One of the most important tasks for systematics is to define species (Mayr 1963), for this purpose, there are different ways, which vary according to three elements: 1 the attributes, 2 the evidence (morphological, genetic, ecological, reproductive, geographic or some combination) and 3 the criteria used to delimit them (Young et al. 2018). The combination of these elements has been articulated in terms of defining species, recapitulated in more than 20 concepts, some of them operational and others theoretical (Mayden 1997).

Another approach has been to view species as hypotheses, or the result of inferences aimed at understanding the properties and relationships of organisms (Fitzhugh 2005). Under this perspective, species can be viewed as explanations of occurrences of the same characters among cross-fertilized individuals, by character origin and fixation during tokogeny (Fitzhugh 2005). So, when an author describes a species, he hypothesizes that all its members can be recognized by the characters provided in the description and that these are the product of causal tokogenetic relationships (Hening 1966).

Based on this framework, in this study, the hypotheses of *Phloeosinus* spp, inhabiting the Mexican Transition Zone were tested, based on many character sources, both morphological and genetic ones, and 14 different analyses. We hypothesize that if the individuals from different geographical localities,

identified to a putative species, under the criteria of their description (i.e. diagnosis), correspond to only one species, then the analyses of their overall phenotype will show, that part of their morphological variation patterns will be shared and will covary among them as a product of an origin and its respective fixation in the population during past tokogenetic events. Also, the monophyly of some species using phylogenomic data was evaluated, we hypothesize that if the patterns of morphological variation among individuals associated with a previous hypothesis are the product of tokogenetic events, then their genetic variation will present a clear structure of linages congruent with that hypothesis.

Collectively the 14 analyses performed, according to the source of the attributes, the nature of their variation, and the sex of the specimens, supported that at least seven species are consistent with their previous hypotheses *P. baumanni, P. tacubayae, P. deleoni, P. cristatus, P. spinosus, P. arizonicus,* and *P. taxodii taxodiicolens* (Table 4).

The phylogenomic analyses in four of them delineated and supported to *P. baumanni*, *P. tacubayae*, and *P. deleoni* as well-structured linages and monophyletic species, corresponding to the most stable species taxonomically in the region, because since their description, they have not had nomenclatural changes (Hopkins 1905, Blackman 1942).

Phloesinus baumanni and *P. tacubayae* were recovered as sister species and the best supported phenotypically by more than seven morphological analyses (Fig. 7, 8 and Table 4). These results agree with the fact that they share many ecological and biological traits and overlap their distribution areas. Both are monophagous, inhabit coniferous, oak, mountain mesophytic, and tropical deciduous forests (Cibrian-Tovar et al. 1995), and develop their life cycle exclusively in the Mexican Cypress, *Hesperocyparis lusitanica* (Atkinson and Equihua 1985). Both species are native of MTZ in Mexico and Central America, *P. baumanni* is distributed from SE Arizona to El Salvador, and *P. tacubayae* from Nuevo Leon to Nicaragua (Wood 1982; Atkinson et al. 1986, Atkinson 2019, Cervantes-Espinoza et al. 2022); in some localities, they can be found in sympatry and syntropy within the same host tree

(Cibrián-Tovar et al. 1995). Respect to their taxonomy, both species were proposed by Hopkins (1905), and supported by contrasting morphological differences between them, the most evident being the larger size and the marked sexual dimorphism in the elytral declivity of *P. baummani*, absent in *P. tacubayae* (Hopkins 1905, Wood 1982, Cervantes-Espinoza et al. 2022). Although they share biological and ecological traits, relationships between these species likely need to be clarified because both have been related to other congenerics based on morphological resemblance (Wood 1982). *Phloesinus baumanni* has been closely related to *P. variolatus*, a species whose distribution is restricted to California and feeds on *Cupressus sargenti*, while *P. tacubayae* is closely related to *P. anntenatus* whose distribution is widespread in the southern Rocky Mountains, where it feeds of Pinaceae and *Libodendrus* spp.

The clade *P. baumanni*-*P. tacubayae* was supported as the sister of the monophyletic *P. deleoni*, whose morphological variation patterns also were consistent with its species status in "11 and 9" morphological analyses respectively, both external and internal attributes (Fig 7, 8 and Table 4). This species is the most distinctive from the other *Juniperus* feeders of the genus within MTZ (Wood. 1982), by its ecological and morphological traits. *Phloeosinus deleoni* is a monophagous species that develop its life cycle in *J. flaccida*, and do not share its host with another *Phloesinus* spp., it inhabits xeric areas and is endemic to four Mexican mountain systems: Sierra Madre Oriental (SMOR), (Nuevo Leon); Sierra Madre Occidental (SMOC), (Chihuahua, Durango); Faja Volcanica Transmexicana (FVTM), (Hidalgo, Michoacán); Sierra Madre del Sur (SMS), (Oaxaca, Puebla); (Atkinson 2023). Due to its degree of trophic specialization and the combination of characters on the frons and elytral declivity, Wood (1982) was unable to establish a clear relationship with other members of the genus.

In the cases of *P. arizonicus*, *P. cristatus*, *P. spinosus* and *P. taxodii taxodiicolens* it was not possible to evaluate their hypothesized lineage structure and monophyly, however, these were supported by different morphological analyses. *Phloeosinus arizonicus* was supported by 2 analyses corresponding to external morphology including qualitative and quantitative data. This species is taxonomically stable

(it has not presented synonymies), is closely related to *P. setosus,* whose distribution is restricted to Arizona where it feeds on *Cupressus arizonica.*

Phloeosinus cristatus was supported by 5 analyses, including traditional morphometrics of quantitative characters (body measurements), as well as the shape of structures such as pronotum and elytra. This species has been synonymized once and is related to *P. sequoia,* whose distribution extends from California to Arizona and Durango, where it feeds on *Cupressus, Juniperus,* and *Thuja* spp.

Phloeosinus spinosus was supported by 2 analyses corresponding to external morphology including qualitative and quantitative data. This species has not presented synonymies and is closely related to *P. swaine* and *P. frontalis,* whose distribution extends to Arizona and New Mexico to Chihuahua, where it feeds on *Cupressus arizonica* and *Juniperus deppeana.* Finally, *P. taxoddii taxodiicolens* was supported by 10 morphological analyses. It was previously considered a different species from *P. taxodii*, supported on specimens from San Luis Potosi. Its distribution is restricted to Mexico from Durango to Puebla, where it feeds on *Taxodium mucronatum.* Wood (1982) categorized it as a subspecies based on morphological variation of specimens from Durango, that display intermediate characters between *P. taxodii* and *P. taxodiicolens*. Its necessary to review type material and evaluate variation of specimens from Sierra Madre Occidental to clarify the status of these taxa.

About *P. serratus*.

This taxon was the only one in which there was evidence that its taxonomic label masks a greater diversity. In our analyses based on genetic data, *P. serratus* showed a very clear lineage structure, concerning the rest of the studied members (Fig. 7 and 8), however, it was not recovered as monophyletic in any of the phylogenies (Fig. 11). Morphologically it was supported by only 5 analyses and in all was the species that occupied the largest area in the multivariate spaces (Fig. 7 and 8), indicating wide phenotypic variation. Interestingly, when the morphological variation of its specimens was analyzed according to the host-locations from which they were obtained, discrete well-differentiated phenotypes were recovered in the multivariate space, corresponding to three groups

whose main differences and characteristics are described in the results section. These groups correspond to populations of *P. serratus* isolated by the patchy distribution of their hosts *Juniperus coahuilensis*, *J. saltillensis* and *Cupressus arizonica*, on the slopes of Cerro del Potosí, which is the highest mountain in the SMOR.

Phloeosinus serratus is a polyphagous species that feeds on 9 species of *Juniperus* and one of *Cupressus*, and has the widest distribution range of the genus, from Washington and Idaho through Texas in the USA to the state of Hidalgo in Central Mexico with a record in Jamaica (Atkinson 2023). Taxonomically it is the oldest species in the region (LeConte 1868) and the one with the most nomenclatural acts, with seven synonymies (Wood 1982). Previous authors have highlighted its wide morphological variation by establishing allopatric units in the northern Rocky Mountain distribution and recognized differences between these and the Mexican populations of the SMOC, without establishing their respective limits and degrees of morphological variation (Blackman 1942, Wood 1982). The specimens included in the present study correspond to the first records in that region of the SMOR and on those hosts, so their morphological variation had not been evaluated.

The complex taxonomic background of *P. serratus*, its geographic-ecological context and our results support that geographic isolation and host specialization are factors that are promoting the diversification of this species. Likewise, the paraphyly of *P. serratus* populations in our analyses is congruent with a peripatric speciation pattern, where new species originate at the periphery of their range and as a result, the ancestral populations become a paraphyletic group, i.e. a lineage that does not include all its descendants (Lukhtanov 2019). Although, it is possible to recognize morphological differences and diagnostic attributes among the allopatric phenotypes of *P. serratus* in the SMOR, and with respect to those presented in previous descriptions (Wood 1982, Blackman 1942), we prefer to maintain these populations without a formal taxonomic assignment due to the lack of genetic evidence.

Character analysis

Our results support that the body measurements, patterns of body sculpture and pubescence, body shape, and morphology of female sternite IX in addition to different multivariate methods of analysis, allow us to recognize morphological variation to support the species. In addition, a set of attributes can be recognized for identification.

For the eight Mexican species tested previously, the characters associated with elytral declivity have been reported as diagnostic (Wood 1982; Hopkins 1905; Blackman 1942), but, they had not been evaluated with statistical methods. This study confirms that in the species where interstria 1 and 3 are armed with teeth, the number of teeth (NDI1-DED, NDI1-DEI, NDI3-DED, NDI3-DEI) is useful to delimit and identify. In *P. serratus* and *P. taxodii taxodiicolens,* these traits are remarkable, because were that most contribute to diagnosticate them. These species have the major number of dentitions in interstriae 3, with 10 and 15 respectively. In addition, it was observed that these traits are useful for discriminating between females and males in some species, mainly in those where these characteristics are very marked among sexes as in *P. baumanni, P. deleoni, P. serratus* and *P. cristatus.* Also, for all species the number of crenulations of each side on the margin on disc elytral (NCI1-DED, NCI1-DEI) allows their recognition and delimitation, mainly for *P. baumanni* with 14, *P. cristatus* with 11 and *P. deleoni* with 12.

Likewise, in this work, it was observed that the use of continuous quantitative characters mainly influences the segregation of groups of species by size. In the scatter plots the small, medium, and big species appear separate each one. The small species (1.9 to 2.4 mm) *P. arizonicus, P. tacubayae, P. taxodii taxodiicolens,* and *P. spinosus* appear on one side of the scatter plot and large species (3 to 4.1 mm) *P. baumanni* and *P. cristatus* appear on the opposite side, while medium-sized species are in the center (2 to 3.7 mm) *P. deleoni* and *P. serratus*).

The sternite IX of females has not previously been studied. In this study the quantitative character analysis supports differences in this structure for all species, with the greatest differences being in the

distance between the lateral apices of the posterior margin, length from posterior to anterior margin, base angle, and arc distance (DALMP, LMPA, AB, DA).

The shape study of body structures like pronotum and elytra in bark beetles has shown that t differences between species and in some cases between sexes are present (García-Román *et al*. 2019, Ospina-Garcés *et al*. 2021). In the genus *Phloeosinus*, the variation of pronotum shape is complex between females and males. The diagram shows a partial segregation of some groups concerning shape configuration, due to the presence of intraspecific variation. Statistically, they are different and based on this it is observed that both males and females present variations in the shape of the pronotum, especially the posterior basal margin, the posterior angles, the anterior angle, and in the lateral area of the middle and posterior section. Although some differences are observed between females and males, the shape configuration does not appear to be a distinguishing feature for each species.

The shape pattern of the elytra shows a slightly more marked segregation compared to the pronotum. The scatter plot between RW1 and RW2 in females and males does not show a total segregation of discrete species groups, because there is a high intraspecific variation. Nevertheless, statistically discrete species groups segregate and show differences in elytral declivity angle, lateral margin, and anterior margin angle. Also, the variation between these regions allows better differentiation of each species compared to the pronotum shape.

Also, the results of geometric morphometry analysis indicate that the shape of sternite IX differs among species, indicating that this structure may be a useful diagnostic character for identification. Previously in other curculionids, a structure similar in shape was found that corresponds to sternite VIII and is commonly referred to as spiculum ventrale (Cristóvão and Lyal 2018, Gültekin and Lyal 2020, Košťál 2018). Although further studies are needed to corroborate whether there is a relationship between these structures.

Sexual dimorphism

Sexual dimorphism has been previously identified in bark beetles via body size or discrete traits (Kirkendall et al. 2015). In this work, we found differences associated with body size, mainly in *P. baumanni*, where females are slightly larger than males. Previously, differences in size have been associated with mating systems, and it has been described that the larger sex in monogamous species is the female and this is related to the fact that females are the pioneer sex in the colonization of the host tree (Foelker and Hofstetter 2014). Also differences in discrete traits from elytral declivity were found between females and males of *P. serratus*, *P. deleoni* and *P. baumanni*. Mainly differences were observed in the shape and number of dentitions present in interstria I and III. In other Scolytinae these differences are associated with the fact that these structures are involved in mating behavior and therefore have undergone a process of sexual selection (Wood 1982; Kirkendall et al. 2015). It has also been described that generally the sex that blocks the entrance of the gallery is usually the one that has more spines or dentitions in the elytral declivity, in this case it is the males that cover these characteristics (Hamilton 1979).

Conclusion

The results of this study provide support for using more than one source of evidence to evaluate species hypotheses in bark beetles and within the genus *Phloeosinus.* The use of different sets of discrete morphological traits, mainly those associated with elytral declivity and body measurements, allow the species to be distinguished. Likewise, the shape and characteristics of the sternite IX of females is a new and useful feature to distinguish all the species evaluated. The power of RAD-seq to evaluate hypotheses through phylogenetic inferences is also corroborated. In addition, the use of an integrative approach such as the one used in this work has not been previously addressed for the study of Scolytinae, so it is presented as a new proposal for it.

Acknowledgements

We thank to María Berenit Mendoza Garfías of the Biodiversity I Photography Laboratory (LANABIO) for her support in obtaining images of SEM, and Montserrat Cervantes-Espinoza for her

help with obtaining photos of light microscopy. We also thank the following institutions for funding this research: PAPIIT-UNAM IA201720, IA203122, IN223924 and Consejo Nacional de Humanidades, Ciencias y Tecnologia CONAHCYT Fronteras de la Ciencia (139030) (FAT). ANFC is a student from Programa de Posgrado en Ciencias Biológicas, Universidad Nacional Autónoma de México (UNAM), and received fellowship with CVU 1146407 from CONAHCYT. FAT, GCR and TRR are members of Sistema Nacional de Investigadores-CONAHCYT.

Author Contributions

Alice Nelly Fernández-Campos (Conceptualization [equal], Data curation [equal], Formal analysis [equal], Investigation [equal], Methodology [equal], Software [equal], Validation [equal], Visualization [equal], Writing – original draft [equal], Writing – review and editing [equal]), Tonatiuh Ramírez-Reyes (Data curation [Equal], Formal analysis [Equal], Methodology [equal], Software [equal], Supervision [equal], Writing – original draft [equal], Thomas H Atkinson (Investigation [equal], Resources [equal], Writing – review and editing [equal]), Gerardo Rodríguez-Cuellar (Funding acquisition [equal], Investigation [equal], Resources [equal]), Francisco Armendáriz-Toledano (Conceptualization [equal], Data curation [equal], Formal analysis [equal], Funding acquisition [equal], Investigation [equal], Methodology [equal], Project administration [equal], Resources [equal], Software [equal], Supervision [equal], Validation [equal], Visualization [equal], Writing – original draft [equal], Writing – review and editing [equal]).

References

Armendáriz-Toledano F, García-Román J, López, MF, Sullivan, BT, and Zúñiga G. New characters and redescription of *Dendroctonus vitei* (Coleoptera: Curculionidae: Scolytinae). *Can. Entomol*. 2017:149:4:413-433.

Armendáriz-Toledano F, Niño A, Sámano JEM, and Zúñiga G. Review of the geographical distribution of *Dendroctonus vitei* (Curculionidae: Scolytinae) based on geometric morphometrics of the seminal rod. *Ann. Entomol. Soc.Am*. 2014:*107*:4:748-755.

Armendáriz-Toledano F, Niño A, Sullivan BT, Kirkendall LR, and Zúñiga GA. New species of bark beetle, *Dendroctonus mesoamericanu*s sp. nov.(Curculionidae: Scolytinae), in southern Mexico and Central America. *Ann. Entomol. Soc. Am*. 2015:108:3:403-414.

Atkinson TH and Equihua A. Notes on biology and distribution of Mexican and Central American Scolytidae (Coleoptera). II. Scolytinae: Cryphalini and Corthylini. *Coleopt. Bull*. 1985:355-363.

Atkinson TH, Flechtmann CA, and Petrov AV. Synopsis of the Neotropical Premnobiina (Coleoptera: Curculonidae: Scolytinae: Ipini) with descriptions of new species, new synonymy and keys to species. *Zootaxa*. 2023:5249(1):69-91.

Atkinson TH, Saucedo CE, Martínez FE, and Burgos SA. Coleópteros Scolytidae y Platypodidae asociados con las comunidades vegetales de clima templado y frío en el estado de Morelos. *Acta Zool. Mex*. 1986:17:1–58.

Atkinson TH. Escarabajos descortezadores y ambrosiales (Coleoptera: Curculionidae: Scolytinae, Platypodinae) de Sonora, México. *Dugesiana*. 2019:*26*(1):41-49.

Atkinson TH. Revisión del género *Phloeocleptus* (Coleoptera: Curculionidae: Scolytinae). *Rev. Mex. Biodiver*s. 2023:94(2):12.

Blackman MW. 1942. Revision of the genus *Phloeosinus* Chapuis in North America (Coleoptera, Scolytidae). *Proceedings of the United States National Museum*.

Burgos-Solorio A, and Atkinson TH. New species and new records of *Chaetophloeus* LeConte (Coleoptera: Curculionidae: Scolytinae) from Mexico. *Zootaxa*. 2022:5174(1):73-84.

Cervantes-Espinoza M, Cuellar-Rodríguez G, Alejandro Ruiz E, Atkinson TH, García Ochaeta JF,

Cervantes-Espinoza M, Ruiz A E, Cuellar-Rodríguez G, Castro-Valderrama U and Armendáriz-Toledano F. Immature stages of *Phloeosinus tacubayae* (Curculionidae: Scolytinae): morphology and chaetotaxy of larval pupae, sexual dimorphism of adults, and development time. *J. In. Sci*. 2023:23:6: 1-23.

Cibrián-Tovar D, Méndez-Montiel J T, Campos-Bolaños R, Yates III H O, and J. Flores-Lara. 1995. Insectos forestales de México/Forest Insects of Mexico. Universidad Autónoma de Chapingo, México: 453 p.

Cognato AI, and Sperling FA. Phylogeny of Ips DeGeer species (Coleoptera: Scolytidae) inferred from mitochondrial cytochrome oxidase I DNA sequence. *Mol. Phylogenet. Evol*. 2000:*14*:3:445-460.

Craighead F, George RST. A new technique in tree medication for the control of bark beetles. *Science*, 1930, 72: 433–435. https://doi.org/10.1126/science.72.1869.433

Cristóvão JP, Lyal CHC. Anchonini in Africa: new species and genus confirming a transatlantic distribution (Coleoptera: Curculionidae: Molytinae). *Diversity*. 2018:10:3:82.

Darriba D, Taboada GL, Doallo R, and Posada D. jModelTest 2: more models, new heuristics and high-performance computing. *Nat. methods*. 2012:9(8):772.

Dayrat B. Towards integrative taxonomy. *Biol. J. Linn.Soc.*, 2005, vol. 85, no 3, p. 407-417.

Dole SA, Jordal BH, and Cognato AI. Polyphyly of Xylosandrus Reitter inferred from nuclear and mitochondrial genes (Coleoptera: Curculionidae: Scolytinae). *Mol. Phylogenet. Evol*. 2010:*54*(3):773-782.

Eaton DAR, Overcast I. ipyrad: Interactive assembly and analysis of RADseq datasets, *Bioinformatics*, Volume 36, Issue 8, April 2020, Pages 2592–2594, https://doi.org/10.1093/bioinformatics/btz966

Estrada-Castillón E, Villarreal-Quintanilla JA, Salinas-Rodríguez MM; Encina-Domínguez JA, Cantú-Ayala CM, González-Rodríguez H, Jiménez-Pérez J. 2014. Coníferas de Nuevo León, México; Universidad Autónoma de Nuevo León: Nuevo León, México.

Faccoli M, and Sidoti A. Description of *Phloeosinus laricionis* sp. n. (Coleoptera: Curculionidae, Scolytinae), a new bark beetle species from southern Europe. *Zootaxa*. 2013:*3722(*1):92-100.

Fettig CJ. 2016. Native Bark Beetles and Wood Borers in Mediterranean Forests of California In Lieutier F, Paine TD (Eds.) Insects and diseases of Mediterranean forest systems Switzerland. Springer International Publishing, Cham, Switzerland. 499–528. https://doi.org/10.1007/978-3-319-24744-1_18

Fitzhugh K. The inferential basis of species hypotheses: the solution to defining the term ‘species’. *Mar. Ecol*. 2005:26(3-4):155-165.

Foelker CJ, Hofstetter RW. Heritability, fecundity, and sexual size dimorphism in four species of bark beetles (Coleoptera: Curculionidae: Scolytinae). *Ann. Entomol. Soc. Am.* 2014:107(1):143-151.

García-Román J, Armendáriz-Toledano F, Valerio-Mendoza O, and Zúñiga G. An assessment of old and new characters using traditional and geometric morphometrics for the identification of *Dendroctonus approximatus* and *Dendroctonus parallelocollis* (curculionidae: Scolytinae). *J. Insect Sci.* 2019:19(1):14.

García-Román J, Ramírez-Reyes T, Armendáriz-Toledano F. The spermatheca in the genus *Dendroctonus* (Curculionidae: Scolytinae): morphology, nomenclature, potential characters for taxonomic use and phylogenetic signal. *Rev. Mex. Biodivers.* 2022:93.

Godefroid M, Meseguer AS, Sauné L, Genson G, Streito JC, Rossi JP, Zaldivar-Riverón A, Mayer F, Cruaud A. and Rasplus JY. Restriction-site associated DNA markers provide new insights into the evolutionary history of the bark beetle genus *Dendroctonus. Mol. Phylogenet. Evol*, 2019:139*:*106528.

Guindon S, Dufayard JF, Lefort V, Anisimova M, Hordijk W, and Gascuel O. New algorithms and methods to estimate maximum-likelihood phylogenies: assessing the performance of PhyML 3.0. *Syst. Biol*. 2010:59(3):307-321.

Gültekin L, Lyal CHC. Two new Larinus Dejean (Coleoptera: Curculionidae) species descriptions from India with taxonomic overview. *J. Insect Biodivers*. 2020:20(2):59-67.

Hamilton WD. 1979. Wingless and fighting males in fig wasps and other insects in Sexual selection and reproductive competition in insects (ed. Blum, MS and Blum, NA) 167–220.

Hammer Ø, and Harper DA. Past: paleontological statistics software package for education and data analysis. *Palaeontol. Electron.* 2001:*4*(1):1.

Hennig, W. 1999. *Phylogenet. Syst*. University of Illinois Press.

Hernández-García JA, Cuellar-Rodríguez G, and Armendáriz-Toledano F. Phylogenetic position of *Geosmithia* spp.(Hypocreales) living in *Juniperus* spp. forests (Cupressaceae) with bark beetles of *Phloeosinus* spp.(Scolytinae) from the northeast of Mexico. *Forests*, 2020:11(11):1142.

Hoang DT, Chernomor O, Von Haeseler A, Minh BQ, and Vinh LS. UFBoot2: improving the ultrafast bootstrap approximation. *Mol. Biol. Evol.* 2018:35(2):518-522.

Hopkins AD. *Notes on some Mexican Scolytidae: with descriptions of some new species*. 1905.

Huelsenbeck JP, Ronquist F. MRBAYES: Bayesian inference of phylogenetic trees. *Bioinformatics*. 2001:17(8):754-755.

Hulcr J, Atkinson TH, Cognato A I, Jordal BH, and McKenna DD. (2015). Morphology, taxonomy, and phylogenetics of bark beetles. In *Bark Beetle* (pp. 41-84). Academic Press. Hulcr J, Mogia M, Isua B, and Novotny V. Host specificity of ambrosia and bark beetles (Col., Curculionidae: Scolytinae and Platypodinae) in a New Guinea rainforest. *Ecol. Entomol*. 2007:32(6):762-772.

Johnson AJ, Hulcr J, Knížek M, Atkinson TH, Mandelshtam MY, Smith SM, Cognato I, Park S, Li Y, and Jordal NH. Revision of the Bark Beetle Genera Within the Former Cryphalini (Curculionidae: Scolytinae), *Insect Syst. Divers*, 2020:4(3):1. https://doi.org/10.1093/isd/ixaa002

Jombart T, and Ahmed I. *adegenet 1.3-1*: new tools for the analysis of genome-wide SNP data, *Bioinformatics*. 2011: 27(21):3070–3071, https://doi.org/10.1093/bioinformatics/btr521

Jordal BH. 2007. Reconstructing the phylogeny of Scolytinae and close allies: major obstacles and prospects for a solution. In: Bentz, Barbara; Cognato, Anthony; Raffa, Kenneth, eds. Proceedings from the Third Workshop on Genetics of Bark Beetles and Associated Microorganisms. Proc. RMRS-P-45. Fort Collins, CO: US Department of Agriculture, Forest Service, Rocky Mountain Research Station. p. 3-9 (Vol. 45).

Jordal BH. Glostatina, a new xyloctonine subtribe for Glostatus (Coleoptera: Curculionidae), based on clear genetic and morphological differences. 2023.

Kirkendall LR; Biedermann PH, Jordal BH. 2015. Evolution and diversity of bark and ambrosia beetles. En *Bark beetles*. Academic Press. p. 85-156.

Knaus BJ, Grünwald NJ. vcfr: a package to manipulate and visualize variant call format data in R. *Molecular ecology resources*, 2017, vol. 17, no 1, p. 44-53.

Knížek M. Scolytinae. In: Löbl I., Smetana A. (eds.), Catalogue of Palearctic Coleoptera, 2011, Vol. 7: 86-87, 204-251. Apollo Books, Stenstrup, 373 p.

Košťál, M. Nanophryodotus gen. n. from South Africa, with three new species. *Koleopterol. Rundsch,* 2018:92:195-208.

López-Buenfil JA, Valdez-Carrasco J, Equihua-Martinez A, Burgos-Solorio A. El proventrículo como estructura para identificar géneros mexicanos de Scolytidae (Coleoptera*). Soc. Mex. Entomol*. 2001.

Lukhtanov VA. Species delimitation and analysis of cryptic species diversity in the XXI century. *Entomol. Rev*. 2019:*99:*463-472.

Mandelshtam MY, Yakushkin EA, Kovalenko YN, and Petrov AV. New Invasive Hypothenemus Westwood, 1834 (Coleoptera, Curculionidae: Scolytinae) Species in the Caucasus and in the Southern Primorskii Territory, Russia. *Entomol. Rev*. 2022:102(4):485-491.

Mayden RL. 1997. A hierarchy of species concepts: the denouement in the saga of the species problem. In M. F. Claridge, H. A. Dawah and M. R. Wilson (eds.), Species: The units of diversity, Chapman and Hall. pp. 381–423

Mayr E. 1963. *Animal species and evolution*. Harvard University Press.

McNichol BH, Sullivan BT, Munro HL, Montes CR, Nowak JT, Villari C, and Gandhi KJ. Density-dependent variability in an eruptive bark beetle and its value in predicting outbreaks. *Ecosphere*. 2021:12(1).

Minh BQ, Schmidt HA, Chernomor O, Schrempf D, Woodhams MD, Von Haeseler A, and Lanfear R. IQ-TREE 2: new models and efficient methods for phylogenetic inference in the genomic era. *Mol. Biol. Evol*. 2020:37(5):1530-1534.

Ospina-Garcés SM, Ibarra-Juarez LA, Escobar F, and Lira-Noriega A. Evaluating sexual dimorphism in the ambrosia beetle *Xyleborus affinis* (Coleoptera: Curculionidae) using geometric morphometrics. *Fla. Entomol*, 2021:*104*(2):61-70.

Pérez-Silva M, Equihua-Martínez A, Atkinson TH, Romero-Nápoles J, and López-Buenfil JA. Claves ilustradas para la identificación de géneros y especies de la tribu Xyleborini (Curculionidae: Scolytinae) de Mexico. *Rev. Mex. Biodivers.* 2021:92.

Pistone D, Gohli J and Jordal BH. Molecular phylogeny of bark and ambrosia beetles (Curculionidae: Scolytinae) based on 18 molecular markers. *Syst. Entomol*. 2018:43(2):387-406.

Pureswaran DS, Hofstetter RW, Sullivan BT, Grady AM, and Brownie C. Western pine beetle populations in Arizona and California differ in the composition of their aggregation pheromones. *J. Chem. Ecol*. 2016:42:404-413.

Ramírez-Reyes T, Armendáriz-Toledano F, and Cuellar-Rodríguez L. Rearranging and completing the puzzle: Phylogenomic analysis of bark beetles *Dendroctonus* reveals new hypotheses about genus diversification. *Mol. Phylogenet. Evol*. 2023:187:107885.

Rohlf FJ. TpsDig, version 1.4, Software, Department of Ecology and Evolution, State University of New York, Stony Brook, NY 11794–5245. *Available in http://life. bio. sunysb. edu/morph (accessed 29 Oct. 2016)*, 2004.

Schedl KE. Some bark and ambrosia beetles from the Tres Maria Islands, Mexico. 143 Contribution. *Pan-Pac. Entomol.* 1956:32:30–32.

Sheets HD. 2003. IMP-integrated morphometrics package. Department of Physics, Canisius Collegue, Buffalo, NY. Available from http://www3.canisius.edu/_sheets/imp7.htm

Stauffer C. Phylogenetic relationships of the bark beetle species of the genus Ips DeGeer. *Insect Mol Biol.* 1997:6:233-240.

Sullivan BT, Grady AM, Hofstetter RW, Pureswaran DS, Brownie C, Cluck D, Coleman TW, Graves A, Willhite E, Spiegel L, Scarbrough D, Orlemann A, and Zúñiga G. Evidence for semiochemical

divergence between sibling bark beetle species: *Dendroctonus brevicomis* and *Dendroctonus barberi*. *Journal of chemical ecology*. 2021:47:10-27.

Valerio-Mendoza O, García-Román J, Becerril M, Armendáriz-Toledano F, Cuéllar-Rodríguez G, Negrón JF, Sullivan BT, and Zúñiga G. Cryptic species discrimination in western pine beetle, *Dendroctonus brevicomis* LeConte (Curculionidae: Scolytinae), based on morphological characters and geometric morphometrics. *Insects*. 2019:10(11):377.

Victor J, and Zuniga G. Phylogeny of *Dendroctonus* bark beetles (Coleoptera: Curculionidae: Scolytinae) inferred from morphological and molecular data. *Syst. Entomol*, 2016:41(1):162-177.

Wood SL, and Bright DE. 1992. A catalog of Scolytidae and Platypodidae (Coleoptera). part 2: taxonomic index. *Great Basin Nat. Mem.* Vol. 13, p. 1-1553.

Wood SL. 1982 The bark and ambrosia beetles of North and Central America (Coleoptera: Scolytidae), a taxonomic monograph. *The Great Basin Naturalist Memoirs.* 6, 1–1359.

Wood SL. 1986. New synonymy and new species of American bark beetles (Coleoptera: Scolytidae), Part XI. *Great Basin Nat*, p. 265-273.

Young MK, Smith RJ, Pilgrim KL, Fairchild MP and Schwartz MK. Integrative taxonomy refutes a species hypothesis: The asymmetric hybrid origin of *Arsapnia arapahoe* (Plecoptera, Capniidae). *Ecol. Evol*. 2019:9(3):1364-1377.

Figures

Figure 1. Characters associated from the head in *Phloeosinus.* **(A)** Color head of *P. baumanni*, "black". **(B)** Color head of *P. deleoni*, "brown". **(C)** Color head in lateral of *P. serratus* "reddish brown". **(D)** Size of head pubescence of *P. tacubayae.* **(E)** Size of head pubescence of *P. deleoni.* **(F)** Size of head pubescence of *P. serratus.* **(G)** Frons sculpting pattern of *P. deleoni.* **(H)** Frons sculpting pattern of *P. serratus.* **(I)** Frons sculpting pattern of *P. baumanni.* White arrows indicate the frons patterns sculpture.

Figure 2. Frons vestiture pattern. **(A)** *P. deleoni,* abundant distributed heterogeneously. **(B)** *P. taxodii taxodiicolens,* sparsely distributed heterogeneously. **(C)** *P. serratus,* sparsely distributed

homogeneously. **(D)** *P. tacubayae,* abundant distributed homogeneously. Doted lines indicate the vestiture patterns on frons.

Figure 3. Vestiture pattern and pubescence size of the epistomal margin. **(A)** Female of *P. serratus,* abundant and uniformly covering entirely the epistomal margin. **(B)** Female of *P. tacubayae* abundant and uniformly covering entirely the epistomal margin. **(C)** Male of *P. taxodii taxodiicolens*. **(D)** Male of *P. deleoni* sparse, showing some areas without pubescence.

Figure 4. Pronotum and elytra color. **(A)** Male of *P. cristatus* "black". **(B)** Male of *P. tacubayae* "brown". **(C)** Male of *P. arizonicus* "dark brown". **(D)** Male of *P. deleoni* "reddish brown ". **(E)** Male of *P. baumanni* "yellowish brown".

Figure 5. Characters associated with sculpture and vestiture of elytra. **(A)** Male of *P. tacubayae,* elytral disc vestiture "abundant". **(B)** Male of *P. taxodii taxodiicolens,* elytral disc vestiture "sparse". **(C)** Male of *P. serratus,* size of the elytral disc pubescence "long". **(D)** Male of *P. deleoni,* size of the elytral disc pubescence "short". **(E)** Male of *P. taxodii taxodiicolens,* size of the elytral disc pubescence "short and long". **(F)** Female of *P. serratus,* vestiture of the elytral declivity "abundant". **(G)** Female of *P. deleoni* vestiture of the elytral declivity "sparse". **(H)** Male of *P. deleoni,* the elytral declivity with "hairs". **(I)** Female of *P. deleoni,* the elytral declivity with "only scales". **(J)** Male of *P. tacubayae,* the elytral declivity with "hairs and scales". **(K)** Male of *P. arizonicus,* pattern of sculpture and vestiture of elytral declivity interstriae II "glabrous". **(L)** Female of *P. serratus,* elytral declivity interstriae II with "hairs". **(M)** Male of *P. serratus,* elytral declivity interstriae II with "scales". **(N)** Male of *P. taxodii taxodiicolens,* elytral declivity interstriae II with "scales and hairs". **(O)** Male of *P. deleoni,* elytral declivity interstriae II with "teeth".

Figure 6. Characters of body measurements of male of *P. baumanni*. **(A)** Dorsal view. **(B)** Ventral view, **(C)** Lateral view. Attribute acronyms are present in methods.

Figure 7. Scatter plots from multivariate analyses using quantitative and qualitative characters. **(A)** Linear discriminant analysis from males and females from 24 quantitative characters. **(B)** Principal

coordinate analysis for males and females from 38 characters. **(C)** Principal component analysis from 6 quantitative characters from sternite IX of females. **(D**) Linear discriminant analysis from 6 quantitative characters from sternite IX of females. **Abbreviations: AB,** angle of base; **DA,** distance between the arch; **DALMP,** distance between lateral apices of posterior margin; **DSC,** distance between the central silks; **LMPA,** length of the posterior to anterior margin; **LPA,** length of the anterior projection; **NCM-DED**, number of crenulations on the right elytral disc margin; **NCM-DEI**, number of crenulations on the left elytral disc margin; **NDI1-DED**, number of dentitions in interstriae I of right elytral declivity; **NDI1-DEI**, number of dentitions in interstriae I of left elytral declivity; **NDI3-DED**, number of dentitions in interstriae III of right elytral declivity; **NDI3-DEI**, number of dentitions in interstriae III of left elytral declivity. Arrows indicate the characters that most influenced in the variation.

Figure 8. Scatter plots of multivariate analyses of body shape structures in *Phoeosinus*. **(A)** Scatter plot of the first and second relative warps with respective deformations grids of males pronotum shape. **(B)** Scatter plot from linear discriminant analysis of male pronotum shape. **(C)** Scatter plots of the first and second relative warps with respective deformations grids of male elytra shape. **(D)** Scatter plot from linear discriminant analysis of male elytra shape. **(E)** Scatter plots of the first and second relative warps with respective deformations grids of female sternite IX shape. **(F)** Scatter plot from linear discriminant analysis of female sternite IX shape. The shape configurations to the right of the graphs represent the mean of each species evaluated.

Figure 9. Scatter plots from multivariate analysis of phenotypic variation among the populations of *P. serratus.* **(A)** Linear discriminant analysis of females and males from 24 quantitative characters. **(B)** Principal coordinate analysis of females and males from 38 quantitative and qualitative characters. **(C)** First and second relative warps with respective deformations grids of male pronotum shape. **(D)** Linear discriminant analysis of male pronotum shape. **(E)** First and second relative warps with respective deformations grids of male elytra shape. **(F)** Linear discriminant analysis of male elytra shape. **(G)** First and second relative warps with respective deformations grids of female sternite IX shape. **(H)**

Linear discriminant analysis of female sternite IX shape. The shape configurations to the right of the graphs represent the mean of each population evaluated.

Figure 10. Principal component analysis of 3,031 SNP's variation. The color points represent each species.

Figure 11. Maximum likelihood phylogenetic tree inferred with IQTREE from the larger matrix (137,897 characters). Bootstrap support values are on branches.

Table 1. Locations, geographical coordinates, and host for examined specimens of *Phloeosinus.*

Specie	Country	State and Municipalty	Latitude	Longitude	Genus host	Species host
P. tacubayae	Mexico	Nuevo Leon, Galeana	24.8223611	-100.084333	*Hesperocyparis*	*lusitanica*
	Mexico	Edo. Mex, Chapingo	19.4806472	-98.865225	*Cupressus*	sp
P. deleoni	Mexico	Nuevo Leon, Galeana	24.8254611	-100.077367	*Juniperus*	*flaccida*
	Mexico	Oaxaca, San Juan Bautista, Coixtlahuaca	17.65	-97.2768611	*Juniperus*	*flaccida*
P. baumanni	Mexico	Michoacan, Patzcuaro	19.5225806	-101.610167	*Hesperocyparis*	*lusitanica*
	Mexico	Iztaccihuatl-Amecameca	19.1727167	-98.6410556	*Hesperocyparis*	*lusitanica*
	Mexico	Edo. Mex, Texcoco	19.4912	-98.88	*Hesperocyparis*	*lusitanica*
P. cristatus	Mexico	Coahuila, Arteaga	-	-	*Cupressus*	*arizonica*
	Mexico	Chihuahua, Urique	-	-	*Cupressus*	*arizonica*
	USA	Oak Creek, AZ.	-	-	-	-
P. arizonicus	Mexico	Coahuila, Saltillo	25.3451	-101.0289	*Cupressus*	*arizonica*
P. spinosus	USA	Oak Creek, AZ.	-	-	*Cupressus*	*glabra*
P. taxodii taxodiicolens	Mexico	Edo. Mex, Texcoco	19.4912	-98.88	*Taxodium*	*mucronatum*
P. serratus	Mexico	Nuevo Leon, Galeana	24.49	-100.07	*Cupressus*	*arizonica*
Phloeosinus serratus	Mexico	Nuevo Leon, Galeana	24.8596667	-100.360333	*Juniperus*	*coahuilensis*
Phloeosinus serratus	Mexico	Nuevo Leon, Aramberri	24.8223611	-100.084333	*Juniperus*	*saltillensis*

Table 2. Multivariate analyses results.

Origin of characters	Number of characters analyzed	Type of analysis	Samples	Number of samples analyzed (n)	PC1 / AXIS 1	PC2 / AXIS 2	PC3 / AXIS 3	Total variation	MANOVA test

External morphology	24 quantitative	PCA/LDA*	♀♂	133	75.25%	15.33%	5.30%	95.88%	p= 1.411E-63
					52.10%	**18.78 %**	**13.10 %**	**83.98%**	
			♀	56	67.35%	14.01%	9.77%	91.13%	p= 1.07E-25
					60.39%	**13.73 %**	**11.63 %**	**85.75%**	
			♂	77	73.58%	15.41%	6.19%	95.18%	p= 6.28E-50
					45.21%	**26.62 %**	**11.84 %**	**83.67%**	
	38 quantitative and qualitative	PCoA	♀♂	133	31.33%	9.25%	5.93%	46.51%	p= 9.336E-107
			♀	56	33.98%	10.84%	7.96%	52.78%	p= 1.122E-241
			♂	77	38%	9.69%	7.66%	55.35%	p= 0

* The values highlighted in black correspond to the linear discriminant analyses.

Table 3. Analyses results from body shape study.

Origin of characters	Type of análisis	Samples	Number of samples analyzed (n)	RW1 / AXIS 1	RW2 / AXIS 2	RW3 / AXIS 3	Total variation	ANOSIM test
Pronotum	PCA/LDA*	♀	56	61.03%	16.67%	9.05%	86.75%	p=0.0001
				61.96%	**16.71%**	**10.26%**	**88.93%**	
		♂	77	74%	10.66%	7.24%	91.90%	p=0.0001
				52.83%	**10.08%**	**14.13%**	**77.04%**	
Elytra	PCA/LDA*	♀	56	65.32%	19.16%	10.34%	94.82%	p=0.002
				79.97%	**10.33%**	**5.89%**	**96.19%**	
		♂	77	55.35%	22.49%	11.28%	89.12%	p= 0.0001
				69.97%	**12.55%**	**6.89%**	**89.41%**	

* The values highlighted in black correspond to the linear discriminant analyses.

Table 4. Matrix with support of each analyses applied.

Method	Characters or structructure analyzed	Analysis applied	Samples	SPECIES HYPOTHESIS							
				P. baumanni	*P. tacubayae*	*P. deleoni*	*P. serratus*	*P. taxodii taxodiicolens*	*P. cristatus*	*P. spinosus*	*P. arizonicus*
Traditional morphometry	38 quantitative and qualitative characters from external morphology	PCA/LDA quantitative	♀♂	x		x	x	X	x	NA	NA
			♀	x	x	x	x	X	x	NA	NA
			♂	x		x	x	X	x	x	x
		PCoA quantitative and qualitative	♀♂		x			X		NA	NA
			♀		x			X		NA	NA
			♂		x			X		x	x
	6 quantitative characters from sternite IX	PCA/LDA	♀	x	x	x	x	X		NA	NA
Body	Pronotum	PCA/LDA	♀	x						NA	NA

Shape Geometric morphometry			♂	x				X	x		
	Elytra		♀	x	x	x			x	NA	NA
			♂	x		x		X			
	Sternite IX		♀	x	x	x	x	X	NA	NA	NA
Phylogenetic inference	RaxML	ML	♀♂	x	x	x	x	NA	NA	NA	NA
	Mr.Bayes	BI		x	x	x	x	NA	NA	NA	NA

Note: The "x" indicates for which character matrix and analysis each species is supported.
"NA" indicates that there were no samples for that analysis.

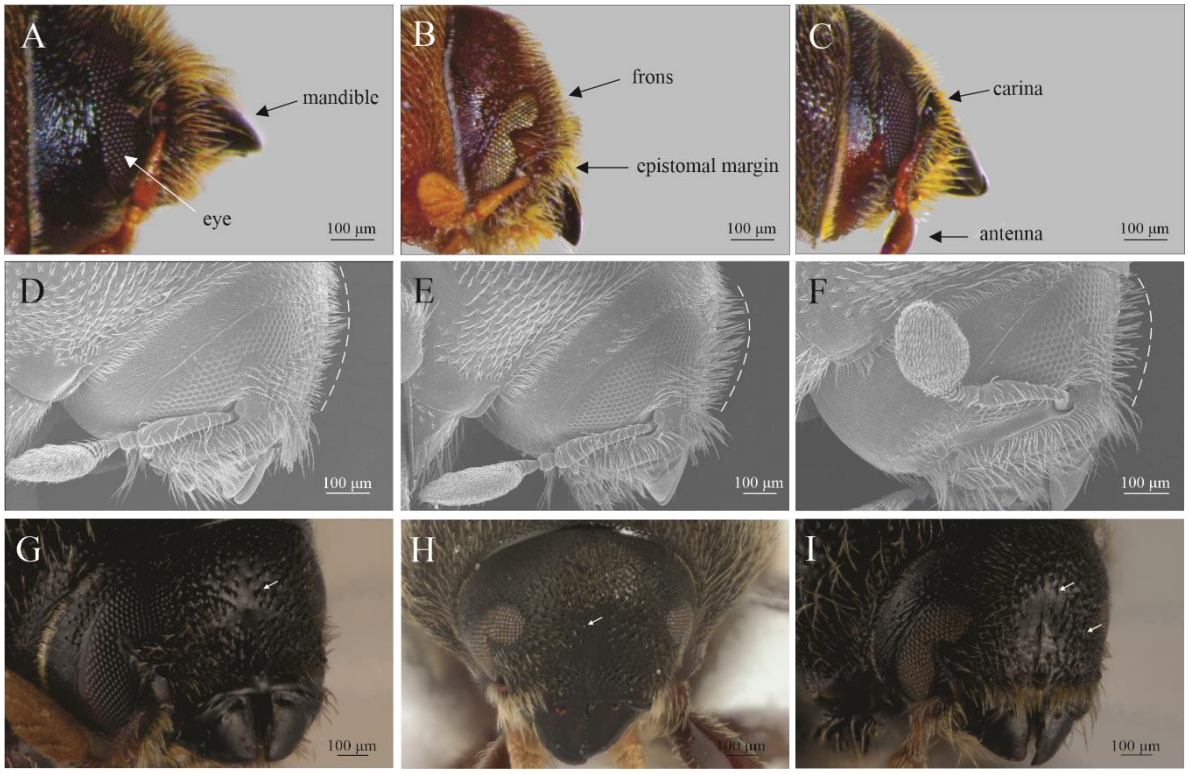

Figure 1

Figure 2

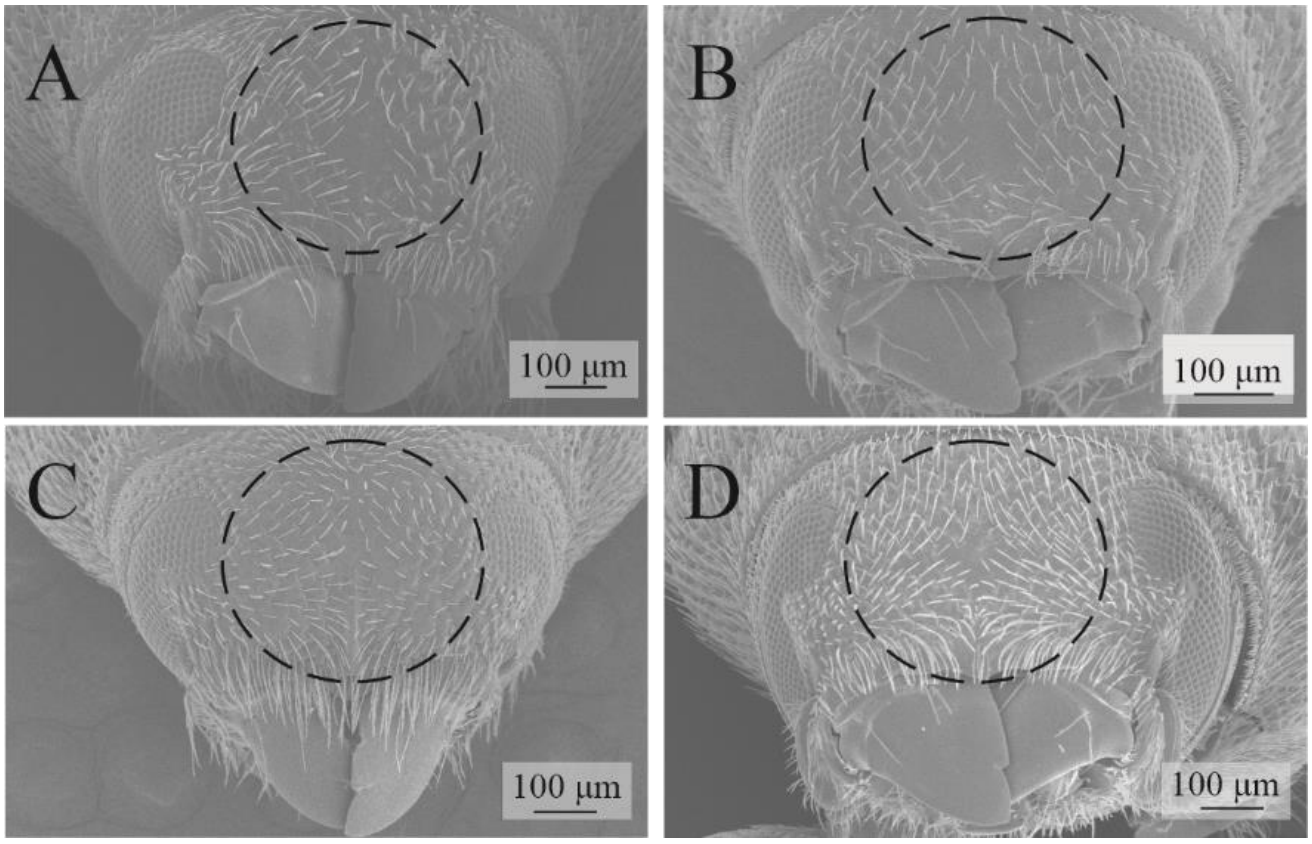

Figure 3

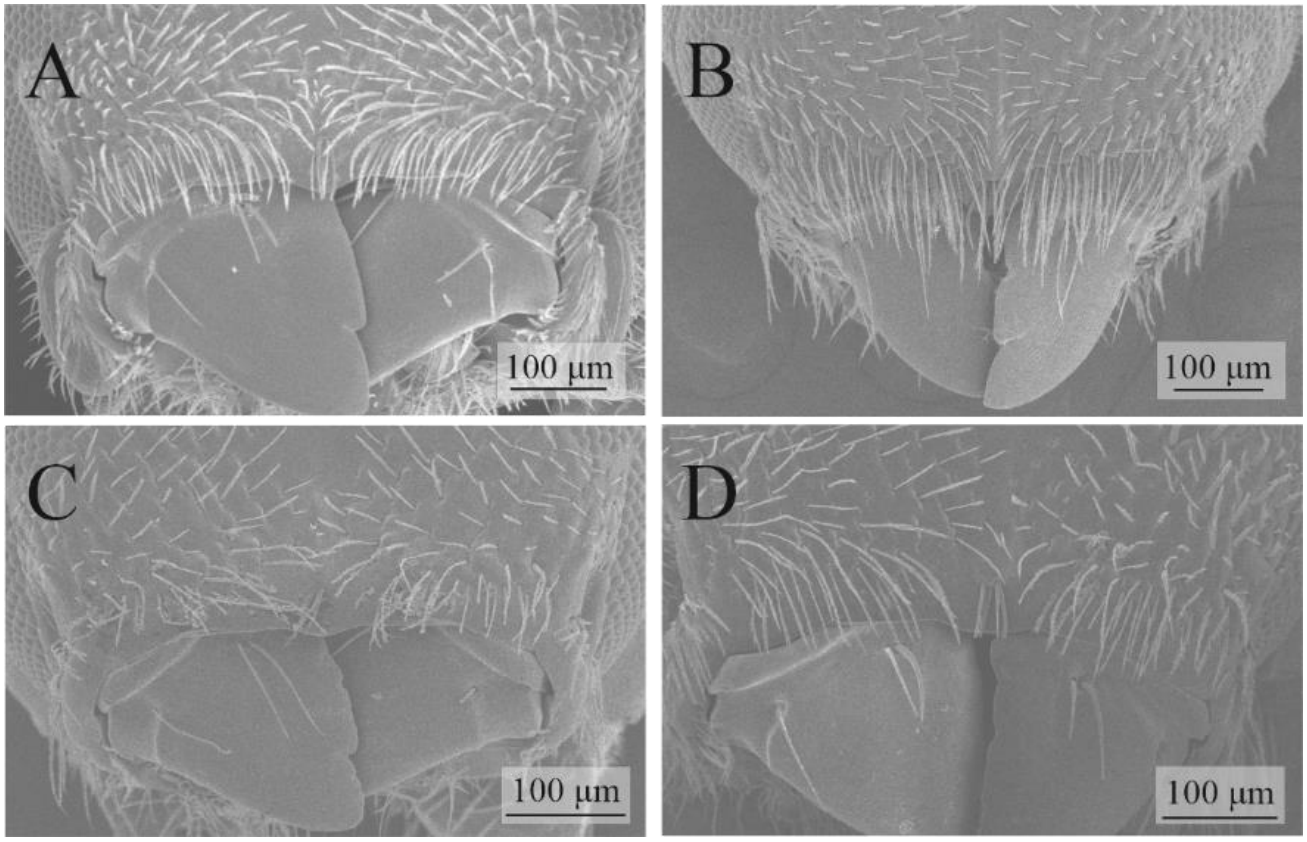

Figure 4

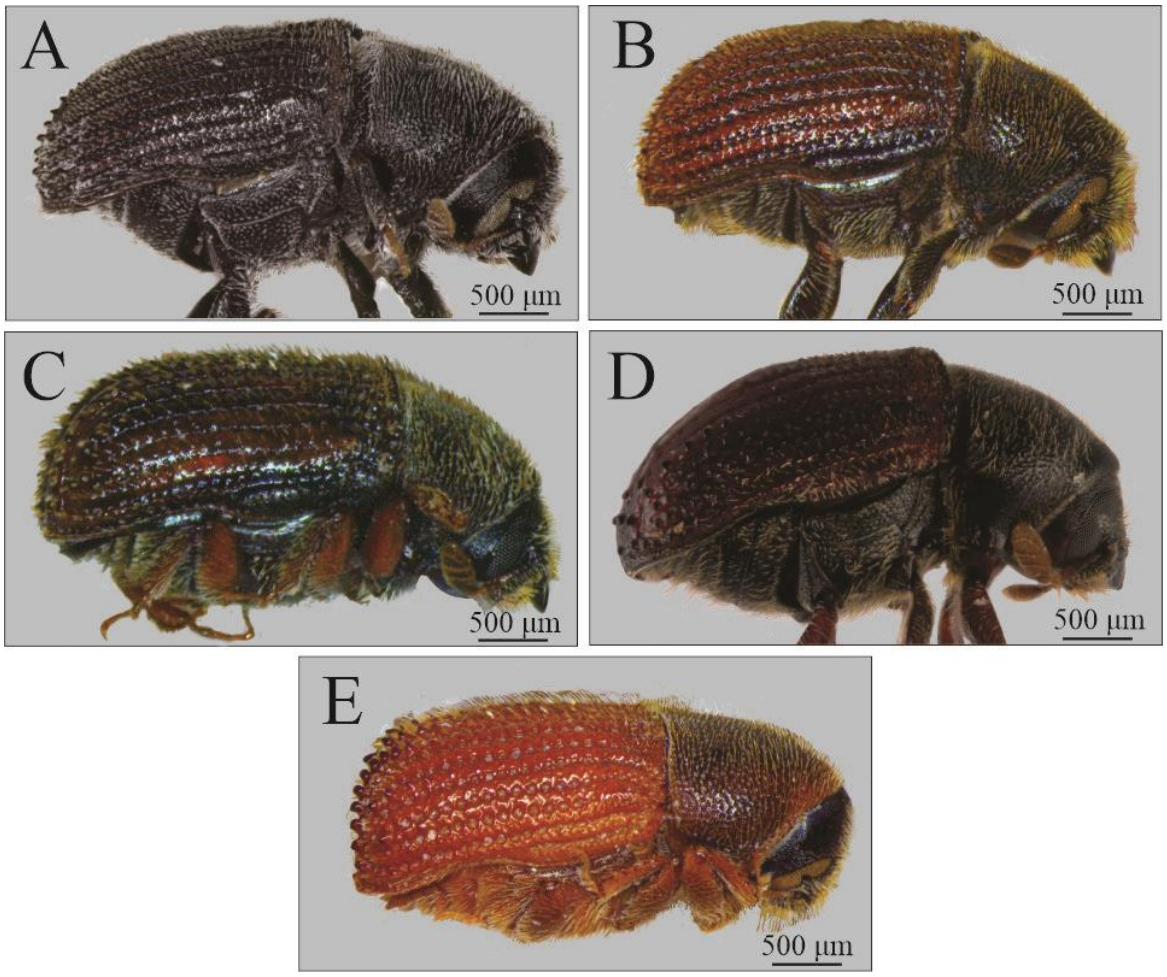

Figure 5

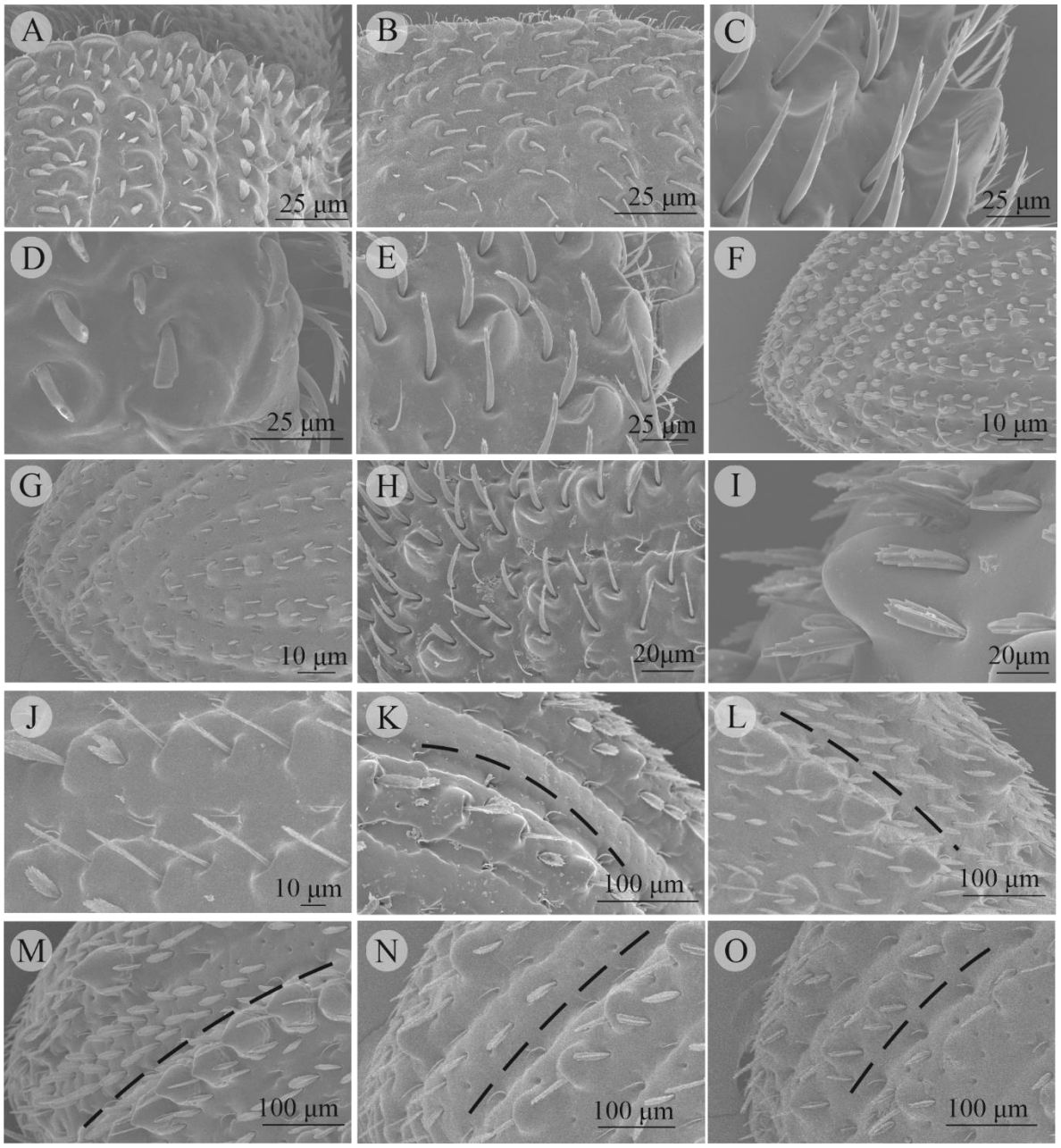
A
25 µm
B
25 µm
C
25 µm
D
25 µm
E
25 µm
F
10 µm
G
10 µm
H
20µm
I
20µm
J
10 µm
K
100 µm
L
100 µm
M
100 µm
N
100 µm
O
100 µm

Figure 6

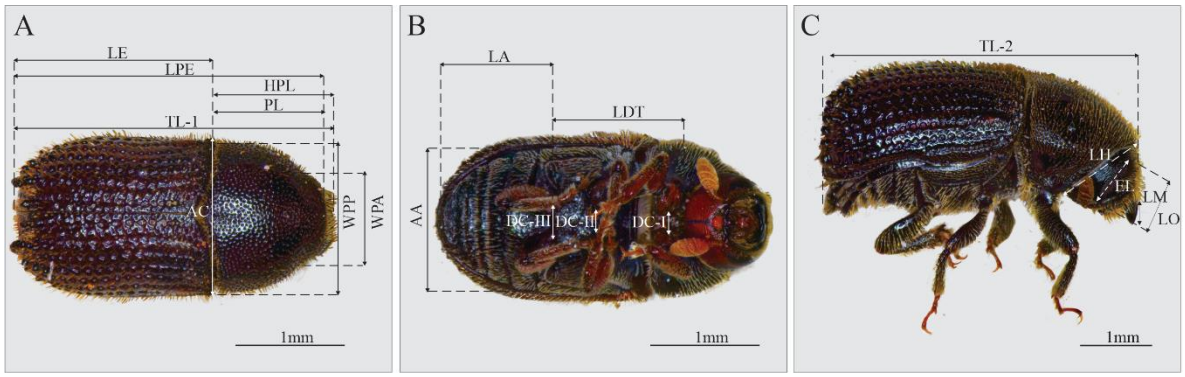

Figure 7

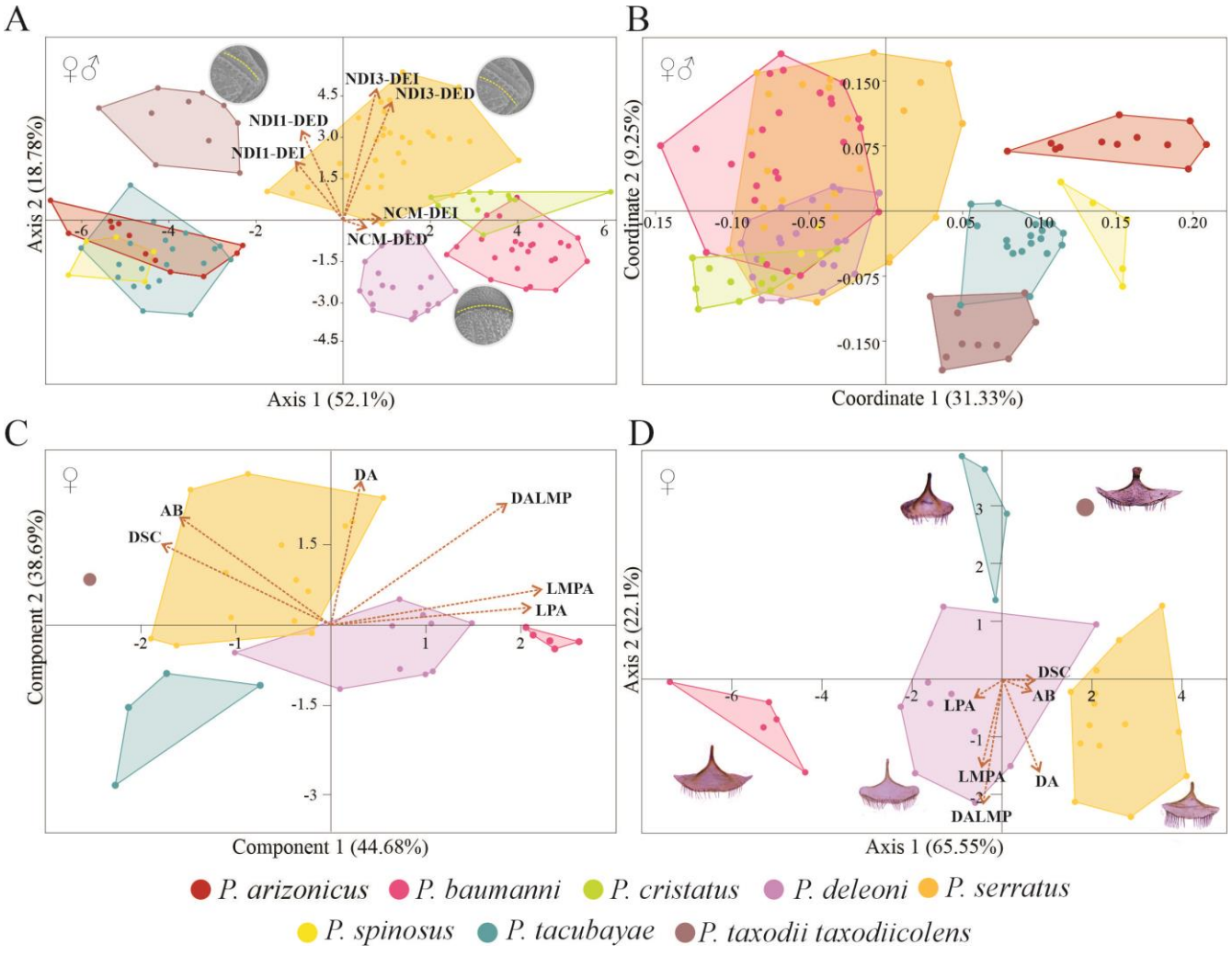

Figure 8

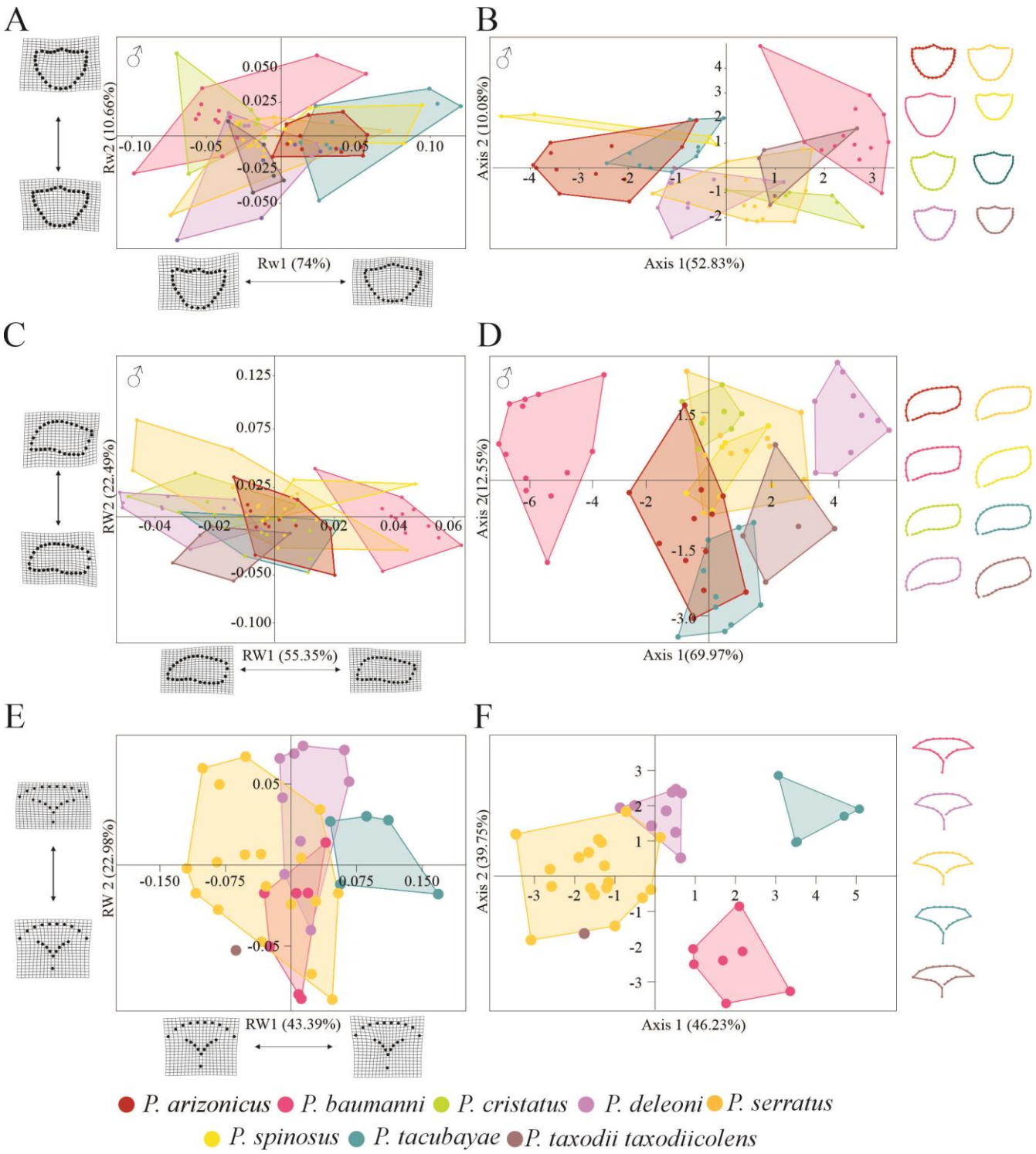
A
B
C
D
E
F
♂
Rw2 (10.66%)
Rw1 (74%)
Axis 2 (10.08%)
Axis 1(52.83%)
RW2 (22.49%)
RW1 (55.35%)
Axis 2(12.55%)
Axis 1(69.97%)
RW 2 (22.98%)
RW1 (43.39%)
Axis 2 (39.75%)
Axis 1 (46.23%)
P. arizonicus
P. baumanni
P. cristatus
P. deleoni
P. serratus
P. spinosus
P. tacubayae
P. taxodii taxodiicolens

Figure 9

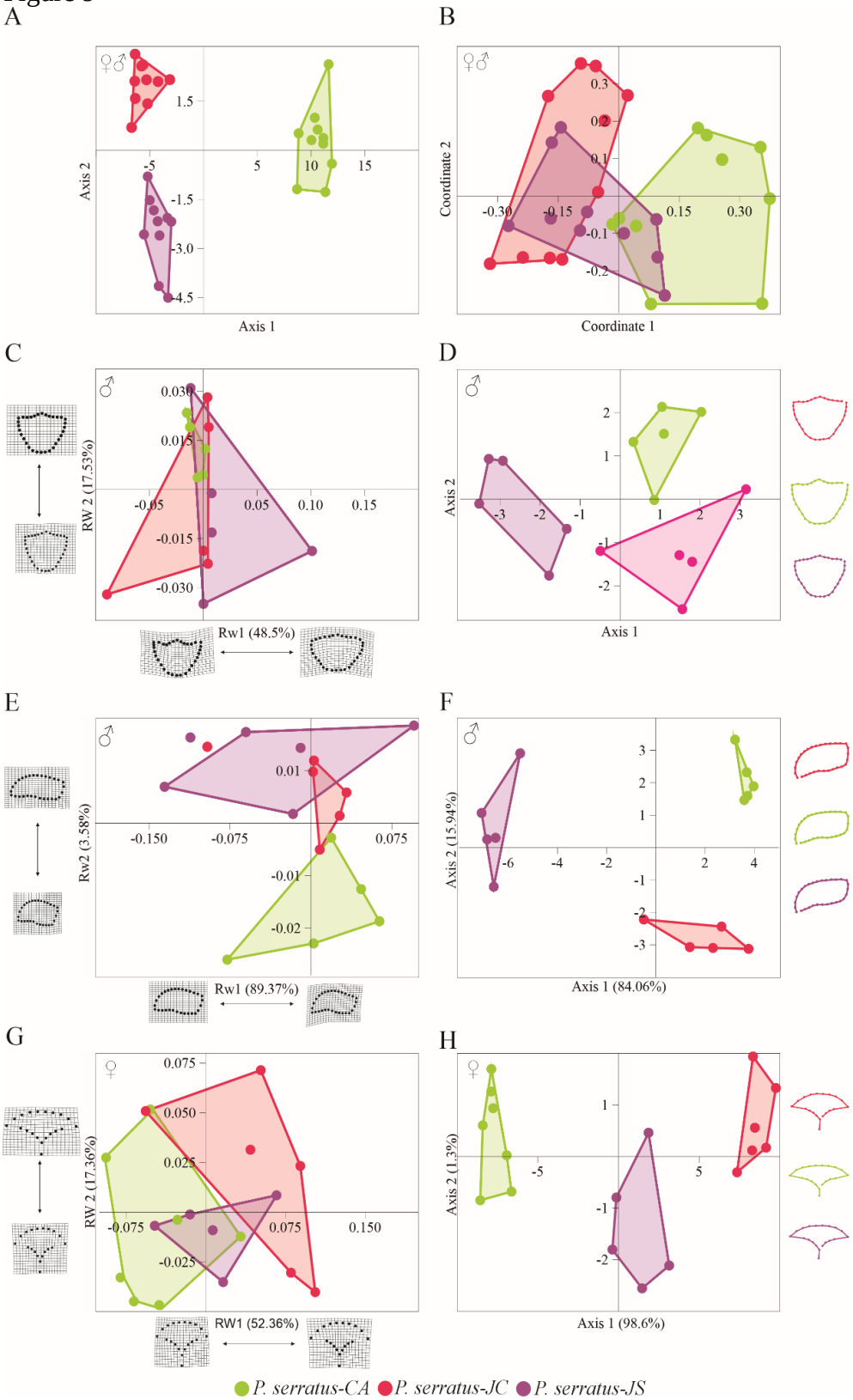

Figure 10

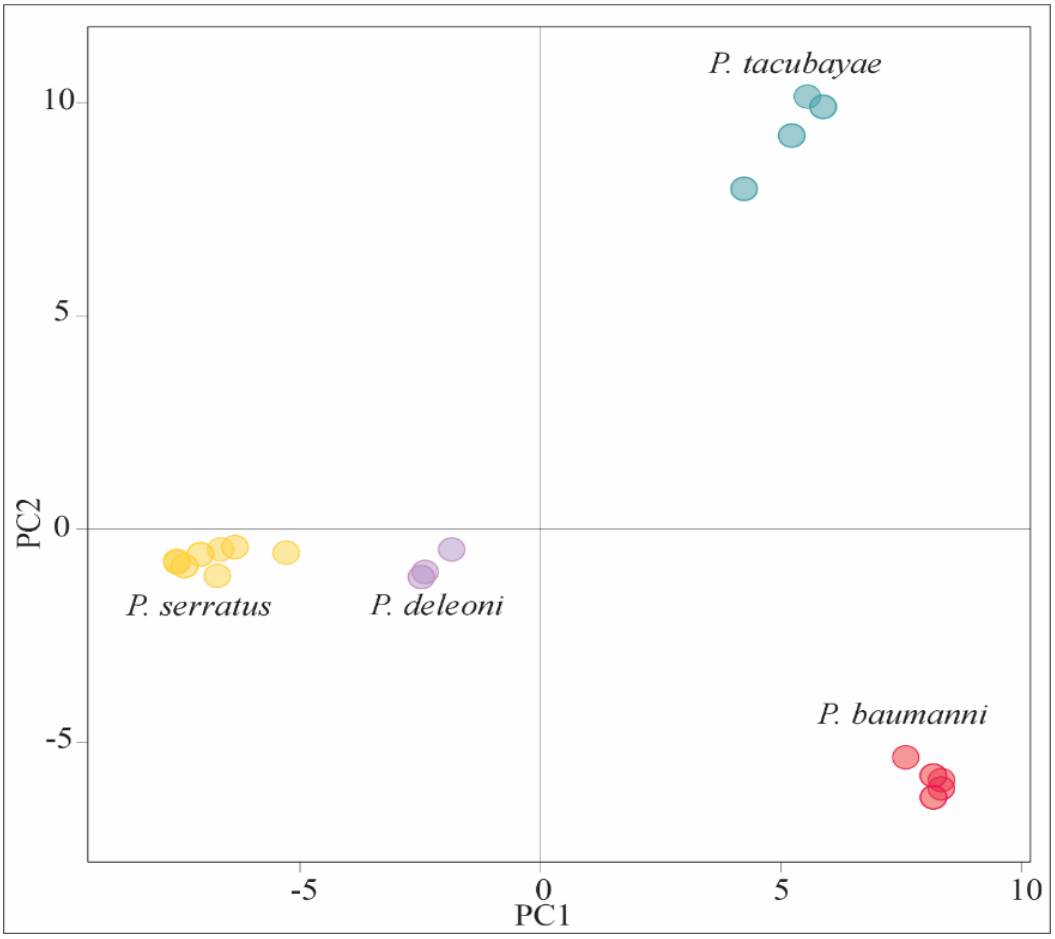
P. tacubayae
P. serratus
P. deleoni
P. baumanni
PC1
PC2
10
5
0
-5
-5
0
5
10

Figure 11.

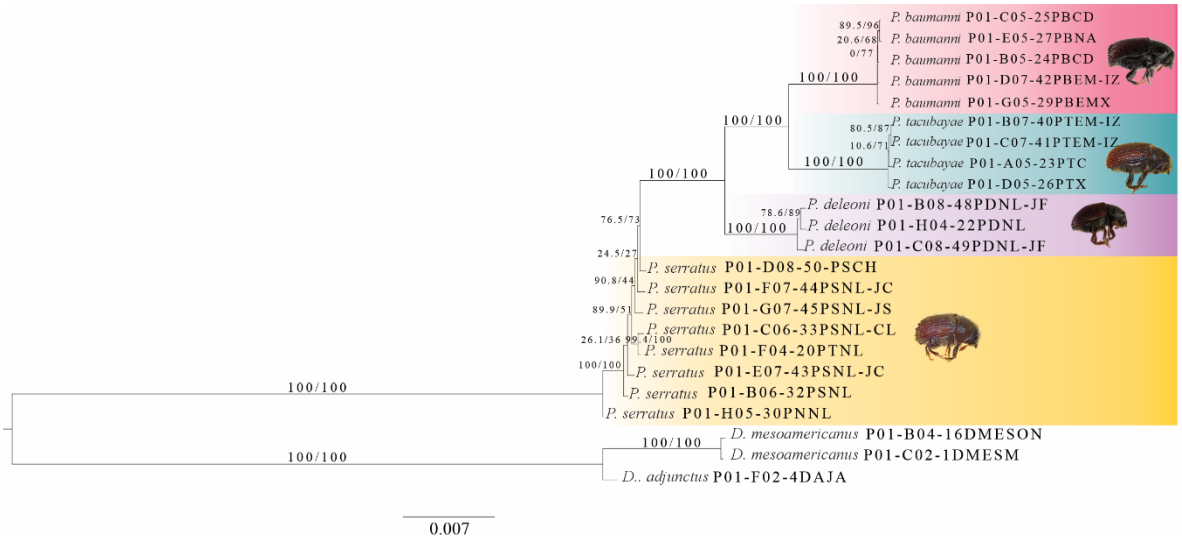
P. baumanni P01-C05-25PBCD
P. baumanni P01-E05-27PBNA
P. baumanni P01-B05-24PBCD
P. baumanni P01-D07-42PBEM-IZ
P. baumanni P01-G05-29PBEMX
P. tacubayae P01-B07-40PTEM-IZ
P. tacubayae P01-C07-41PTEM-IZ
P. tacubayae P01-A05-23PTC
P. tacubayae P01-D05-26PTX
P. deleoni P01-B08-48PDNL-JF
P. deleoni P01-H04-22PDNL
P. deleoni P01-C08-49PDNL-JF
P. serratus P01-D08-50-PSCH
P. serratus P01-F07-44PSNL-JC
P. serratus P01-G07-45PSNL-JS
P. serratus P01-C06-33PSNL-CL
P. serratus P01-F04-20PTNL
P. serratus P01-E07-43PSNL-JC
P. serratus P01-B06-32PSNL
P. serratus P01-H05-30PNNL
D. mesoamericanus P01-B04-16DMESON
D. mesoamericanus P01-C02-1DMESM
D.. adjunctus P01-F02-4DAJA
0.007

DISCUSIÓN GENERAL Y CONCLUSIONES

Un reto importante en la taxonomía de los escarabajos descortezadores es el establecimiento de caracteres que permitan la correcta identificación y delimitación de las especies, sobre todo en especies cripticas. Sin embargo, debido a los hábitos de estos insectos, su morfología se ha homogeneizado dificultando su identificación, por lo que es necesario encontrar otros caracteres y técnicas que sean útiles para este propósito.

Asimismo, la utilización en conjunto de más de una disciplina en la taxonomía de estos insectos ofrece resultados más robustos y la fiabilidad de las hipótesis aumenta con la independencia de las disciplinas analizadas. En este trabajo a través de la implementación de dos líneas de evidencia: morfológica y genética se obtuvieron resultados congruentes entre sí que respaldan en mayor o menor medida las hipótesis de las especies del género *Phloeosinus* distribuidas en México. Específicamente, los resultados de este trabajo respaldan que el uso de caracteres morfológicos externos y su análisis a través de estadística mutivariada es útil para delimitar a las especies. Si bien, previamente este tipo de caracteres ya han sido reportados como diagnósticos para *Phloeosinus* (Hopkins, 1909; Blackman, 1964; Wood, 1982), no se habían evaluado con métodos estadísticos y las descripciones de los mismos eran muy ambiguas.

El análisis de la forma de estructuras corporales anteriormente ha sido pobremente abordado en escarabajos descortezadores, sin embargo, en los géneros *Dendroctonus* y *Xyleborus*, se ha demostrado que la forma del pronoto y los élitros difiere entre especies y en algunos casos entre sexos (García-Román *et al.,* 2019; Ospina-Garcés *et al.,* 2021). En el género *Phloeosinus* no es tan evidente la variación de la forma de estas estructuras entre especies, sin embargo, si presentan diferencias, sobre todo en la curvatura del declive elitral y la curvatura de los bordes anteriores y posteriores del pronoto. El estudio la forma del esternito IX de las hembras no había sido abordado previamente. En este trabajo se encontraron diferencias en esta estructura para todas las especies, por lo que esta estructura puede constituir un carácter diagnostico útil para la identificación y delimitación de las especies dentro del género. Asimismo, el análisis filogenómico realizado a partir de datos Rad-seq y el apoyó obtenido a tres de las hipótesis estudiadas, corrobora la utilidad de la aplicación de datos de esta magnitud para la realización de inferencias filogenéticas dentro de la subfamilia Scolytinae.

REFERENCIAS BIBLIOGRÁFICAS

Armendariz-Toledano, F., and Zúñiga, G. 2017. Illustrated key to species of the genus *Dendroctonus* (Coleoptera: Curculionidae) occurring in Mexico and Central America. *International Journal of Insect Science*, 17, 1–15.

Armendáriz-Toledano, F., Niño, A., Sámano, J. E. M., and Zúñiga, G. (2014). Review of the geographical distribution of *Dendroctonus vitei* (Curculionidae: Scolytinae) based on geometric morphometrics of the seminal rod. *Annals of the Entomological Society of America*, *107*(4), 748-755.

Atkinson, T. H. (2023). Revisión del género *Phloeocleptus* (Coleoptera: Curculionidae: Scolytinae). *Revista Mexicana de Biodiversidad*, *94*(2), 12.

Atkinson, T. H., Flechtmann, C. A., and Petrov, A. V. (2023). Synopsis of the Neotropical *Premnobiina* (Coleoptera: Curculonidae: Scolytinae: Ipini) with descriptions of new species, new synonymy and keys to species. *Zootaxa*, *5249*(1), 69-91.

Blackman, M. W. (1942). Revision of the genus *Phloeosinus* Chapuis in North America (Coleoptera, Scolytidae). *Proceedings of the United States National Museum*.

Burgos-Solorio A, and Atkinson TH. (2022). New species and new records of *Chaetophloeus* LeConte (Coleoptera: Curculionidae: Scolytinae) from Mexico. Zootaxa. 5174(1):73-84.

Cervantes-Espinoza, M., Cuellar-Rodríguez, G., Alejandro Ruiz, E., Atkinson, T. H., García Ochaeta, J. F., Alfredo Hernández-García, J., and Armendáriz-Toledano, F. (2022). Distribution of *Phloeosinus tacubayae* Hopkins, 1905 (Curculionidae, Scolytinae), the Cypress Bark Beetle, and new records from potential distribution models. *Check List*, *18*(5).

Cognato, A. I., and Sperling, F. A. (2000). Phylogeny of *Ips* DeGeer species (Coleoptera: Scolytidae) inferred from mitochondrial cytochrome oxidase I DNA sequence. *Molecular Phylogenetics and Evolution*, *14*(3), 445-460.

Dole, S. A., Jordal, B. H., and Cognato, A. I. (2010). Polyphyly of *Xylosandrus* Reitter inferred from nuclear and mitochondrial genes (Coleoptera: Curculionidae: Scolytinae). *Molecular Phylogenetics and Evolution*, *54*(3), 773-782.

Estrada-Castillón, A. E., Villarreal-Quintanilla, J. Á., Salinas-Rodríguez, M. M., Cantú-Ayala, C. M., González-Rodríguez, H., and Jiménez-Pérez, J. (2014). Coníferas de Nuevo León, México [Conifers of Nuevo León, Mexico], Universidad Autónoma de Nuevo León, México.

García-Román, J., Armendáriz-Toledano, F., Valerio-Mendoza, O., and Zúñiga, G. (2019). An assessment of old and new characters using traditional and geometric morphometrics for the identification of *Dendroctonus approximatus* and *Dendroctonus parallelocollis* (curculionidae: Scolytinae). *Journal of Insect Science*, *19*(1), 14.

García-Román, J., Ramírez-Reyes, T., and Armendáriz-Toledano, F. (2022). The spermatheca in the genus *Dendroctonus* (Curculionidae: Scolytinae): morphology, nomenclature, potential characters for taxonomic use and phylogenetic signal. *Revista mexicana de biodiversidad*, *93*.

Godefroid M, Meseguer AS, Sauné L, Genson G, Streito JC, Rossi JP, Zaldivar-Riverón A, Mayer F, Cruaud A (2019). Restriction-site associated DNA markers provide new insights into the evolutionary history of the bark beetle genus *Dendroctonus. Molecular phylogenetics and evolution*, *139*, 106528.

Hernández-García, J. A., Cuellar-Rodríguez, G., Aguirre-Ojeda, N. G., Villa-Tanaca, L., Hernández-Rodríguez, C., and Armendáriz-Toledano, F. (2020). Phylogenetic position of *Geosmithia* spp.(Hypocreales) living in *Juniperus* spp. forests (Cupressaceae) with bark beetles of *Phloeosinus* spp.(Scolytinae) from the rortheast of Mexico. *Forests*, *11*(11), 1142.

Hopkins, A. 1909. Contributions toward a monograph of the scolytid beetles: I the genus *Dendroctonus*. U.S. Department of Agriculture Bureau of Entomology Technical Series 17 (Part I). Washington D.C.: Washington Govt.

Hulcr, J., Atkinson, T. H., Cognato, A. I., Jordal, B. H., and McKenna, D. D. (2015). Morphology, taxonomy, and phylogenetics of bark beetles. In *Bark Beetles* (pp. 41-84). Academic Press.

Johnson, A. J., Hulcr, J., Knížek, M., Atkinson, T. H., Mandelshtam, M. Y., Smith, S. M., Cognato, I., Park, S., Li, Y. and Jordal, B. H. (2020). Revision of the bark beetle genera

within the former Cryphalini (Curculionidae: Scolytinae). *Insect Systematics and Diversity*, *4*(3), 1.

Jordal BH. (2007). Reconstructing the phylogeny of Scolytinae and close allies: major obstacles and prospects for a solution. In: Bentz, Barbara; Cognato, Anthony; Raffa, Kenneth, eds. Proceedings from the Third Workshop on Genetics of Bark Beetles and Associated Microorganisms. Proc. RMRS-P-45. Fort Collins, CO: US Department of Agriculture, Forest Service, Rocky Mountain Research Station. p. 3-9 (Vol. 45).

Jordal BH. (2023). Glostatina, a new xyloctonine subtribe for *Glostatus* (Coleoptera: Curculionidae), based on clear genetic and morphological differences.

Kirkendall, L. R., Biedermann, P. H., and Jordal, B. H. (2015). Evolution and diversity of bark and ambrosia beetles. In *Bark beetles* (pp. 85-156). Academic Press.

Lopez-Buenfil, J. A., Valdez-Carrasco, J., Equihua-Martinez, A., and Burgos-Solorio, A. (2001). El proventrículo como estructura para identificar generos mexicanos de Scolytidae (Coleoptera*)*. *Sociedad Mexicana de Entomologia*, Veracruz (Mexico).

Mandelshtam MY, Yakushkin EA, Kovalenko YN, and Petrov AV. (2022). New Invasive *Hypothenemus* Westwood, 1834 (Coleoptera, Curculionidae: Scolytinae) Species in the Caucasus and in the Southern Primorskii Territory, Russia. *Entomol. Rev*. 102(4):485-491.

McNichol, B. H., Sullivan, B. T., Munro, H. L., Montes, C. R., Nowak, J. T., Villari, C., and Gandhi, K. J. (2021). Density-dependent variability in an eruptive bark beetle and its value in predicting outbreaks. *Ecosphere*, *12*(1), e03336.

Ospina-Garcés, S. M., Ibarra-Juarez, L. A., Escobar, F., and Lira-Noriega, A. (2021). Evaluating sexual dimorphism in the ambrosia beetle *Xyleborus affinis* (Coleoptera: Curculionidae) using geometric morphometrics. *Florida Entomologist*, *104*(2), 61-70.

Pérez Silva, M.; Equihua Martinez, A.; Atkinson, T.H. (2015). Identificación de las especies mexicanas del género *Xyleborus* Eichhoff, 1864 (Coleoptera: Curculionidae: Scolytinae). Insecta Mundi 440: 135.

Pistone, D., Gohli, J., and Jordal, B. H. (2018). Molecular phylogeny of bark and ambrosia beetles (Curculionidae: Scolytinae) based on 18 molecular markers. *Systematic Entomology*, *43*(2), 387-406.

Ramírez-Reyes, T., Armendáriz-Toledano, F., and Rodríguez, L. G. C. (2023). Rearranging and completing the puzzle: Phylogenomic analysis of bark beetles *Dendroctonus* reveals new hypotheses about genus diversification. *Molecular Phylogenetics and Evolution*, *187*, 107885.

Stauffer, C. (1997). Phylogenetic relationships of the bark beetle species of the genus *Ips* DeGeer. *Insect Molecular Biology*, *6*, 233-240.

Valerio-Mendoza, O., García-Román, J., Becerril, M., Armendáriz-Toledano, F., Cuéllar-Rodríguez, G., Negrón, J. F., ... and Zúñiga, G. (2019). Cryptic species discrimination in western pine beetle, *Dendroctonus brevicomis* LeConte (Curculionidae: Scolytinae), based on morphological characters and geometric morphometrics. *Insects*, *10*(11), 377.

Victor, J., and Zuniga, G. (2016). Phylogeny of *Dendroctonus* bark beetles (Coleoptera: Curculionidae: Scolytinae) inferred from morphological and molecular data. *Systematic Entomology*, *41*(1), 162-177.

Wood, S.L. (1982) The bark and ambrosia beetles of North and Central America (Coleoptera: Scolytidae), a taxonomic monograph. *The Great Basin Naturalist Memoirs,* 6, 1–1359.

ANEXO

THE CANADIAN ENTOMOLOGIST

CAMBRIDGE UNIVERSITY PRESS

Endophallus inflation: A potential taxonomic tool for the subfamily Scolytinae (Coleoptera: Curculionidae)

Journal:	*The Canadian Entomologist*
Manuscript ID	Draft
Manuscript Type:	Research Paper
Date Submitted by the Author:	n/a
Complete List of Authors:	Fernández-Campos, Alice; 1Posgrado en Ciencias Biológicas, Universidad Nacional Autónoma de México, Unidad de Posgrado, Edificio D, 1° Piso, Circuito de Posgrados, Ciudad Universitaria, Coyoacán, C.P. 04510, CDMX, México Guzmán-Robles, Ana; 1Posgrado en Ciencias Biológicas, Universidad Nacional Autónoma de México, Unidad de Posgrado, Edificio D, 1° Piso, Circuito de Posgrados, Ciudad Universitaria, Coyoacán, C.P. 04510, CDMX, México Cuellar-Rodríguez, Gerardo; Universidad Autónoma de Nuevo León Facultad de Ciencias Forestales Armendáriz-Toledano, Francisco; Universidad Nacional Autonoma de Mexico Instituto de Biologia, Zoología
Abstract:	The taxonomy of the subfamily Scolytinae has traditionally been based on external morphological attributes corresponding to the elytral declivity, head, and pronotum. Some traits from the general morphology of the aedeagus and spermatheca have been proposed in scarce genera. In this study, we explore and improve a technique of endophallus inflation, to apply it in Scolytinae members and describe its morphology for the first time in 16 species from Dendroctonus Erichson, Ips De Geer, and Phloeosinus Chapuis. These taxa display differences in the attachment types of endophallus and two distinct inflate and retraction mechanisms. Our results support that the internal sac is a useful tool for taxonomy in Scolytinae because each tribe, genera, and species display a particular morphological pattern, and in Dendroctonus also suggests its value to phylogenetic inferences.

Endophallus inflation: A potential taxonomic tool for the subfamily Scolytinae (Coleoptera: Curculionidae)

Alice Nelly Fernández-Campos [1,2], Ana Valeria Guzmán-Robles[2], Gerardo Cuellar Rodríguez[3], Francisco Armendáriz-Toledano[2]*

[1]Posgrado en Ciencias Biológicas, Universidad Nacional Autónoma de México. Unidad de Posgrado, Edificio D, 1° Piso, Circuito de Posgrados, Ciudad Universitaria, Coyoacán, C.P. 04510, CDMX, México

[2]Instituto de Biología, Departamento de Zoología, Colección Nacional de Insectos, Universidad Nacional Autónoma de México, Circuito Zona Deportiva S/N, C.U. Coyoacán, 04510 Ciudad de México, México.

[3]Universidad Autónoma de Nuevo León, Facultad de Ciencias Forestales, Campus Linares, Nuevo León, México

ANFC: alicenelly18@gmail.com, AVGR: avaleriaguzman@gmail.com FAT: farmendariztoledano@ib.unam.mx *

*Corresponding author

Abstract

The taxonomy of the subfamily Scolytinae has traditionally been based on external morphological attributes corresponding to the elytral declivity, head, and pronotum. Some traits from the general morphology of the aedeagus and spermatheca have been proposed in scarce genera. In this study, we explore and improve a technique of endophallus inflation, to apply it in Scolytinae members and describe its morphology for the first time in 16 species from *Dendroctonus* Erichson, *Ips* De Geer, and *Phloeosinus* Chapuis. These taxa display differences in the attachment types of endophallus and two distinct inflate and retraction mechanisms. Our results support that the internal sac is a useful tool for taxonomy in Scolytinae because each tribe, genera, and species display a particular morphological pattern, and in *Dendroctonus* also suggests its value to phylogenetic inferences.

Introduction

The taxonomy of the subfamily Scolytinae has traditionally been based on external morphological attributes corresponding to the elytral declivity, head, and pronotum because their variation allows the recognition of species, and because they display cuticle elements easily observable and quantifiable in terms of abundance, size, and distribution (Wood 1982; Hopkins 1909; Hulcr *et al.* 2015).

In insects, particularly in Coleoptera, male genital attributes are of great importance for their taxonomy (Coca-Abia and Robbins 2006; Pardo-Díaz *et al.* 2020; Yang *et al.* 2020; Gao and Coca-Abia 2021), however, these have been poorly integrated in bark beetles' studies, due to the difficulty of manipulating small specimens and structures (Hurl *et al.* 2015). Although the genitalia have been little explored for the Scolytinae for taxonomic purposes, some attributes from the general morphology of the aedeagus and spermatheca have been proposed in scares genera (Wood 1957; Hopping 1963; Lanier 1972, 1987; Pajares and Lanier 1990; Lanier *et al.* 1991; Furniss 1996; Mandelshtam *et al.* 2006, 2012). In a few taxa, specialized parts of male genitalia also provided good taxonomic traits such as seminal rod and anchor shape in *Dendroctonus* Erichson (Coleoptera: Curculionidae) and receptacle

in *Xyleborus* Eichhoff (Coleoptera: Curculionidae) (Ríos-Reyes *et al.* 2008; Armendáriz-Toledado *et al.* 2014; Pérez–Silva *et al.* 2015; García-Román *et al.* 2019, 2022; Valerio-Mendoza *et al.* 2019).

A little explored structure, but with taxonomic potential is the endophallus, an eversible membranous sac located within the aedeagus (Torre-Bueno *et al.* 1989; Tuxen 1970). During the copulation process the endophallus is placed inside the bursa copulatrix functioning as a key-lock system and as a prezygotic isolation mechanism (Düngelhoef and Schmitt 2010), so it is useful for defining species boundaries and estimating phylogenetic relationships (Coca-Abia 2007; Düngelhoef and Schmitt 2010; Sasabe *et al.* 2010, Erbey and Candan 2018). In several Coleoptera taxa, the endophallus is a powerful taxonomic tool, to delimit and recognize problematic species (Danilevsky *et al.* 2004; Bollino and Sandel 2017).

The first comparative study of the anatomy of the male genitalia in the order Coleoptera corresponds to Sharp and Muir (1912), they described characteristics of the shape and structures of endophallus, also incorporated a technique for its eversion and emphasized the importance of including it in taxonomic studies. Since this work, the study of the endophallus morphology has contributed significantly to the taxonomy of different beetle families such as Lucanidae (Imura 2007), Glaphyridae (Uliana and Sabatinelli 2010; Bollino and Ruzzante 2015), Chrysomelidae (Bukejs and Anichtchenko 2019; Daccordi *et al.* 2020), Carabidae (Anichtchenko 2010; Janovska *et al.* 2013), Curculionidae (Bollino and Sandel 2017; Meregalli *et al.* 2020) and Cerambycidae (Danilevsky *et al.* 2004; Yamasako and Ohbayashi 2011).

In some taxa of Scarabaeoidea, the structural characteristics of the everted and non-inflated endophallus, such as sclerites, spines, and silks, have been used as attributes for phylogenetic inferences (Coca-Abia 2007). In Scolytinae, the endophallus has only been studied in *Dendroctonus monticolae* Hopk. (= *D. ponderosae*), focusing on the description of the inflated endophallus and the musculature associated with its eversion movement; however, the technique used for inflation was not presented (Cerezke 1964).

The diversity of Coleoptera groups in which the study of the endophallus has been approached allowed the development of several inflation techniques, using different substances to inflate and/or fill this structure. The Berti-Vachon technique or "air filling" (Bontems 2013), is one of the most used, since it achieves the recovery of the endophallus shape, respecting the integrity of the structures of the internal sac; however, its execution is complicated, especially in small specimens. Another commonly used technique is Berlov´s technique, which consists of filling the sac using toothpaste (Berlov 1992). Although with this method the endophallus shape is well recovered, the details of the sclerotized structures are lost by the toothpaste color, and the sac loss volume during the drying process. To avoid this problem, a modification to Berlov´s technique was proposed (Uliana and Sabatinelli 2010), adding micronized silica to reduce this effect. The use of glycerin as a filling substance has also proven effective (Yamasako and Ohbayashi, 2011), the only disadvantage is that the structure cannot be preserved dry as with the previous techniques. A new inflation technique was adapted to small curculionids, applicable to both fresh and museum specimens, which consists of cleaning the aedeagus with an enzymatic solution and then using K-Y gel to fill the endophallus (Van Dam 2014). Although this technique yields effective results and maintains the transparency of the membrane, the sample cannot be kept dry. In this study, we propose some modifications to Van Dam's technique (2014) for the study of the endophallus of Scolytinae members. In addition, the anatomy and morphology of internal sac are described for the first time in 16 species from *Dendroctonus* Erichson, *Ips* De Geer, and *Phloeosinus* Chapuis, emphasizing its usefulness for taxonomic use, also the inflation patterns of the sac are described and discussed.

Materials and methods

Sixty specimens corresponding to sixteen species of three genera of Scolytinae were analyzed: ten *Dendroctonus* spp. (*D. adjunctus* Blandford, *D. approximatus* Dietz, *D. barberi* Hopkins, *D. frontalis* Dietz, *D. mesoamericanus* Armedáriz-Toledano and Sullivan, *D. parallelocollis* Chapuis, *D. pseudotsugae barragani* Furniss, *D. vitei* Wood; *D. rhizophagus* Thomas and Bright, and *D. valens*

LeConte), four of *Phloeosinus* Chapuis (Coleoptera: Curculionidae) (*P. baumanni* Hopkins, *P. deleoni* Blackman, *P. tacubayae* Hopkins, *P. serratus* LeConte) and three of *Ips* De Geer (Coleoptera: Curculionidae) (*I. lecontei* Swaine and *I. calligraphus* Germar) (Table 1). The specimens examined were obtained from infested trees in 21 localities from Mexico and Honduras; also, museum specimens, both mounted and preserved in alcohol were included. Specimens were borrowed from Colección Nacional de Insectos, Instituto de Biología, Universidad Nacional Autónoma de México, Mexico. Specimens from different populations were included in *D. valens* and *P. serratus*, because cryptic diversity is recognized within them (Ramírez-Reyes *et al.* 2023).

For the sexing and identification of specimens, dichotomous keys were used. *Dendroctonus* spp., were sexed based on body external traits and the shape of the seventh tergite (Armendáriz-Toledano *et al.* 2015) and by the presence of stridulatory apparatus in males (Lyon 1958). Species identification was made based on external and internal morphology attributes, like the presence or absence of frontal tubercules, length and abundance of pubescence of elytral declivity (*D. adjunctus* and *D. approximatus*) (García-Román *et al.* 2019), the presence of coarse rugosities on the elytral interspaces and impressed striae, and short pubescence on the elytral declivity (*D. barberi*) (Valerio-Mendoza *et al.* 2019), the shape of the lateral margins of the epistomal process and pronotum (*D. parallelocollis* and *D. pseudotsugae*) (García-Román *et al.* 2019, Armendáriz-Toledano *et al.* 2017), characteristics of the antennal club (*D. rhizophagus, D. valens* and *D. vitei*) (Armendáriz-Toledano *et al.* 2014) and characteristics of the male genitalia such as the seminal rod and anchor (*D. frontalis* and *D. mesoamericanus*) (Armendáriz-Toledano *et al.* 2014, 2015).

Phloeosinus specimens were sexed based on whether the eighth tergite was visible (males) or not (females) (Hopkins 1905: Cervantes-Espinoza, *et al.* 2023). The species were identified based on external morphological characters (Blackman 1942; Wood 1982). Characters from the head were used, like frons shape, elevation of the carina concerning the epistomal margin and the shape of antennal sutures, density of pubescence and punctuations of pronotum, shape of elytral declivity, width of

interstriae, and number and shape of the declivital teeth (*P. baumanni, P. deleoni, P. serratus* and *P. tacubayae*)

Finally, the *Ips* specimens were identified using the dichotomous keys of Lanier (1987), LaBonte and Valley (2019), and Douglas *et al.* (2019). While the *I. calligraphus* specimens were sexed based on the shape of the hook shape of the third spine of the elytral declivity; meanwhile, *I. lecontei* males were recognized by the presence of bifurcate tubercles at the center of the epistomal margin.

Male adults were dissected to obtain the genitalia. The method of obtaining the aedeagus was different depending on the method of preservation of the specimens (dry, alcohol, or fresh) and is described below.

Rehydration of dry-mounted specimens. For optimal extraction of the genitalia, the specimens were first rehydrated using a "softening solution" (distilled water and 50% commercial meat tenderizer). The ingredients of meat tenderized indicated on the label of the product were iodized salt, dextrose, papain, and calcium stearate. The procedure consisted of placing the insects in vials with this solution and incubating them for 45-60 min at 60° C.

Obtaining and cleaning of the aedeagus. After rehydration, the dissection to obtain the aedeagus was performed for all specimens (preserved dry, in alcohol, and fresh). The abdomen was removed and placed in a vial with a pancreatin solution to facilitate tissue digestion (Alvarez-Padilla and Hormiga 2007; Van Dam 2014), the samples were incubated for 1 to 2 hours at 37°C, although they can also be left at room temperature for two to three days. Once the samples were clean, they were rinsed with distilled water and then transferred to alcohol. If the tissue did not dissolve completely, the samples were incubated for 30 min at 60°C with 10% NaOH to finish cleaning and softening, then neutralized with 10% HCl, rinsed with distilled water, and preserved in 70% alcohol.

Endophallus inflation. Once the aedeagous were clean, the endophallus inflation was made. Thus, the Van Dam´s (2014) technique was performed with certain modifications. An insulin syringe was used to inflate the endophallus, the tip of the needle was filed to a right angle and the contour was filed to

obtain a conical shape and facilitate inflation. A lubricant K-Y gel was used as an inflation substance. Due to the density of the gel, before inflation, a 50% dilution with 96% alcohol was performed. A drop of the gel solution was placed on a slide and then the aedeagus was placed in it. The procedure was performed using a stereo microscope. With the help of fine-tipped forceps the body of the aedeagus was held taking care not to crush it and it was placed in a dorsal position or in a position that allowed easy manipulation for inflation. With the syringe, the gel was injected through the basal orifice of the aedeagus located between the apodemes (Fig. 1). Once the endophallus was everted, photographs were taken in different positions: dorsal, lateral, and ventral for their subsequent description. The photographs were taken using a compound microscope with a camera at 40x, 100x, and 400x magnification depending on species size. Finally, the samples were preserved in a vial with 70% alcohol. For some species, the inflation process was recorded on video to visualize the movement of the structures involved, however, in the case of the genus *Ips,* this was the only option to describe it due to the intrinsic characteristics of the endophallus (see results). From the photographs and videos, drawings of the different views of the endophallus of all species were made.

The description of the endophallus anatomy was performed using the nomenclature of Cerezke (1964), Yamasako and Ohbayashi (2011), Daccordi *et al.* (2020), and Meregalli *et al.* (2020), Torre-Bueno 1989 and Tuxen 1970. The following is a list of abbreviations with respective definitions for describing the structures of the aedeagus and endophallus. The definitions were based on the glossary of Torre-Bueno (1989), Cerezke (1964), Tuxen (1970) and Armendáriz-Toledano *et al.* (2015). The term ‘aedeagus’ or “penis” is here restricted to the part commonly known as the median lobe, containing the accessory apparatus and the internal sac, and it not including the spicule and tegmen.

LIST OF ABBREVIATIONS

acap, accessory apparatus. An ensemble of two sclerotized structures located within the aedeagus and connected by muscles and involved in seminal flow, it consists of the anchor, and the seminal rod.

anch, anchor. Flat, chitinous, “u” shaped plate supporting the seminal rod.

apod, apodemes. A paired fine needle at the base of the aedeagal shaft.

bor, basal orifice. Basal opening of aedeagus through which the ejaculatory duct enters.

edvlb, endophallus' distal ventral lobe. The lobe arises in the ventral-lateral region of the median lobe of the endophallus, situated below the proximal dorsal lobes.

dlb, aedeagus' dorsal lobe. Single or subdivided lobe in the dorsal region of the aedeagus.

ellb, endopallus' lateral lobes. Lobes arise laterally from the median lobe of the endophallus.

emlb, endophallus' median lobe. The main lobe of the endophallus, is attached to the accessory apparatus, the ***ellb,*** and ***epdlb*** arise from it.

epdlb, endophallus' proximal dorsal lobes. Lobes arise on the dorso-lateral region of the median lobe, located above the distal-ventral lobes.

ost, ostium. Opening or area in the distal region in which the endophallus is everted.

lfd, aedeagus lateral folds. Folds located on the dorsal-distal sides of the ostium in *Phloeosinus.*

lpen, lateral lobes of pennis/aedeagus. Two prominent lobes lie on the dorsal aspect of the aedeagus in *Dendroctonus* and *Ips.*

smrd, seminal rod. The chitinous structure of the penis attached to the anchor, within the aedeagus, is involved in seminal flow.

smt, seminal trough. Or ejaculatory duct.

spcl, spicule. A small needlelike spine, attached by membranes to the outside of the aedeagus.

vlb, aedeagus' ventral lobe. Subdivided lobe in the ventral region of the aedeagus.

y, possible sensory structure. Located on the endophallus median lobe, it has been to sensorial function (Cerezke 1964).

Results

Inflation. Of the sixteen species analyzed, only two were partially inflated, because they were dry-preserved specimens with very small aedeagus. In members of *Dendroctonus* and *Phloeosinus,* the inflated endophallus was maintained for days after the procedure, which facilitated their observation

and description. For *Ips* spp., the endophallus only maintained its shape when the pressure of the injection fluid was constant, when the fluid was no longer applied, the sac retracted into the aedeagus, suggesting a stronger mechanism of retraction (Supplementary Video 1).

Morphology. The genital organ of the *Dendroctonus*, *Ips*, and *Phloeosinus*, consists of three sclerotized structures, the spicule, tegmen, and penis (*sensu* Cerezke 1964) or aedeagus (*sensu* Nichols 1999). The tegmen and spicule lie adjacent to the penis but are attached ventrally to it by muscle and membrane. The tegmen is a small transversal segment, irregular in shape, attached to apodemes; this structure serves as musculature support during eversion (Cerezke 1964). In *Dendroctonus* the tegmen is a u-shaped structure located in the ventral region of the aedeagus close to the apodemes, while in *Plhoeosinus* is v-shaped, and in *Ips* is a ring that surrounds the aedeagus. The spicule is a small parallel needlelike spine attached by membranes to the outside of the aedeagus (Tuxen 1970), distally the spine is bifurcated partially rounding the aedeagus this structure serves as a support within the aedeagus. Among all species, the spicule is similar in shape, but the principal difference is its size.

In both *Dendroctonus* and *Phloeosinus* members within the aedeagus, the endophallus and an accessory apparatus are present, the last in turn consists of the seminal rod and an anchor.

The aedeagus is a capsule with two orifices, the basal one in the proximal region and the apical one, or ostium, in the distal region. In the basal region are the apodemes, which correspond to a pair of thin extensions that support the spermatic duct; the length of apodemes vary among genera and species mainly in *Ips*. The seminal rod and anchor conform to the accessory apparatus in *Dendroctonus* and *Phloeosinus*, these structures show variation within species mainly in *Dendroctonus*. Both structures are involved in the process of eversion of the endophallus during copulation.

The endophallus in the taxa studied is a sac continuously connected to the distal end of the aedeagus. When the endophallus is fully everted and inflated, it looks like a semitransparent membrane, which is composed of lobes (Fig. 2). During the process of eversion, the endophallus exits through the ostium in *Dendroctonus*, driven by the movement of the accessory apparatus to which it is attached (Fig. 2A). In

Phloeosinus the endophallus ascends through the dorsal-distal region of the aedeagus, where it joins at the lateral folds, and in the dorsal-proximal region it joins with the accessory apparatus (Fig. 2B). In both *Dendroctonus* and *Phloeosinus* when the endophallus is everted, the accessory apparatus is displaced at an angle of 45 to 90° concerning its uninflated position. In *Ips* the endophallus is attached dorsally to the median lobe of the aedeagus and laterally to the ventral lobe, both the median and ventral lobe limit the movement of the endophallus during the eversion process, giving it the characteristic of being retractile (Fig. 2C).

The number of endophallus lobes is different among genera and species, *Dendroctonus* spp. display three to five lobes, *Phloeosinus* spp. three lobes, and finally *Ips* spp. have two (Fig. 2). Comparing the relative position of lobes, a common morphological pattern in endophallus can be recognized, the presence of a pair of lateral lobes (*ellb*), in ventral and lateral view (Fig. 2), whose arrangement, and shape are different among genera. The lateral lobes (*ellb*) are oval and smaller than the median one (*emlb*) in *Dendroctonus*, meanwhile, these are rounded and equally or larger than the median one in *Phloeosinus*; in *Ips* only the lateral lobes are present, and their shape is uniform and oval (Fig. 2C). An additional pair of lobes can be recognized in lateral view (*epdlb* and e*dvlb*) in members of *Dendroctonus frontalis* complex (Fig. 2A).

Similarities among genera were recognized. In *Dendroctonus* and *Phloeosinus*, a median lobe and a yellow pore-like circular structure located in the posterior region of the median lobe, are preserved, both structures absent in *Ips* species (Figure 2). The pore-like circular structure was previously recognized "Y" structure (Fig. 12, in Cerezke 1964). Spiny sclerite patterns are observed on the outer surface of the lobes in all species. Lateral lobes have evenly arranged conical spines. In *Dendroctonus*, the median lobe has smaller spines in closely spaced groups, the spines become smaller towards the posterior end of the lobe, and no sclerotization's are observed on its ventral side.

Dendroctonus. The endophallus is attached to the anchor arms and below the seminal rod. When pressure is exerted to evert the endophallus, the seminal rod and anchor move forward, positioning

themselves outside the capsule and forming an angle between 45 to 90° concerning its initial position, in lateral view. The size of the endophallus varies among the species, although, in *D. adjunctus, D. approximatus* and *D. pseudotsugae barragani* the internal sac is bigger than aedeagus, and in *D. barberi, D. frontalis, D. mesoamericanus, D. parallelocollis* and *D. vitei* is smaller than it.

Dendroctonus adjunctus

The length of the endophallus (321 µm) is more than half the total length of the aedeagus (493 µm). The sac is composed of five lobes, one median lobe, two proximal dorsal lobes (Fig. 3A, D), and two distal ventral lobes (Fig. 3B, E). The median lobe is very pronounced with a rounded shape. The proximal dorsal lobes are small, located on the apical region of the median lobe (Fig. 3C, F). The distal lobes are smaller than the upper ones and are in the ventral region of the median lobe (3B, E). The "Y" structure is located on the distal region of the sac (Fig. 3).

Dendroctonus approximatus

The total length of the endophallus (449 µm) is almost equal to that of the aedeagus (581 µm). The endophallus is composed of five lobes, a prominent rounded median lobe in dorsal view (Fig. 4B, F), a pair of narrower and shorter distal lobes arising from the ventral surface of the median lobe (Fig. 4D, E), and a pair of proximal lobes arising from the dorsal surface of the median lobe (Fig. 4B, C, F, G,). The "Y" structure is located on the distal region of sac.

Dendroctonus barberi

The size of the endophallus (490 µm) is almost proportional to that of the aedeagus (512.54 µm). It is formed by five lobes, a rounded median lobe in dorsal view (Fig. 5B, E), a pair of wider and larger proximal lobes arising from the ventral surface of the median lobe (Fig. 5C, F), and a pair of narrower and long distal lobes arising from the dorsal surface of the median lobe (Fig. 5). The proximal and distal lobes are similar in shape, but the proximal lobes are larger than the distal lobes. In the posterior region in the central part of the median lobe is the Y structure on a small evaginated surface of endophallus (Fig. 5).

Dendroctonus frontalis

The endophallus (140 µm) is shorter than the aedeagus (297.03 µm). It consists of three lobes, an inconspicuous median lobe, and two larger lateral lobes (Fig. 6B, E). In dorsal view, the size of the lateral lobes and the median lobe is almost proportional. The median lobe in the distal region presents the Y" structure (Fig. 6D, G). The lateral lobes are covered with small spines evenly distributed over the entire outer surface (Fig. 6C, F).

Dendroctonus mesoamericanus

The length of the endophallus (181 µm) is proportional to that of the capsule (172 µm). It consists of three lobes, a conspicuous median lobe, and two well-defined lateral lobes (Fig. 7B, D). The median lobe is bigger than the lateral ones. The Y structure is in the distal region of the endophallus between lateral lobes. On the surface of the lobes, there are two types of spines, some small and others large and conical. The surface of the median lobe is covered by large, evenly distributed conical spines, while the lateral lobes are covered by smaller spines (Fig. 7).

Dendroctonus parallelocollis

The length of the endophallus (307 µm) is proportional to that of the capsule (582 µm). It consists of three lobes, a well-defined median lobe in dorsal and lateral view (Fig. 8A, B) and two distal lateral lobes extending perpendicular to the median lobe and arising from the sides of the posterior region of the median lobe (Fig. 8B, E). The shape of the lateral lobes is very different from that of the median lobe, as it has some folds that give it an irregular shape widest at de base of the lobes. In the posterior region of the median lobe is the Y structure. On the dorsal surface of the median lobe and in the anterior region of the lateral lobes small conical spines are distributed, in the median lobe the density of spines decreases to the laterals (Fig. 8).

Dendroctonus pseudotsugae

The length of the endophallus in dorsal view (382 µm) is almost half the total length of the aedeagus (774 µm). The endophallus of this species consists of three lobes, poorly differentiated among them, a

prominent median lobe, and two small distal lateral lobes (Fig. 9B, D). The surface of the median lobe covers almost the entire endophallus. In the dorsal region, the median lobe is covered by small spines, the density decreases towards the lateral lobes. The Y structure is found in the ventral posterior region of the median lobe (Fig. 9).

Dendroctonus rhizophagus

A partial inflation of the endophallus was obtained. In dorsal view, it can be observed that it is formed by at least three lobes, resembling a "T" shape in dorsal view (Fig 10A), a poorly developed median lobe, and two well-defined distal lateral lobes (Fig. 10A, C). The median lobe is larger than the lateral lobes. The Y structure is between the two distal lateral lobes on the distal region of the endophallus (Fig. 10B, D).

***Dendroctonus valens* from Mexico**

The length of the endophallus is almost proportional to the capsule of the aedeagus (655 µm). It is formed by three lobes resembling a "y" shape in ventral view, an inconspicuous median lobe, and two prominent distal lateral lobes (Fig. 11A, D). The median lobe is poorly differentiated from the lateral lobes (Fig. 11B, E). The apices of the lateral lobes end in a point. The dorsal and lateral surface of the endophallus is covered by small spines, in the ventral region, the density of the spines decreases (Fig. 11).

***Dendroctonus valens* from Honduras**

The endophallus is like those of *D. rhizophagus*, formed by three lobes resembling a short "T" shape in ventral view, a conspicuous median lobe divided into two well-defined regions (distal and proximal) (Fig. 12A, D), the proximal region is rounded in dorsal view, while the distal region is fused with the two lateral lobes. The apical edge of each lateral lobe is divided in two small lobes equal in size and shape, both rounded. The median lobe is equal in length to the lateral lobes. The Y structure is between the two distal lateral lobes on distal region of endophallus. The entire surface of the endophallus is covered by small spines whose density decreases towards the ventral region (Fig. 12).

***Dendroctonus vitei* Wood, 1975**

The length of the endophallus (208 µm) is almost one-third of the total length of the aedeagus (367 µm). The endophallus is formed by three lobes, a prominent rounded median lobe, in dorsal view (Fig. 13A), and two lateral distal lobes that in dorsal view are small and very rounded, as large as wide (Fig. 13A, D). The lateral lobes are smaller than the median one. The Y structure is in the posterior ventral region of the median lobe (Fig. 13C, F). The entire surface of the endophallus is covered by small spines whose density decreases from the center of the dorsal region of the median lobe towards the ventral region (Fig. 13).

Phloeosinus

The endophallus in this genus is a thin membranous sac whose base is attached to the accessory apparatus, and the dorsal-distal region of the ostium. The sac surrounds the seminal rod and is fused with the anchor, which is located above the seminal rod (Fig. 14). When the endophallus is everted or inflated, the seminal rod performs a 45° movement. In general, the endophallus of *Phloeosinus* is formed by three lobes, a median lobe, and two lateral lobes, whose shape is quite uniform in all the species analyzed. In all species, the size of the internal sac is similar and is not bigger than seminal capsule. In addition, in the posterior region of the median lobe is the Y structure that in lateral view has a conical shape.

Phloeosinus baumanni

The length of the endophallus in the dorsal view (280 µm) is approximately half the total length of the aedeagus (242 µm). The sac consists of a conspicuous median lobe extending from the basal orifice connected to the accessory apparatus to the ostium (Fig. 15A), and a pair of poorly marked lateral lobes that protrude more than the median lobe and expand beyond the ostium (apical region of the aedeagus). The shape of the endophallus lobes is rounded. The lateral lobes are not well differentiated from the median lobe, and they appear the same size as the median lobe, in lateral view (Fig. 15B, E). All lobes

are covered by small spines whose density is higher at the base (anterior region) near the accessory apparatus and the Y structure is in the posterior region of the median lobe (Fig. 15F).

Phloeosinus deleoni

The length of the endophallus (328.58 µm) corresponds to more than half of the total length of the aedeagus (537.35 µm) in dorsal view. The median lobe is prominent compared to the lateral lobes (Fig. 16B, E). In the posterior region, the median lobe is rounded and the lateral lobes display oval edges (Fig. 16C, F). The Y structure is in the median lobe apex (Fig. 16C, F). All lobes have spines in the dorsal region, the density of these is higher at the base (next to the accessory apparatus) and decreases towards the anterior region (Fig. 16).

Phloeosinus tacubayae

The length of the endophallus (294.33 µm) is approximately three-quarters of the total length of the aedeagus (441.09 µm) in dorsal view. The endophallus consists of three inconspicuous lobes (Fig. 17B). The median lobe is prominent compared to the lateral lobes and is rounded in the anterior region. Lateral lobes are poorly differentiated from the median lobe, and much less evaginated than the median lobe, in fact in some views appear an unilobate endophallus (Fig. 17A, D). In the apex of the median lobe is a protruding "Y" structure in the anterior region near the base of the endophallus it presents spines whose density decreases towards the posterior-apical region (Fig. 17).

Phloeosinus serratus

For this species, specimens from three populations collected from different host plants *Hesperocyparis lusitanica* (Mill) Bartel, *J. coahuilensis* (Martínez) Gaussen ex R.P. Adams and *J. saltillensis* M.T. Hall were studied. For each one a description is shown below. Specimens from these hosts present conspicuous morphological differences in external and female genital morphology. For the three populations of *P. serratus* the characteristics of the endophallus were similar (Fig. 18). The endophallus consists of a median lobe and two smaller lateral lobes. In the region near the accessory apparatus, the surface of the endophallus is covered by small spines whose density decreases towards

the sides. In the apical and central region of the endophallus is the Y structure that protrudes from the median lobe (Fig. 18).

Ips

The endophallus is a retractile eversible sac and presents two lateral lobes. The sac attached to the dorsal lobes of the aedeagus in the median part of the dorsal region (junction point of both lobes) and on the sides it is joined with the ventral lobes, (Fig. 19). In the central part of the aedeagus is the seminal trough, which at the time of inflation descends slightly towards the posterior part of the endophallus. When inflation is performed, the ventral lobes expand to the sides, allowing the eversion of the endophallus, the movement performed resembles the opening movement of a fan. However, when the pressure exerted during inflation is removed, the endophallus retracts and the ventral lobes return to their initial position. In the two species analyzed the size of the lobes is proportional to the length of the ventral lobes of the aedeagus.

Ips calligraphus

In this species when the endophallus is inflated and everted, the ventral (*vlb*) and dorsal lobes (*dlb*) of aedeagus are strongly moved together with the endophalus lobes. The vlb expands to the sides, forming an angle of 90 degrees, concerning to dlb, meanwhile, dorsal lobes are slightly separated between them (Fig. 20). The endophallus lateral lobes (*ellb*) are longer than wide, and their length is slightly higher than *vlb*, and their width is equivalent to *dlb* length (Fig. 20).

Ips lecontei

In this species when the endophallus is inflated and everted, the ventral (*vlb*) and dorsal lobes (*dlb*) of aedeagus are slightly moved together with the endophallus lobes. The point of *vlb* expands poorly to the sides, forming an angle of less than 45°, concerning to *dlb*, meanwhile, dorsal lobes are slightly separated between them (Fig. 21). The *ellb* is as long as wide, and longer than the aedeagus lobes (Fig. 21).

Discussion

In this study, modifications to Van Dam's technique (2014) were proposed for the study of the endophallus of Scolytinae, which allows describing the morphology of the internal sac and the inflation patterns in 16 species from *Dendroctonus*, *Ips*, and *Phloeosinus*. The species display differences in the attachment type of endophallus and display two distinct inflate and retraction mechanisms. Our results support that the internal sac is a useful tool for taxonomy in Scolytinae, because each tribe, genera, and species display a particular morphological pattern, and in *Dendroctonus* also supports its value to phylogenetic inferences.

The diversity studies that use the endophallus, promoted the generation of several techniques that facilitate its processing, evertion, and allow its conservation once inflated (Berlov 1992; Uliana and Sabatinelli 2010; Janovska *et al.* 2013; Daccorti *et al.* 2020). An important problem of previously proposed methods, including the most widely used technique, Berti-Vachon (Bontems, 2013), is its applicability in small and pin-mounted specimens. Van Dam (2014) presented an easy and fast technique for endophallus eversion, that requires, a relatively short time and can be used in a wide taxa diversity within Curculionidae. The adaptations of this technique implemented in the present study, such as the previous rehydration step of specimens, the combination of two digestion steps (enzyme and KOH), the dilution of inflation fluid, and the modifications of the tools (forceps and syringes), together allow satisfactory results in the Scolytinae members, under different preservation conditions. First, we were able to inflate the endophallus from large species, such as *D. rhizophagus* (5.0-6.3 mm), and *D. valens* (5.3-8.3 mm), and small ones, such as *D. frontalis* (2.0-3.2 mm) and *P. tacubayae* (1.9-2.4 mm), which represent in a good way the body size variation in the group. Also, the technique worked properly, both in fresh, and pin-mounted specimens, and allowed the inflation in a relatively short time, facilitating the analysis of at least two specimens per species.

Two techniques have been implemented in other curculionids to endophallus eversion, the first one is the Berti-Vachon (Bollino and Sandel 2017; Meregalli *et al.* 2020), and the second (and more recent) is the Van Dam technique, both consists of three general steps: 1 the dissection and enzymatic digestion

of the aedeagus, 2 the inflation of the endophallus, and 3 the preparation of the endophallus for photography. In specimens of Scolytinae, it is possible to obtain relatively good results in fresh specimens by following these three steps, however, in specimens preserved in alcohol for several years and those dry mounted, the muscle tissues are very hard, and it is very difficult to dissect without breaking the segments of the abdomen and pieces of the aedeagus. The incorporation of a previous rehydration step using a "brine" (softening solution) allowed a much softer consistency of the cuticular membranes and muscle fibers, allowing cleaner dissections and obtaining the aedeagus with greater ease and integrity.

In other curculionids, the use of a pancreatin enzymatic solution alone allows tissue digestion within a couple of hours (Van Dam *et al.* 2014). However, according to our results, in dry preserved specimens or those with highly chitinized structures such as *D. adjunctus, D. approximatus, D. parallelocollis, D. rhizophagus, D. valens*, and *P. baumanni*, the pancreatin solution alone was not sufficient for soft tissue degradation, so it was necessary to add a further digestion step with a low concentration solution of KOH. The use of K-Y gel as a filling substance allowed the observation of the details of the endophallus as it is a transparent gel, as opposed to other substances such as toothpaste (Uliana and Sabatinelli 2010; Janovska *et al.* 2013), whose coloration masks the sclerotized structures present in the endophallus. However, it was necessary to dilute the gel (50%), because at the density provided by the manufacturer, it couldn't flow through the structures and consequently they did not inflate. Despite the decrease in density, the gel provided firmness to the sample, and allowed its manipulation with a very low risk of collapse, like when other fluids such as alcohol and glycerin are used (Yamasako and Ohbayashi 2011).

One of the key points to achieve successful inflation is a good coupling and clamping of the base of the aedeagus with the forceps. Van Dam *et al.* (2014), propose the use of microvascular corneal forceps (no. 18155-13). However, the use of these forceps in Scolytinae is not useful, as the size of the aedeagus is very small and the forceps are very coarse and stiff, which hinders the manipulation of the

aedeagus and therefore the inflation process. In the case of very small specimens such as the Scolytinae, we conclude and highly recommend the use of very fine-tipped forceps, as this gives better control when manipulating the sample during the inflation process. Also, in this work, 70% alcohol is proposed as a preservation method for the inflated samples, although the duration is not yet defined, it seems to be an efficient preservation method.

Anatomy and nomenclature

Studies on the anatomy of the endophallus in the Coleoptera have focused mainly on descriptions of the lobes and sclerotized structures that make it up, especially in related species or individual species (Bollino and Ruzzante 2015; Bollino and Sabatinelli 2017; Meregalli *et al.* 2020). A recent study proposed a standardization of the nomenclature of several sclerosed elements of the insect endophallus (Génier 2019). However, there is no homogenization of the terms used to name and describe the aedeagal lobes mainly because, their number, position, and shape display great intra and interspecific variation among taxa (Bollino and Ruzzante 2015; Bollino and Sandel 2017; Meregalli *et al.* 2020). The assignment of names and descriptions of lobes have been based mainly on their position concerning the aedeagus, for example, the basal lobe, the median lobe, the lateral lobes, and the apical lobe, etc. (Yamasako and Ohbayashi 2011; Daccordi *et al.* 2020; Meregalli *et al.* 2020). In this study, the description of the lobes and structures that conform to the endophallus was made according to the nomenclature described by Cerezke (1964), whose criteria for naming the lobes were also positional. The endophallus elements previously described for *Dendroctonus ponderosa* were the median lobe, the lateral lobes, the "Y" structure, and the spines. In our descriptions, these terms could be adopted in the three genera analyzed, and a general pattern of two lateral lobes arrangement was recognized in *Dendroctonus, Ips,* and *Phloeosinus.* Although the scope of the nomenclature proposed in this study could not be extrapolated to the entire subfamily, by the representation of a few taxa (Bollino and Sandel 2017; Meregalli *et al.* 2020), our data supported by three genera from different tribes (Hylurgini, Phloeosinini, and Ipini, *sensu* Hulcr *et al.* 2015) suggest that within Scolytinae, at least two

lobes are maintained, and the number, position, and shape of them are variable among genera and tribes. Thus, some terms such as "median lobe and lateral lobes" could apply to the whole group.

Another important point is the presence of the circular structure, or "Y-structure" previously defined by Cerezke in the genus *Dendroctonus* and now in the genus *Phloeosinus*. Although this structure is not the same in both genera, it is very similar in shape and location, and is probably a feature that is maintained within the subfamily Scolitynae.

Taxonomy

The endophallus is a key structure in the taxonomy and evolution of Coleoptera (Zhou *et al.*2020; Bienkowski 2021), and has been widely incorporated into species descriptions, phylogenetic reconstructions and evolutionary biology studies, because attributes present on the endophallus surface, such as sclerites, provide a rich source of taxonomic characteristics (Zunino and Halffter 1988; Coca-Abia 2007; Medina *et al.* 2013; Roggero *et al.* 2015; Uliana and Sabatinelli 2010).

Our results support the endophallus morphology as a useful tool for taxonomy in Scolytinae because each genus displays a particular pattern of shape of the endophallus and the arrangement, number, size, and shape of its lobes are specific among genera and species. The inflation patterns display two different types of attachment between the aedeagus and the internal sac, in *Phloeosinus* the base is attached to ventral folds around the ostium, while in *Dendroctonus* and *Ips* the attachment of the sac membrane is by distal lobes, three and four respectively. In addition, the genera also differed in terms of sac retraction, as in *Ips* members the sac is retracted by the resistance applied by the ventral and dorsal lobes of the aedeagus, whereas in *Dendroctonus* and *Phloeosinus*, there is no apparent mechanism of retraction, suggesting that it is due solely to the lack of seminal fluid pressure and muscular action (Cerezke 1964).

In *Dendroctonus*, the taxa with a major representation in this study, the morphological patterns of endophallus, also suggests its value to phylogenetic inferences. The similarities of endophallus among species agree with the groups or complexes, previously supported with morphological, cariological,

biological, and molecular characteristics (Sullivan *et al.* 2021; Armendáriz-Toledano *et al.* 2014, 2015; Victor and Zuñiga 2015; Godefroid *et al.* 2019; García-Román *et al.* 2019, 2022; Ramirez-Reyes *et al.* 2023).

The species *D. vitei, D. mesoamericanus, D. frontalis, D. approximatus,* and *D. adjunctus* are grouped within the *Dendroctonus frontalis* complex (Lanier 1987; Victor and Zúñiga 2015; Ramírez-Reyes *et al.* 2023). In this study, this group was characterized by a rounded median lobe and two small lateral lobes arising in the dorsal apical region of the median lobe. In the members of *Dendroctonus frontalis* complex *sensu stricto* (Lanier 1987) or clades IV and V (Ramírez-Reyes *et al.* 2023), *D. frontalis, D. mesoamericanus,* and *D. vitei*, three lobes similar in position are present. Meanwhile, the other members of this complex, corresponding to clade III (Ramírez-Reyes *et al.* 2023), *D. adjunctus, D. approximatus* and *D. barberi* share five lobes similar in position. However, comparing the morphological patterns within these clades, discordances are observed in closely related species, as the case of the endophallus of *D. vitei* is more similar to that of *D. mesoamericanus* than to *D. frontalis,* even though the latter ones are sister species.

Members of the *D. valens* group also share endophallus similarities, *D. rhizophagus* and *D. valens* display three lobes, resembling a "T" and “Y”shape in dorsal view, a poorly developed median lobe, and two well-defined distal lateral lobes. Differences in lobe shape were observed among specimens of *D. valens* from Honduras and Mexico. The endophallus of *D. valens* from Honduras is formed by three lobes resembling a short "T" shape in ventral view, with the apical lateral lobe divided into two rounded small lobes equal in size and shape, meanwhile, *D. valens* from Central Mexico, are more similar to *D. rhizophagus,* displaying an endophallus formed by three lobes resembling a "y" shape in ventral view, and two prominent distal lateral lobes with the apices ending in a point.

These morphological differences are consistent with the hypothesis that the Central American populations of *D. valens* correspond to a different species (Cai *et al.* 2008; Armendáriz-Toledano and

Zuñiga 2017)), which was previously recognized as *D. beckeri* by Tatcher (1954) and later synonymized with *D. valens* (Wood 1963).

Dendroctonus pseudotsugae and *D, parallelocollis* present well-defined morphological patterns, distinct from those of *D. frontalis* and *D. valens* groups. The second species displays some shared attributes with the *D frontalis* complex, two small lateral rounded lobes attached to the distal end of the median lobe, agree with the most recently phylogeny, whose topology supports to *D. parallelocollis* as sister species of the *D. frontalis* complex (Ramírez-Reyes *et al.* 2023).

A possible lock-and-key role between the endophallus and bursa copulatrix has been proposed in related species with variable endophallus morphology (Sasabe *et al.* 2010). However, this theory is debated in genera whose endophallus is highly uniform (Janovska *et al.* 2013. In our study we observed variation in the shape of the endophallus within the genus *Dendroctonus,* indicating that the lock-and-key condition is possibly being met, however, it remains to be complemented with a study of the shape and attributes that make up the bursa copulatrix to corroborate whether they complement each other.

In the genus *Phloeosinus,* the morphological differences among species are less evident and are focused on the shape of the endophallus lobes, however, the species amount included avoid, taxonomic and phylogenetic interpretations. Finally, the two *Ips* spp. display a less complex endophallus morphological pattern, with only two lateral lobes, which are different between the two species analyzed. Further analysis is required in other species of *Ips* to identify the presence of any pattern and to identify some other type of substance used for inflation with a higher density that avoids the retraction of the endophallus and maintains its shape for a longer time to facilitate its anatomical study.

Although this work recognizes the attributes of the endophallus and the importance of its study within the subfamily Scolytinae, it is still necessary to further investigate the possible evolutionary patterns of this structure for its application in the construction of phylogenetic inferences.

Acknowledgements

We thank the following institutions for funding this research: PAPIIT–UNAM, (IA203122, IN223924), and Consejo Nacional de Humanidades Ciencias y Tecnologia CONAHCYT Fronteras de la Ciencia (139030). Alice Nelly Fernández Campos is a student at Programa de Posgrado en Ciencias Biológicas, Universidad Nacional Autónoma de México (UNAM) and received fellowship 1146407 from CONAHCYT. Francisco Armendáriz Toledano and Gerardo Cuellar Rodríguez are a members of Sistema Nacional de Investigadores-CONAHCYT.

References

Álvarez-Padilla, F., and G. Hormiga. 2007. A protocol for digesting internal soft tissues and mounting spiders for scanning electron microscopy. *The Journal of Arachnology*, *35*(3): 538–542.

Anichtchenko, A. V. 2010. Nueva especie de *Platyderus* Stephens, 1828 (Coleoptera Carabidae) de España y nuevos datos sobre *Platyderus toribioi*. *Arquivos Entomolóxicos*, (3): 103–06.

Armendariz-Toledano, F., and G. Zúñiga. 2017. Illustrated key to species of the genus *Dendroctonus* (Coleoptera: Curculionidae) occurring in Mexico and Central America. *International Journal of Insect Science*, 17: 1–15. https://doi.org/10.1093/jisesa/iex009

Armendáriz-Toledano, F., A. Niño, J. E. Macías S., and G. Zúñiga. 2014. Review of the geographical distribution of *Dendroctonus vitei* (Curculionidae: Scolytinae) based on geometric morphometrics of the seminal rod. *Annals of the Entomological Society of America*, *107*(4): 748–755.

Armendáriz-Toledano, F., A. Niño, B. T. Sullivan, *et al.* 2015. A new species of bark beetle, *Dendroctonus mesoamericanus* sp. nov. (Curculionidae: Scolytinae), in southern Mexico and Central America. *Annals of the Entomological Society of America*, *108*(3): 403–414.

Berlov, O. 1992. Preparati permanenti a secco dell'endofallo nel genere *Carabus* L. (Coleoptera, Carabidae). *Bolletino della Società entomologica italiana*, 124(2): 141–143.

Bieńkowski, A. 2021. The Structure of the Endophallus Is a New Promising Feature and a Key to Study of Taxonomy of the Subgenus *Metallotimarcha* of the Genus *Timarcha* (Coleoptera, Chrysomelidae) in the Caucasus. *Insects*, 12(10):937.

Blackman, M. W. 1942. Revision of the genus *Phloeosinus* Chapuis in North America (Coleoptera, Scolytidae). *Proceedings of the United States National Museum*. 92: 397–474. https://doi.org/10.5479/si.00963801.92-3154.397

Bollino, M., and G. Ruzzante. 2015. Corological notes on some species of *Pygopleurus* (Coleoptera: Glaphyridae) from the Greek Island of Lesbos. *Munis Entomology and Zoology*, *10* (1), 69–74.

Bollino, M., and Sandel, F. 2017. Two new taxa of the Subgenus *Artapocyrtus* Heller, 1912, Genus *Metapocyrtus* Heller, 1912 from the Philippines (Coleoptera, Curculionidae, Entiminae, Pachyrhynchini). *Baltic Journal of Coleopterology*, *17*(1): 1–14.

Bontems, C. 2013. Le procédé Berti-Vachon d'évagination du sac interne. *Nouvelle Revue d'Entomologie (Nouvelle Série)* 29 (1): 85–91.

Bukejs, A., and Anichtchenko, A. 2019. Description of fully inflated endophallus in some *Cassida* Linnaeus (Coleoptera: Chrysomelidae: Cassidinae). *Baltic Journal of Coleopterology*, *19* (1): 29–34.

Cai, Y.-W., X.-Y. Cheng, R.-M. Xu, *et al.* 2008. Genetic diversity and biogeography of red turpentine beetle *Dendroctonus valens* in its native and invasive regions. Insect Science. 15: 291–301.

Cerezke, H. F. 1964. The Morphology and Functions of the Reproductive Systems *of Dendroctonus monticolae* Hopk. (Coleoptera: Scolytidae)2. *The Canadian Entomologist*, *96*(3): 477–500.

Cervantes-Espinoza, M, Ruiz, AE., Cuellar-Rodríguez, G., Castro-Valderrama, U., and Armendáriz-Toledano, F. 2023. Immature stages of *Phloeosinus tacubayae* (Curculionidae: Scolytinae): morphology and chaetotaxy of larval pupae, sexual dimorphism of adults, and development time. *J. In. Sci.* 23:6: 1-23.

Coca-Abia, M. M. 2007. Phylogenetic relationships of the subfamily Melolonthinae (Coleoptera, Scarabaeidae). *Insect Systematics and Evolution*, *38*(4): 447–472.

Coca-Abia, M. M., and Robbins, P. S. 2006. Taxonomy and phylogeny of a new Central American beetle genus:(Coleoptera: Scarabaeidae). *Revista de Biología Tropical*, *54*(2), 519-529.

Daccordi, M., Bollino, M. and Vela, J. M. 2020. Some techniques for the study of useful characters in the taxonomy of the genus *Timarcha* Samouelle, 1819 (Coleoptera, Chrysomelidae). *European Journal of Taxonomy*, (630). DOI: https://doi.org/10.5852/ejt.2020.630

Danilevsky, M. L., and D. G. Kasatkin. 2004. Revision of the taxonomic structure of the tribe Dorcadionini (Coleoptera: Cerambycidae) on the base of endophallic morphology. *Russian Entomological Journal*, *13*(3): 127–149.

Douglas, H. B., Cognato, A. I., Grebennikov, V., and Savard, K. 2019. Dichotomous and matrix-based keys to the *Ips* bark beetles of the World (Coleoptera: Curculionidae: Scolytinae). *Canadian Journal of Arthropod Identification*, (38).

Düngelhoef, S., and M. Schmitt, M. 2010. Genital feelers: the putative role of parameres and aedeagal sensilla in Coleoptera Phytophaga (Insecta). *Genetica*, *138*: 45-57.

Erbey, M., and S. Candan. 2018. Comparative Morphology of the Endophallus (Male Internal Genitalia) in Eight Species of the Genus *Lixus* Fabricius, 1801 (Coleoptera: Curculionidae: Lixinae): A Scanning Electron Microscope Study. *Life: The Excitement of Biology*, *5*(4).

Furniss, M. M. 1996. Taxonomic status of *Dendroctonus punctatus* and *D. micans* (Coleoptera: Scolytidae). *Annals of the Entomological Society of America*, *89*(3), 328-333.

Gao, C. B. and Coca-Abia, M. M. 2021. Revision of the genus Miridiba Reitter, 1902 (Coleoptera, Scarabaeidae, Melolonthinae): genital morphotypes and new taxonomic data. *European Journal of Taxonomy*, *749*, 1-94.

García-Román, J., F. Armendáriz-Toledano, O. Valerio-Mendoza, and G. Zúñiga. 2019. An assessment of old and new characters using traditional and geometric morphometrics for the identification of *Dendroctonus approximatus* and *Dendroctonus parallelocollis* (curculionidae: Scolytinae). *Journal of Insect Science*, *19*(1): 14.

García-Román, J., Ramírez-Reyes, T., and Armendáriz-Toledano, F. 2022. The spermatheca in the genus *Dendroctonus* (Curculionidae: Scolytinae): morphology, nomenclature, potential characters for taxonomic use and phylogenetic signal. *Revista mexicana de biodiversidad*, *93*.

Godefroid M, A. S. Meseguer, L. Sauné, *et al*. 2019. Restriction-site associated DNA markers provide new insights into the evolutionary history of the bark beetle genus *Dendroctonus*. *Molecular phylogenetics and evolution*, *139*: 106528.

Hopkins, A.D. 1905. Notes on some Mexican Scolytidae: with descriptions of some new species.

Hopkins, A.D. 1909. Contributions toward a monograph of the scolytid beetles: I the genus *Dendroctonus*. U.S. Department of Agriculture Bureau of Entomology Technical Series 17 (Part I). Washington D.C.: Washington Govt.

Hopping, G. R. 1963. Generic Characters in the Tribe Ipini (Coleoptera: Scolytidae), with a New Species, a New Combination, and New Synonymy1. *The Canadian Entomologist*, *95*(1), 61-68.

Hulcr, J., Atkinson, T. H., Cognato, A. I., Jordal, B. H., and McKenna, D. D. 2015. Morphology, taxonomy, and phylogenetics of bark beetles. In *Bark Beetles* (pp. 41-84). Academic Press.

Imura, Y. 2007. Endophallic structure of the genus *Platycerus* (Coleoptera, Lucanidae) of Japan, with descriptions of two new species. *Elytra*, *35*, 471-489.

Janovska, M., Anichtchenko, A. V., and Erwin, T. 2013. Significant new taxonomic tool for Carabidae (Insecta: Coleoptera): endophallus inflation methods revised. *Кавказский энтомологический бюллетень*, *9*(1), 39-42.

LaBonte, J. R., and Valley, S. A. 2019. Illustrated Key to the Species of Ips, *Orthotomicus*, and *Pseudips* of North America (or Spines, Spines, and More Spines). Oregon Department Agriculture.

Lanier, G. N. 1972. Biosystematics of the genus *Ips* (Coleoptera: Scolytidae) in North America. Hopping's groups IV and X. *The Canadian Entomologist*, *104*(3), 361-388.

Lanier, G. N. 1987. The validity of *Ips cribricollis* (Eich.)(Coleoptera: Scolytidae) as distinct from *I. grandicollis* (Eich.) and the occurrence of both species in Central America. *The Canadian Entomologist*, *119*(2), 179-187.

Lanier, G. N., Teale, S. A., and Pajares, J. A. 1991. Biosystematics of the genus Ips (Coleoptera: Scolytidae) in North America: review of the *Ips calligraphus* group. *The Canadian Entomologist*, *123*(5), 1103-1124.

Lyon, R. L. 1958. A useful secondary sex character in Dendroctonus bark beetles. *The Canadian Entomologist*, *90*(10), 582-584.

Mandelshtam, M. Y., Petrov, A. V., and Korotyaev, B. A. 2012. To the knowledge of the herbivorous scolytid genus *Thamnurgus* Eichhoff (Coleoptera, Scolytidae). *Entomological review*, *92*, 329-349.

Mandelshtam, M. Y., Petrov, A. V., Axentjev, S. I., and Knížek, M. 2006. A new and a poorly known species of bark beetles (Coleoptera: Scolytidae) from Middle Asia. *Труды Русского энтомологического общества*, *77*, 213-218.

Medina C.A., Molano F., and Scholtz C.H. 2013. Morphology and terminology of dung beetles (Coleoptera: Scarabaeidae: Scarabaeinae) male genitalia. *Zootaxa* 3626: 455–476.

Meregalli, M., Boriani, M., Taddei, A., Hsu, C. F., Tseng, W. Z., and Mouttet, R. 2020. A new species of *Aclees* from Taiwan with notes on other species of the genus (Coleoptera: Curculionidae: Molytinae). *Zootaxa*, *4868*(1), zootaxa-4868.

Pajares, J. A., and Lanier, G. N. 1990. Biosystematics of the turpentine beetles *Dendroctonus terebrans* and *D. valens* (Coleoptera: Scolytidae). *Annals of the Entomological Society of America*, *83*(2), 171-188.

Pardo-Diaz, C., Toro, A. L., Tovar, S. A. P., Sarmiento-Garcés, R., Herrera, M. S., and Salazar, C. 2019. Taxonomic reassessment of the genus *Dichotomius* (Coleoptera: Scarabaeinae) through integrative taxonomy. *PeerJ*, *7*, e7332.g

Pérez Silva, M.; Equihua Martínez, A.; Atkinson, T.H. 2015. Identificación de las especies mexicanas del género *Xyleborus* Eichhoff, 1864 (Coleoptera: Curculionidae: Scolytinae). *Insecta Mundi* 440: 135.

Ramírez-Reyes, T., Armendáriz-Toledano, F., and Rodríguez, L. G. C. 2023. Rearranging and completing the puzzle: Phylogenomic analysis of bark beetles *Dendroctonus* reveals new hypotheses about genus diversification. *Molecular Phylogenetics and Evolution*, *187*, 107885.

Rios-Reyes, A. V., Valdez-Carrasco, J., Equihua-Martínez, A., and Moya-Raygoza, G. 2008. Identification of Dendroctonus frontalis (Zimmermann) and D. mexicanus (Hopkins)(Coleoptera: Curculionidae: Scolytinae) through structures of the female genitalia. *The Coleopterists Bulletin*, *62*(1), 99-103.

Roggero, A., Barbero, E., Palestrini, C. 2015 Phylogenetic and biogeographical review of the Drepanocerina (Coleoptera: Scarabaeidae: Oniticellini). *Arthropod Systematics and Phylogeny*, 73(1): 153-174

Sasabe, M., Takami, Y., and Sota, T. 2010. QTL for the species-specific male and female genital morphologies in *Ohomopterus* ground beetles. *Molecular Ecology*, *19*(23), 5231-5239.

Sharp, D., and Muir, F. 1912. XI. The comparative anatomy of the male genital tube in Coleoptera. *Transactions of the Royal Entomological Society of London*, *60*(3), 477-642.

Sullivan, B. T., Grady, A. M., Hofstetter, R. W., Pureswaran, D. S., Brownie, C., Cluck, D., and Zúñiga, G. 2021. Evidence for semiochemical divergence between sibling bark beetle species: *Dendroctonus brevicomis* and *Dendroctonus barberi*. *Journal of chemical ecology*, *47*, 10-27.

Thatcher, T.O., 1954. A New Species of *Dendroctonus* from Guatemala (Scolytidae) Publication No. 6. *Coleopt. Bull*. 3–6.

Torre-Bueno, J. R., Nichols, S. W., and Tulloch, G. S. 1989. The Torre-Bueno glossary of entomology.

Tuxen, S. L. 1970. Taxonomist's glossary of genitalia in insects.

Uliana, M., and Sabatinelli, G. 2010. Revision of *Eulasia genei* Truqui, with description of *Eulasia rittneri* n. sp. from Israel and synonymic notes on related species (Coleoptera: Scarabaeoidea: Glaphyridae). *Zootaxa*, *2436*(1), 28-56.

Valerio-Mendoza, O., García-Román, J., Becerril, M., Armendáriz-Toledano, F., Cuéllar-Rodríguez, G., Negrón, J. F., ... and Zúñiga, G. 2019. Cryptic species discrimination in western pine beetle, *Dendroctonus brevicomis* LeConte (Curculionidae: Scolytinae), based on morphological characters and geometric morphometrics. *Insects*, *10*(11), 377.

Van Dam, M. H. 2014. A simple, rapid technique for the inflation of the endophallus, with particular focus on the Curculionoidea (Coleoptera). *The Coleopterists Bulletin*, *68*(2), 263-268.

Victor, J., and Zuniga, G. (2016). Phylogeny of *Dendroctonus* bark beetles (Coleoptera: Curculionidae: Scolytinae) inferred from morphological and molecular data. *Systematic Entomology*, *41*(1), 162-177.

Wood, S.L. 1982. The bark and ambrosia beetles of North and Central America (Coleoptera: Scolytidae), a taxonomic monograph. *The Great Basin Naturalist Memoirs*, 6, 1–1359.

Wood, S.L. 1957. Ambrosia beetles of the tribe Xyloterini (Coleoptera: Scolytidae) in North America. Can. Entomol. 89: 337-354.

Yamasako, J., and Ohbayashi, N. 2011. Review of the genus *Paragolsinda* Breuning, 1956 (Coleoptera, Cerambycidae, Lamiinae, Mesosini), with reconsideration of the endophallic terminology. *Zootaxa*, *2882*(1), 35-50.

Yang, G., Yang, X., and Shi, H. 2020. Taxonomy and phylogeny of the genus *Gastrocentrum* Gorham (Coleoptera, Cleridae, Tillinae), with the description of five new species. *ZooKeys*, *979*, 99.

Zhou, Y.L., Zhou, H.Z., Ski, A.L. and Beutel, R.G. 2020. Evolution of a hyper-complex intromittent organ in rovebeetles – the endophallus of Xantholinini (Staphylinidae: Coleoptera). Zoological Journal of the Linnean Society,188, 1277–1295.

Zunino, M. y G. Halffter. 1988. Análisis taxonómico, ecológico y biogeográfico de un grupo americano de Onthophagus (Coleoptera: Scarabaeidae). Museo Regiona-le di Scienze Naturali, Monografie, (9): 1-211

Tables

Table 1. Locations, geographical coordinates, and host of examined specimens.

Species	Country	Locality	Latitude	Longitude	Host	Collection
D. adjunctus	Mexico	Nevado de Colima	19.568835	-103.6165512	*Pinus hartwegii*	CNIN
D. approximatus	Mexico	Oaxaca, Portillo, Cajones (OPC)	16.2389472	-95.4774778	*Pinus* sp.	CNIN
D. barberi	Mexico	Nuevo León, Galeana-Carretera Linares-Galeana la 'Y'	24.7791667	-99.955	*P. engelmannii*	CNIN
D. frontalis	Mexico	Michoacán, Charo, La mesa	19.6	-100.93	*Pinus* sp.	CNIN
D. mesoamericanus	Honduras	Francisco Morazán	14.0161111	-86.8955556	*Pinus ocarpa*	CNIN
	Mexico	Michoacán, Villa Madero, Balcones	19.0833333	-100.942222	*Pinus pringlei*	CNIN
D. parallelocollis	Honduras	Potrerillos, Zihuatepeque (HPZI)	14.5869892	-86.1699111	Lindgren trap	CNIN
D. pseudotsugae	México	Arteaga, Coahuila.	25.4372222	-99.2916667	*Pseudotsugae menziessi*	CNIN
D. valens	Honduras	Comayagua, Villa de San Antonio; Chagüite Grande	14.5969444	-86.1405556	Lindgren trap	CNIN
	Mexico	Ajusco, Parque Ejidal San Nicolas Totolapan.	19.2525	-98.7566667	*Pinus* sp.	CNIN
D. vitei	Mexico	Nuevo León, Iturbide, Los Pinos del Sur	24.7166667	-98.1	*P. teocote*	CNIN
D. rhizophagus	Mexico	México, Durango, El Salto,	23.763	-105.365	*P. duranguensis*	CNIN
P. deleoni	Mexico	Oaxaca, San Juan Bautista, Coixtlahuaca	17.65	-97.276861	*P. flaccida*	CNIN
P. baumanni	Mexico	CDMX, Ciudad Universitaria.	-19.315	-99.181	*H. lusitanica*	CNIN
P. tacubayae	Mexico	Iturbide, Ejido la Purisima	24.5422222	-98.175	*H. lusitanica*	CNIN
P. serratus	Mexico	Nuevo León, Galeana	24.49	-100.07	*J. deppeana*	CNIN
	Mexico	Nuevo León, Aramberri	24.8596667	-100.360333	*J. saltillensis*	CNIN
	Mexico	Nuevo León, Aramberri	24.8223611	-100.084333	*J. coahuilensis*	CNIN
I. lecontei	Mexico	Durango, La victoria, Chavarría	-	-	*Pinus* sp.	CNIN
I. calligraphus	Mexico	Nuevo León, Galeana, Camino a la Y de abajo	24.7791667	-99.955	*Pinus* sp.	CNIN

Figure captions

Figure 1. Endophallus inflation process: A, first the forceps are fixed around the base of the basal orifice with the blunt-tipped syringe in the center B, then the endophallus is inflated C, all the process is realized in a stereoscopic microscope with a slide and syringe.

Figure 2. Inflated endophallus patterns in Scolytinae. A *Dendroctonus* in lateral view, B *Phloeosinus* in lateral view, and C *Ips* in dorsal view. Distal lobes (*edvlb*), lateral lobes (*ellb*), median lobe (*emlb*), Y structure (*Y*), and proximal lobes (*epdlb*).

Figure 3. Endophallus of *D. adjunctus.* (A, D) dorsal view, (B, E) lateral view, (C, F) ventral view. Accessory apparatus (*acap*), anchor (*anch*), distal lobes (*edvlb*), median lobe (*emlb*), proximal lobes (*epdlb*), seminal rod (*smrd*).

Figure 4. Aedeagus and endophallus of *D. approximatus.* (A, E) aedeagus in dorsal view; (B, F) endophallus in dorsal view; (B, F) endophallus in lateral view; (D, H) endophallus in ventral view. Accessory apparatus (*acap*), apodemes (*apod*), basal orifice (*bor*), distal lobes of endophallus (*edvlb*), median lobe (*emlb*), ostium (*ost*); spicule (*spcl*), Y structure (*y*).

Figure 5. Aedeagus and endophallus of *D. barberi.* (A, D) aedeagus in dorsal view; (B, E) endophallus in dorsal view; (C, F) endophallus in ventral view. Accessory apparatus (*acap*), apodemes (*apod*), basal orifice (*bor*), distal lobes (*edvlb*), median lobe (*emlb*), ostium (*ost*) proximal lobes (*epdlb*), spicule (*spcl*), "Y"structure (y).

Figure 6. Aedeagus and endophallus of *D. frontalis.* (A, E) aedeagus in dorsal view; (B, F) endophallus in dorsal view; (B, F) endophallus in lateral view; (D, H) endophallus in ventral view. Accessory apparatus (*acap*), apodemes (*apod*), basal orifice (*bor*), lateral lobes (*ellb*), median lobe (*emlb*), the ostium (ost), spicule (*spcl*), "Y" structure (*y*).

Figure 7. Aedeagus and endophallus of *D. mesoamericanus*. (A, F) aedeagus in dorsal view; (B, F) endophallus in dorsal view; (B, D) endophallus in ventral view; (C, E) endophallus in lateral view.

Accessory apparatus (*acap*), apodemes (*apod*), basal orifice (*bor*), lateral lobes (*ellb*), median lobe (*emlb*), the ostium (ost), seminal rod (smrd).

Figure 8. Endophallus of *D. parallelocollis.* (A, D) aedeagus in dorsal view; (B, E) endophallus in lateral view; (C, F) endophallus in ventral view. Accessory apparatus (*acap*), apodemes (*apod*), basal orifice (*bor*), lateral lobes (*ellb*), median lobe (*emlb*), the ostium (*ost*), seminal rod (*smrd*).

Figure 9. Aedeagus and endophallus of *D. pseudotsugae barragani.* (A, C) aedeagus in dorsal view; (B, D) endophallus in dorsal view. Accessory apparatus (*acap*), apodemes (*apod*), basal orifice (*bor*), lateral lobe (*ellb*), median lobe (*emlb*), ostium (*ost*), spicule (*spcl*), "Y"structure (y).

Figure 10. Endophallus of *D. rhizophagus.* (A, C) dorsal view; (B, D) lateral view.
displaying the median lobe (emlb) and the lateral lobes (llb). Accessory apparatus (*acap*), apodemes (*apod*), basal orifice (*bor*), lateral lobes lobes (*ellb*), median lobe (*emlb*), ostium (*ost*), spicule (*spcl*), "Y" structure (y).

Figure 11. Aedeagus of *D. valens* from Mexico. (A, D) dorsal view; (B, E) lateral view; (C, F) ventral view. Accessory apparatus (*acap*), apodemes (*apod*), basal orifice (*bor*), lateral lobes lobes (*ellb*), median lobe (*emlb*), ostium (*ost*), spicule (*spcl*), "Y" structure (*y*).

Figure 12. Endophallus of *D. valens* from Honduras. (A, D) dorsal view; (B, E) lateral view; (C, F) ventral view. Accessory apparatus (*acap*), apodemes (*apod*), basal orifice (*bor*), lateral lobes (*ellb*), median lobe (*emlb*), ostium (*ost*), spicule (*spcl*), "Y" structure (*y*).

Figure 13. Aedeagus and endophallus of *D. vitei*. (A, D) dorsal view; (B, E) lateral view; (C, F) ventral view. Accessory apparatus (*acap*), apodemes (*apod*), basal orifice (*bor*), lateral lobe (*ellb*), median lobe (*emlb*), ostium (*ost*), spicule (*spcl*), "Y" structure (*y*).

Figure 14. The structures that conform to the genital organ of *Phloeosinus.* (A, B) Aedeagus in dorsal view; (C) anchor lateral view; (D) seminal rod lateral view; (E) endophallus. Accessory apparatus (*acap*), anchor (*anch*), apodemes (*apod*), basal orifice (*bor*), endophallus (*enph*), lateral folds (*lfd*) ostium (*ost*), seminal rod (*smrd*).

Figure 15. Aedeagus and endophallus of *Phloeosinus baumanni*. (A, D) Aedeagus in dorsal view; (B, E) endophallus in lateral view. Accessory apparatus (*acap*), lateral lobes (*ellb*), median lobe (*emlb*), seminal rod (*smrd*) the "Y" structure (*y*).

Figure 16. Aedeagus and endophallus of *Phloeosinus deleoni.* (A, D) Aedeagus in dorsal view, (B, E) endophallus dorsal view; (C, F) endophallus in lateral view. Accessory apparatus (*acap*), apodemes (*apod*), basal orifice (*bor*), endophallus (*enph*), lateral lobes (*ellb*), lateral plates (*lp*), median lobe (*emlb*), seminal rod (*smrd*), spicule (*spcl*), "Y" structure (*y*).

Figure 17. Aedeagus and endophallus of *Phloeosinus tacubayae*. (A) Aedeagus dorsal view; (B, D) endophallus dorsal view; (C, E) endophallus lateral view. Accessory apparatus (*acap*), apodemes (*apod*), basal orifice (*bor*), lateral lobes (*ellb*), endophallus (*enph*), lateral folds (*lfd*), median lobe (*emlb*), spicule (*spcl*), the "Y" structure (*y*).

Figure 18. Aedeagus and endophallus of *Phloeosinus serratus.* (A, C, E) Aedeagus dorsal view; (B, D, F, G) endophallus lateral view; (H, I) Y structure in dorsal and lateral view, respectively. Images correspond to specimens from *Hesperocyparis lusitanica* (A, B), from *Juniperus coahuilensis* (C, D), and from *J. saltillensis. A*ccessory apparatus (*acap*), apodemes (*apod*), basal orifice (*bor*), endophallus (*enph*), lateral folds (*lfd*) spicule (*spcl*), Y structure (*y*).

Figure 19. Complete genital organ in dorsal view of *Ips*. (A) Aedeagus; (B) spicula; (C) tegmen; (E) seminal trough. Dorsal lobe (dlb), endophallus (enph), ventral lobes (vlb).

Figure 20. Aedeagus (A) and endophallus (B) of *Ips calligraphus* in dorsal view. Apodemes (*apod*), dorsal lobe (*dlb*), lateral lobe (*llb*), seminal trough (*smt*), ventral lobe (*vlb*).

Figure 21. Aedeagus and endophallus of *Ips lecontei.* (A) Aedeagus dorsal view, (B, C) endophallus dorsal view; (C, E) endophallus ventral view. Apodemes (*apod*), dorsal lobe (*dlb*), lateral lobes (*llb*), seminal though (*smt*), spicule (*scl*), ventral lobe (*vlb*), ventral lobes (*vlb*).

Figure 1

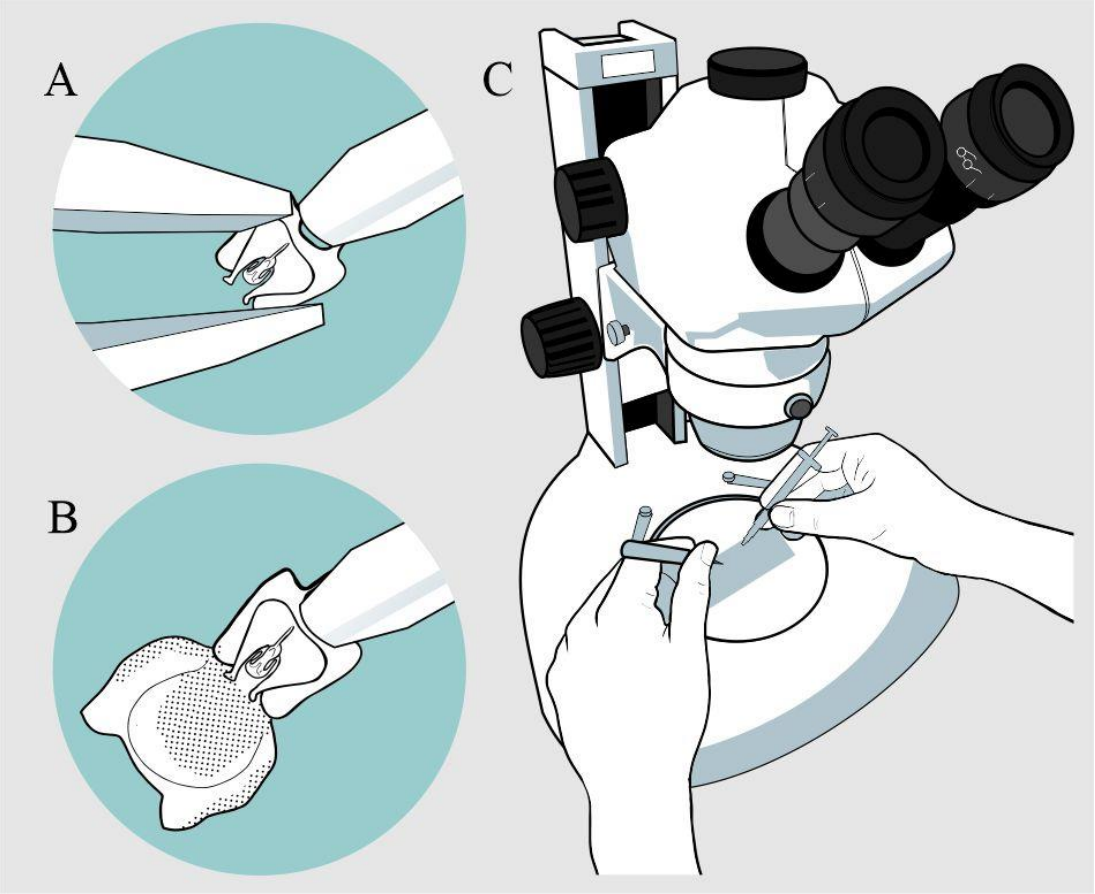

Figure 2

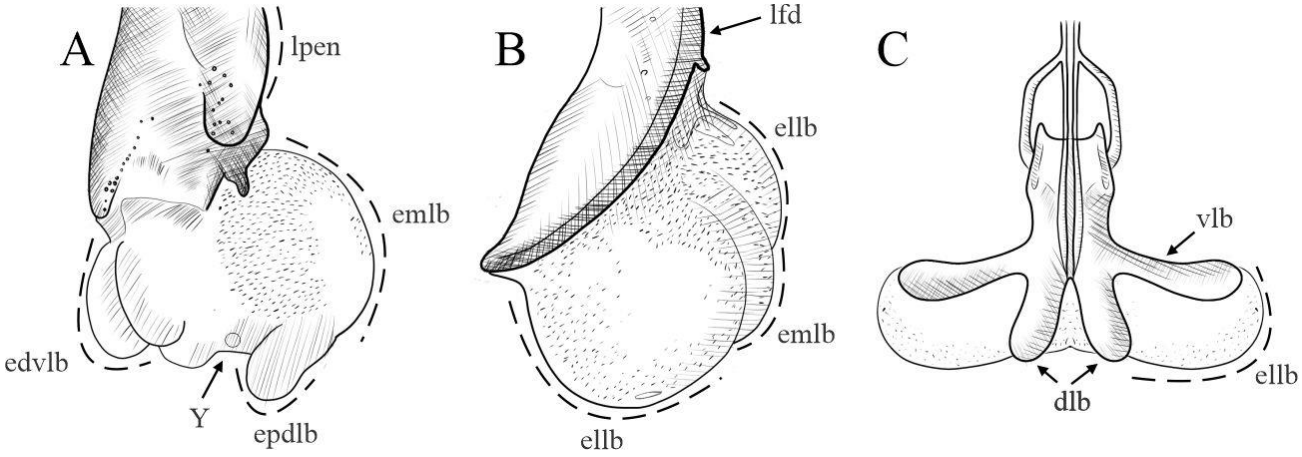

Figure 3

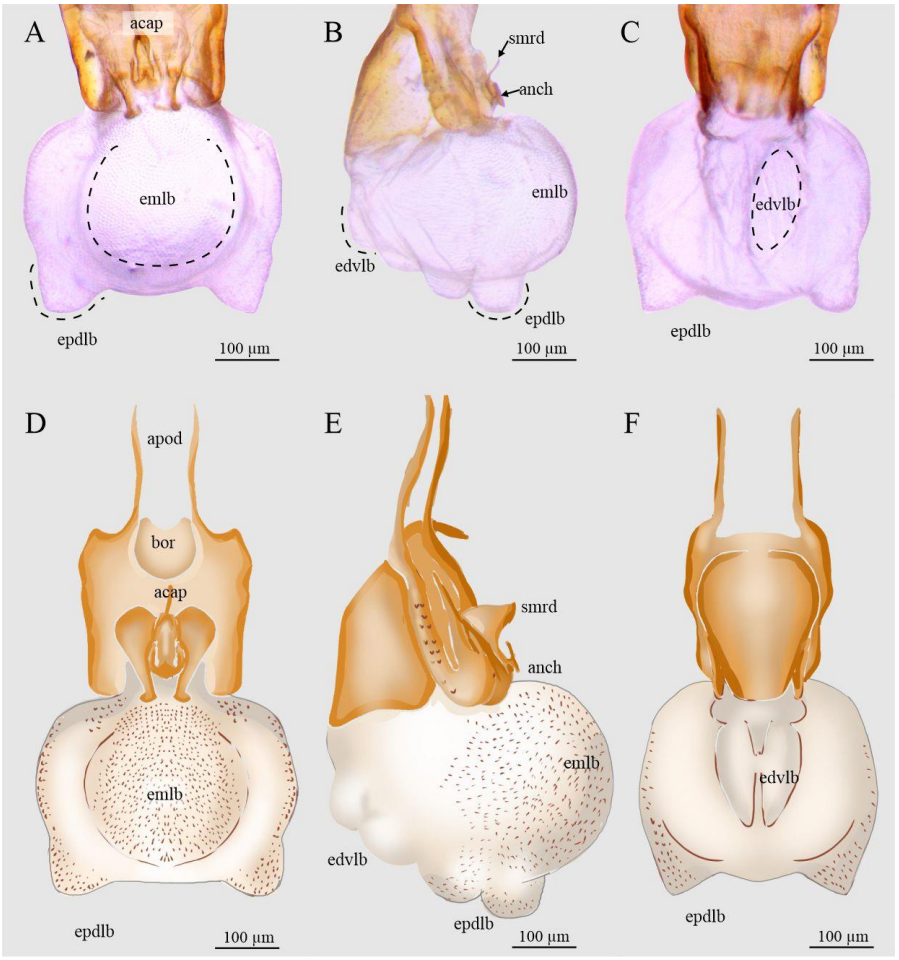
A
acap
emlb
epdlb
100 µm
B
smrd
anch
emlb
edvlb
epdlb
100 µm
C
edvlb
epdlb
100 µm
D
apod
bor
acap
emlb
epdlb
100 µm
E
smrd
anch
emlb
edvlb
epdlb
100 µm
F
edvlb
epdlb
100 µm

Figure 4

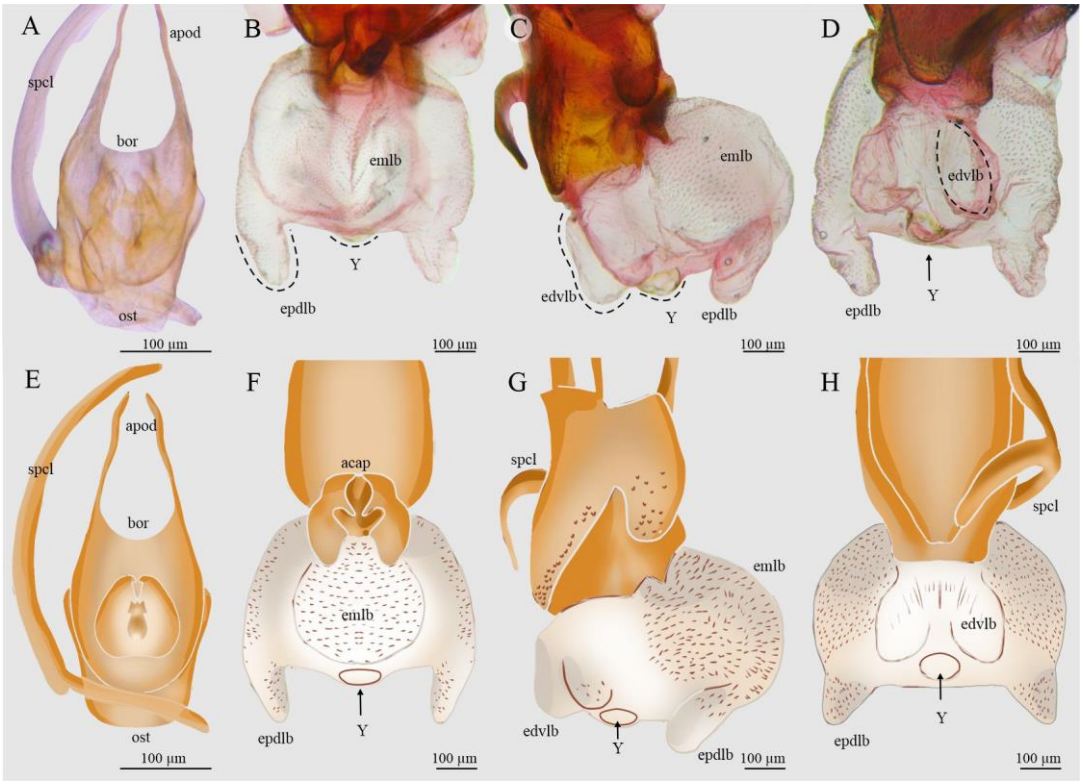
A
apod
spcl
bor
ost
100 µm
B
emlb
Y
epdlb
100 µm
C
emlb
edvlb
Y
epdlb
100 µm
D
edvlb
Y
epdlb
100 µm
E
apod
spcl
bor
ost
100 µm
F
acap
emlb
Y
epdlb
100 µm
G
spcl
emlb
edvlb
Y
epdlb
100 µm
H
spcl
edvlb
Y
epdlb
100 µm

Figure 5

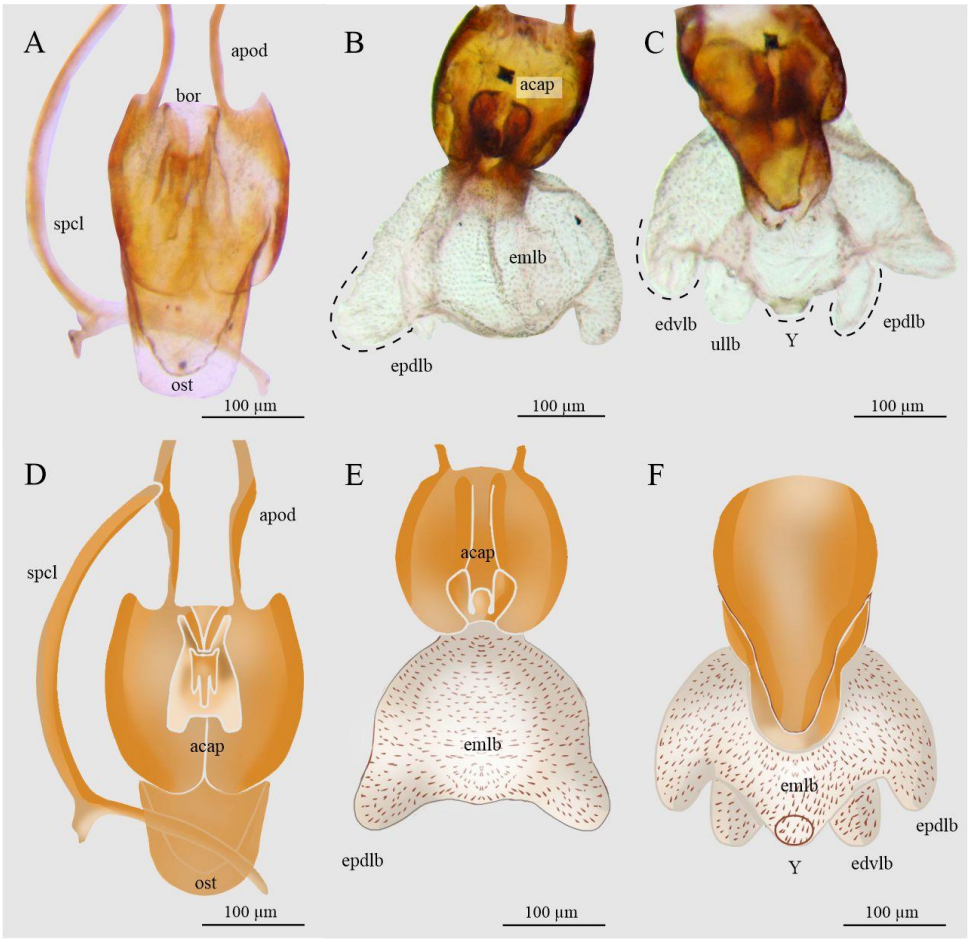

Figure 6

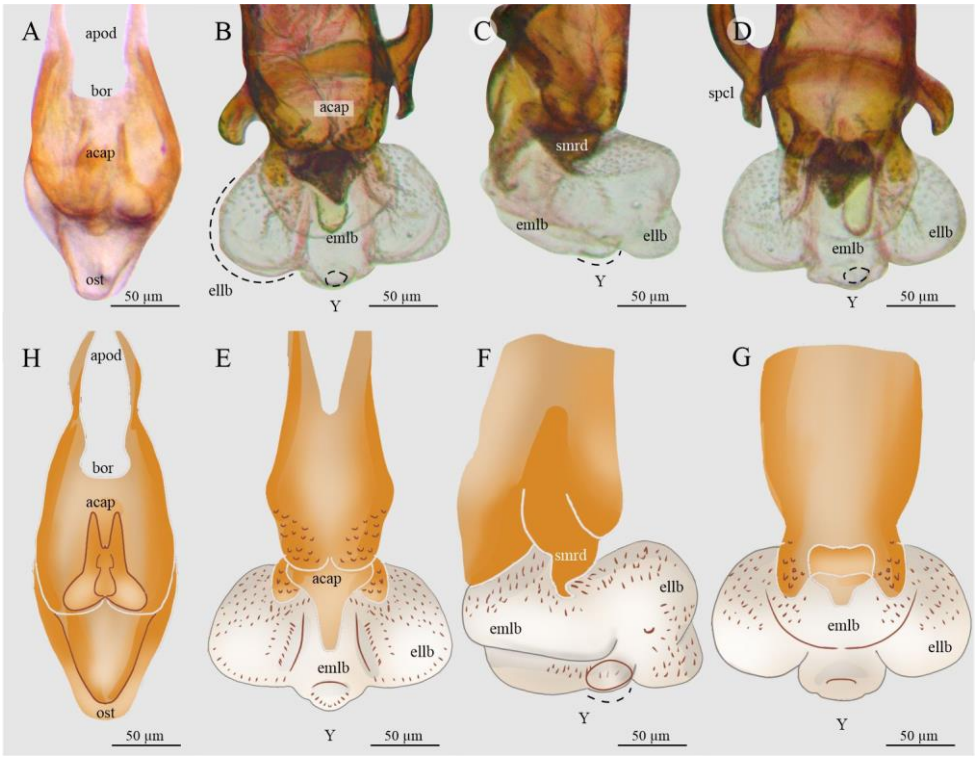
A
apod
bor
acap
ost
50 µm
B
acap
emlb
ellb
Y
50 µm
C
smrd
emlb
ellb
Y
50 µm
D
spcl
emlb
ellb
Y
50 µm
H
apod
bor
acap
ost
50 µm
E
acap
emlb
ellb
Y
50 µm
F
smrd
ellb
emlb
Y
50 µm
G
emlb
ellb
Y
50 µm

Figure 7

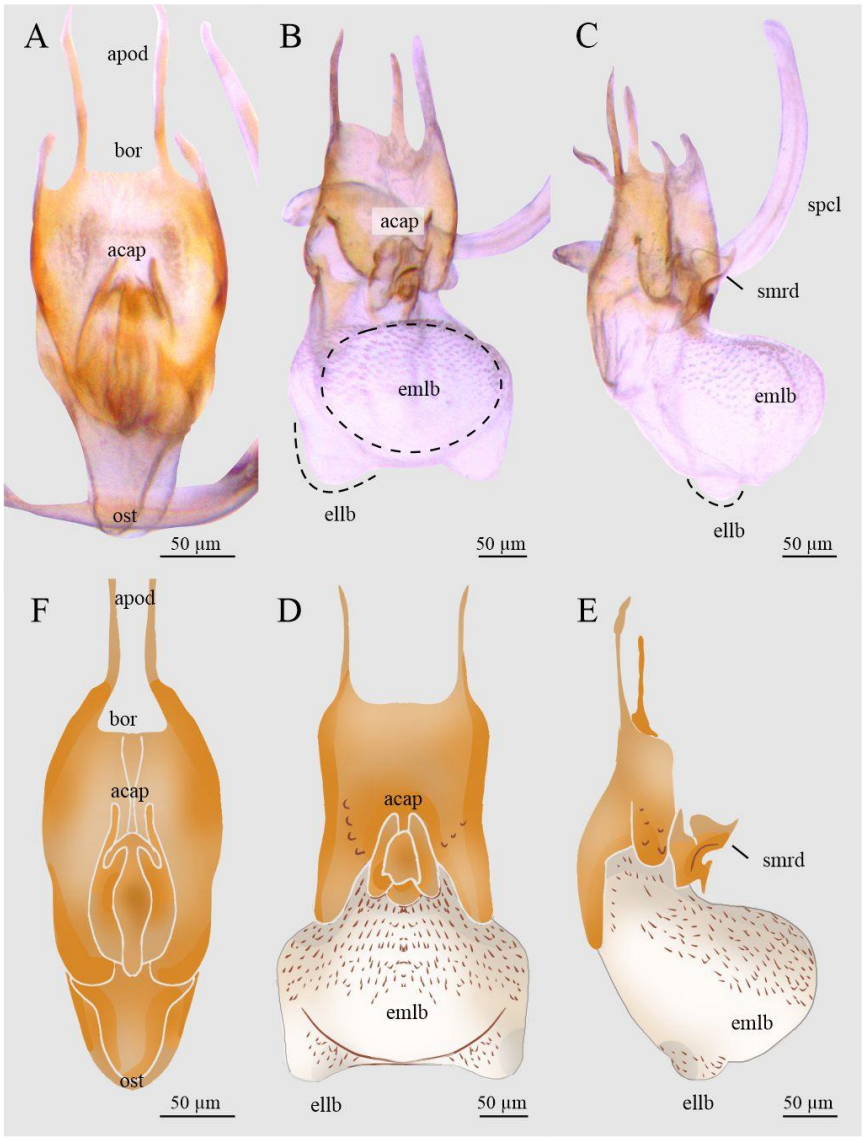
A
apod
bor
acap
ost
50 µm
B
acap
emlb
ellb
50 µm
C
spcl
smrd
emlb
ellb
50 µm
F
apod
bor
acap
ost
50 µm
D
acap
emlb
ellb
50 µm
E
smrd
emlb
ellb
50 µm

Figure 8

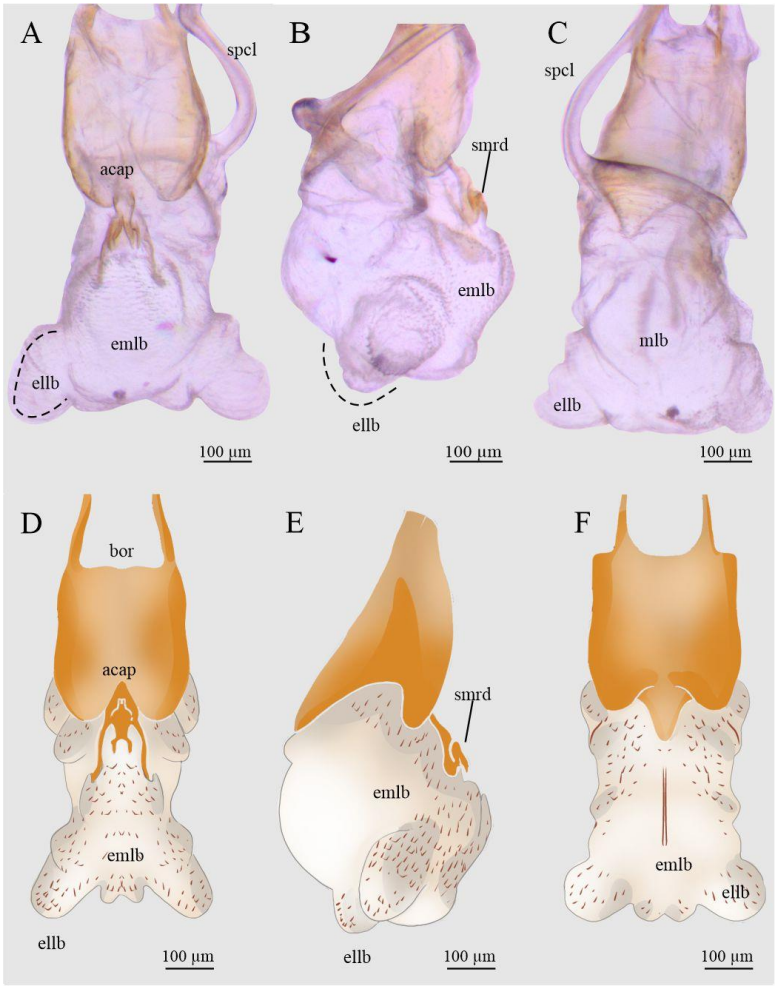
A
spcl
acap
emlb
ellb
100 µm
B
smrd
emlb
ellb
100 µm
C
spcl
mlb
ellb
100 µm
D
bor
acap
emlb
ellb
100 µm
E
smrd
emlb
ellb
100 µm
F
emlb
ellb
100 µm

Figure 9

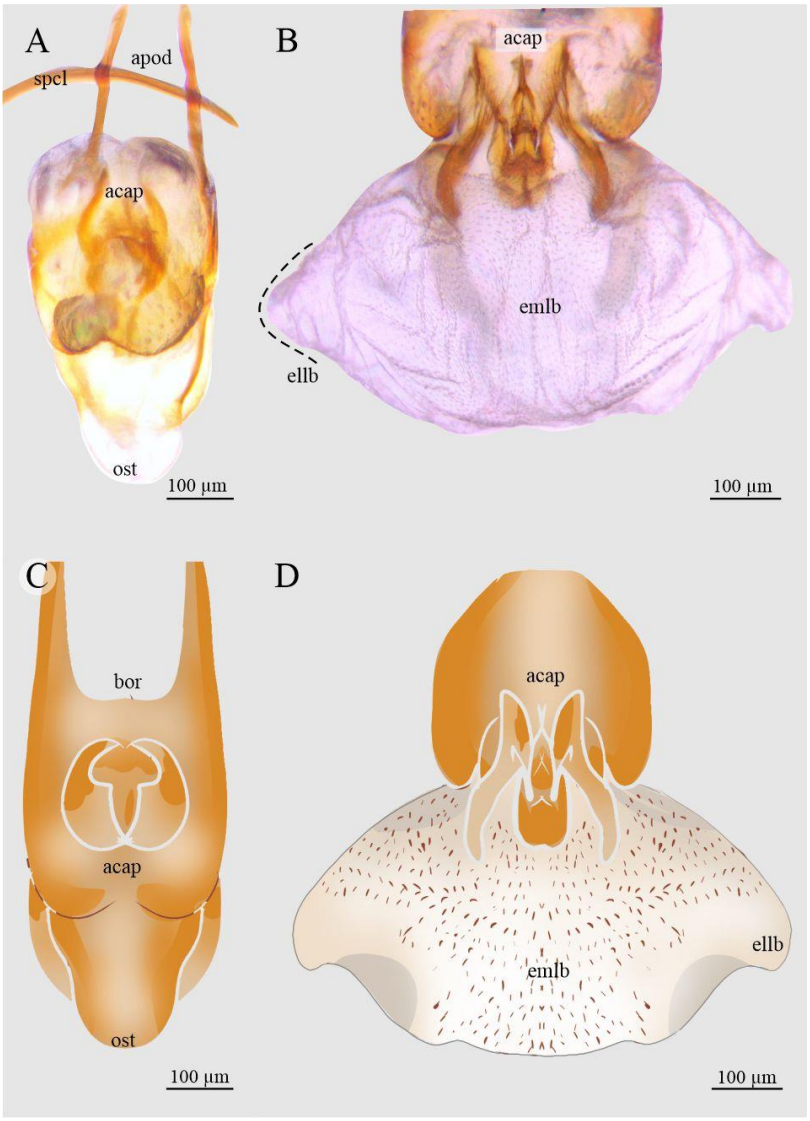
A
apod
spcl
acap
ost
100 µm
B
acap
emlb
ellb
100 µm
C
bor
acap
ost
100 µm
D
acap
ellb
emlb
100 µm

Figure 10

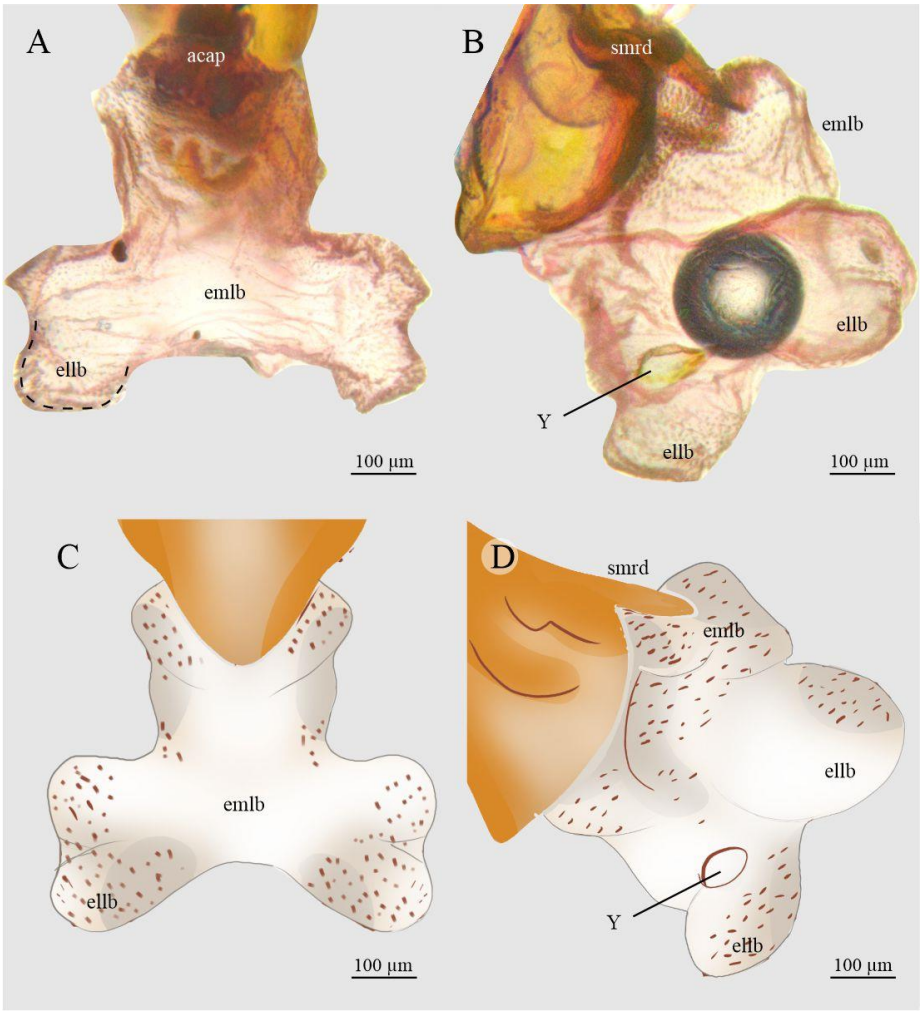
A
acap
emlb
ellb
100 µm
B
smrd
emlb
ellb
Y
ellb
100 µm
C
emlb
ellb
100 µm
D
smrd
emlb
ellb
Y
ellb
100 µm

Figure 11

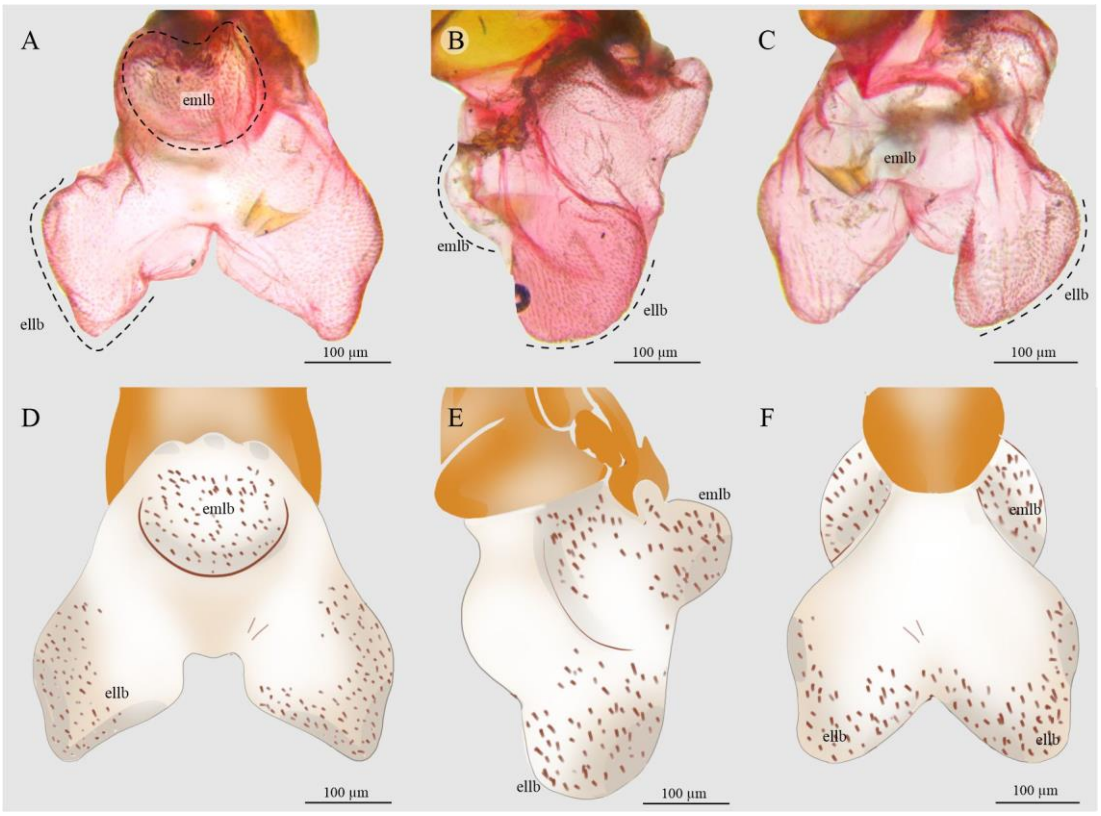
A
emlb
ellb
100 µm
B
emlb
ellb
100 µm
C
emlb
ellb
100 µm
D
emlb
ellb
100 µm
E
emlb
ellb
100 µm
F
emlb
ellb
ellb
100 µm

Figure 12

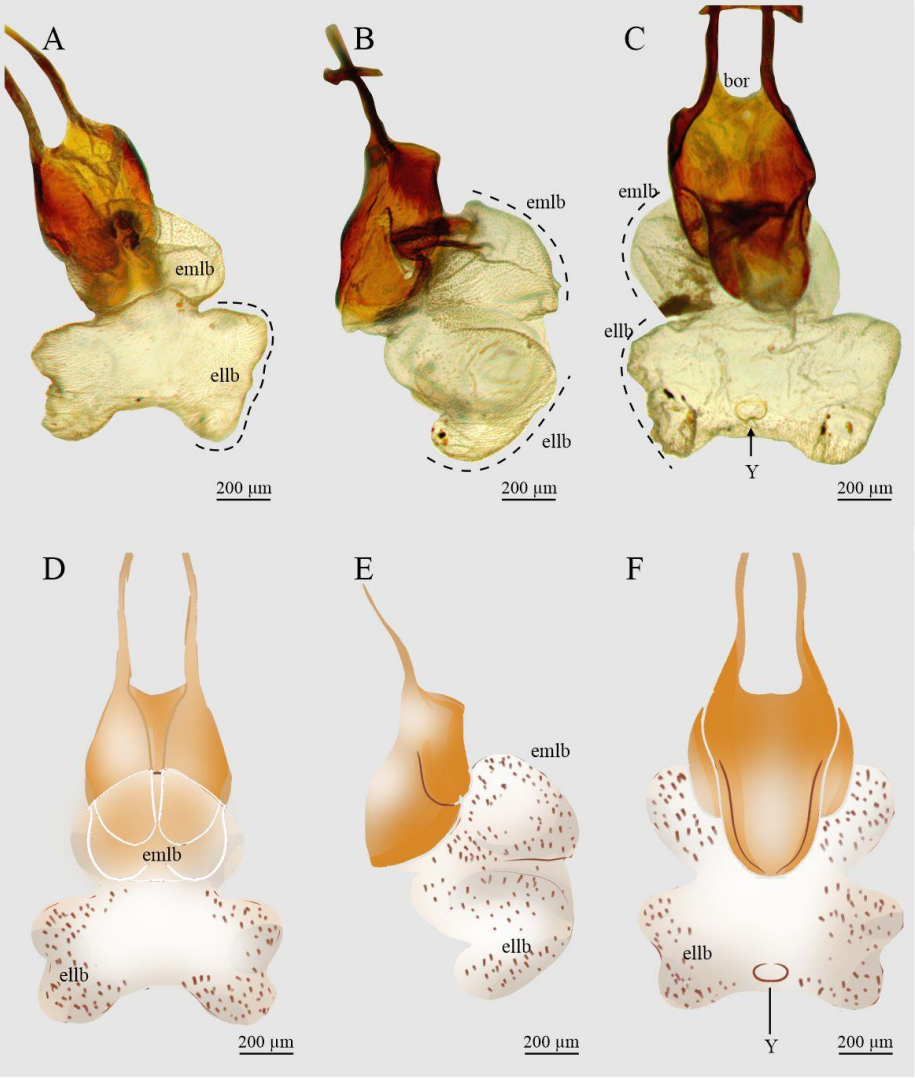
A
emlb
ellb
200 µm
B
emlb
ellb
200 µm
C
bor
emlb
ellb
Y
200 µm
D
emlb
ellb
200 µm
E
emlb
ellb
200 µm
F
ellb
Y
200 µm

Figure 13

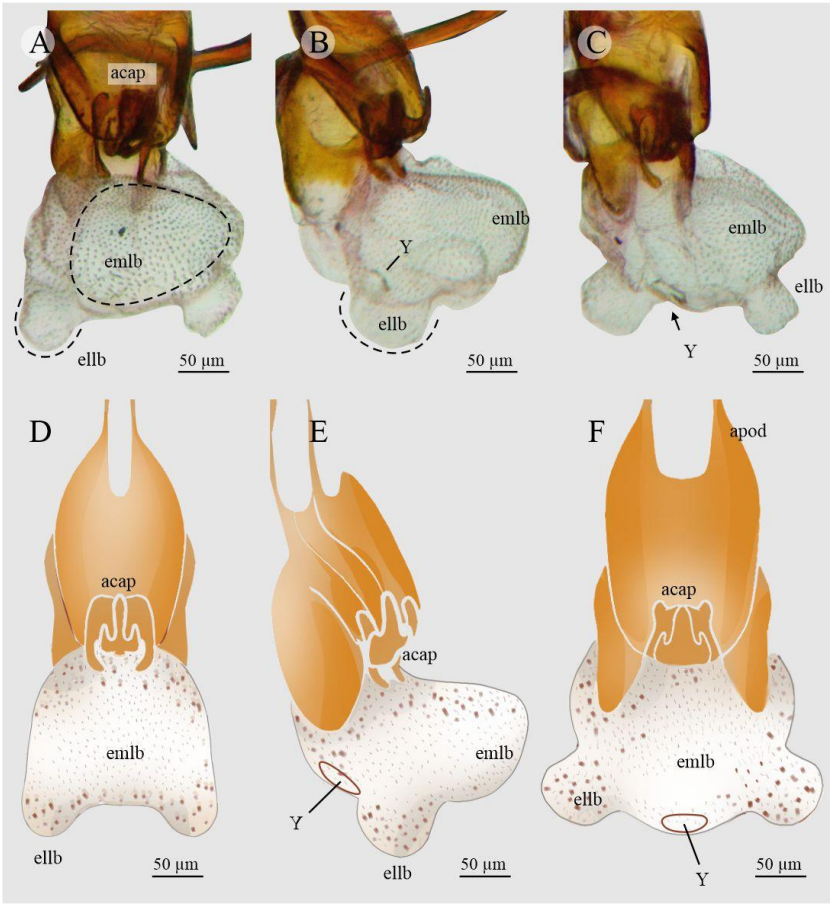

Figure 14

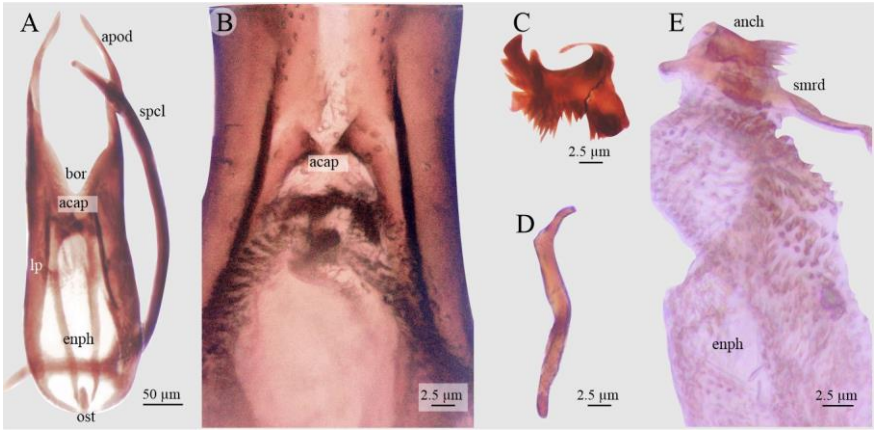

Figure 15

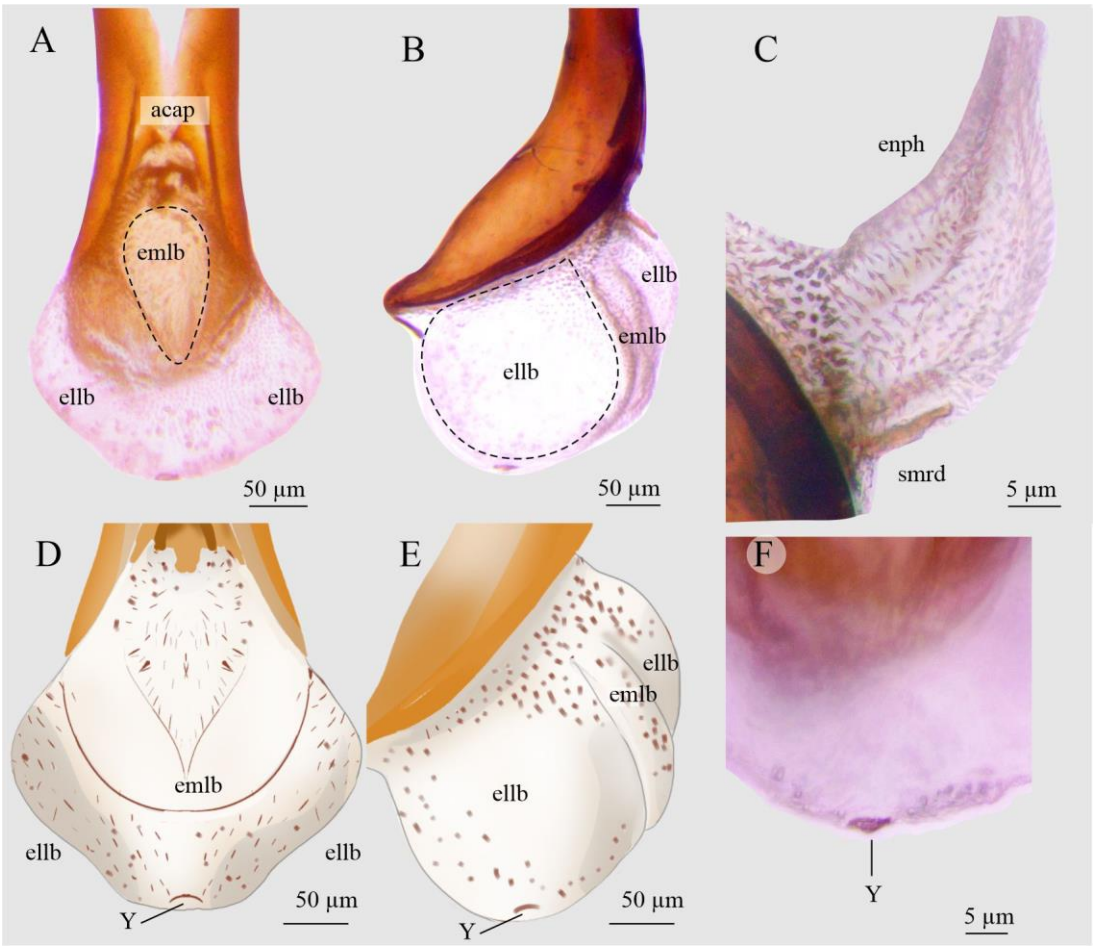
A
acap
emlb
ellb
ellb
50 µm
B
ellb
emlb
ellb
50 µm
C
enph
smrd
5 µm
D
emlb
ellb
ellb
Y
50 µm
E
ellb
emlb
ellb
Y
50 µm
F
Y
5 µm

Figure 16

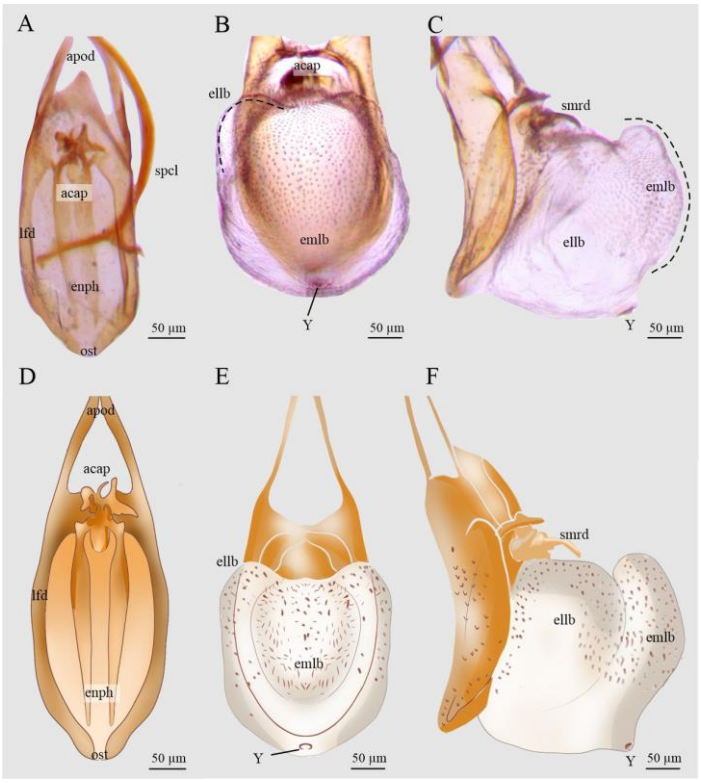

Figure 17

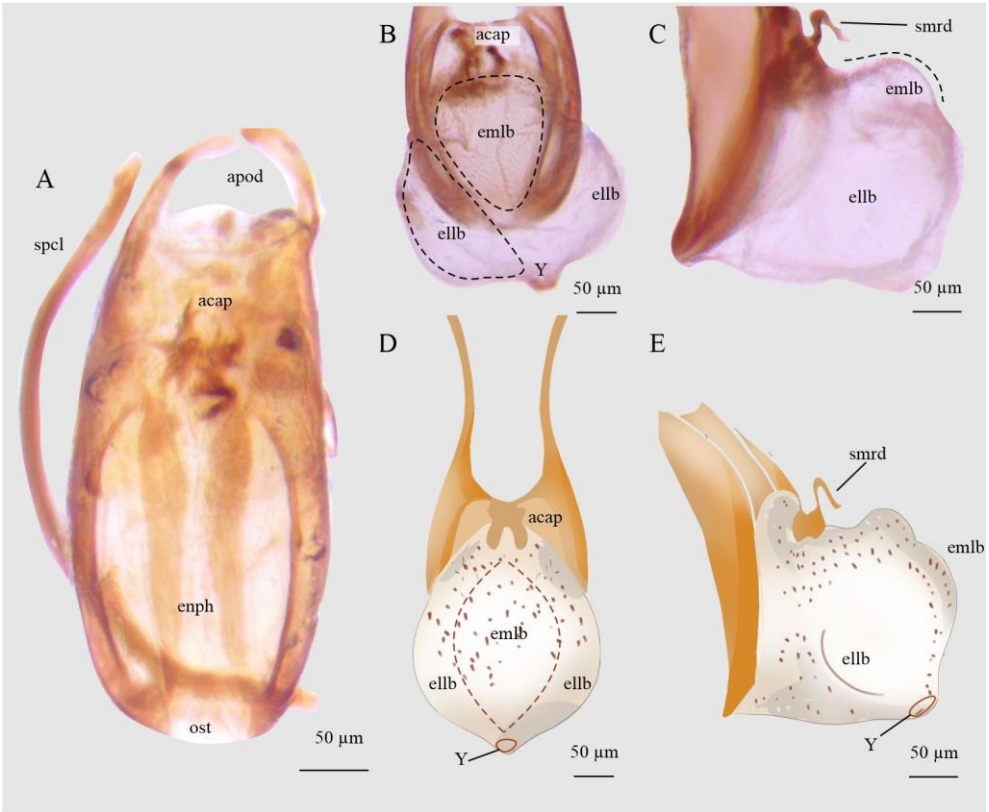

Figure 18

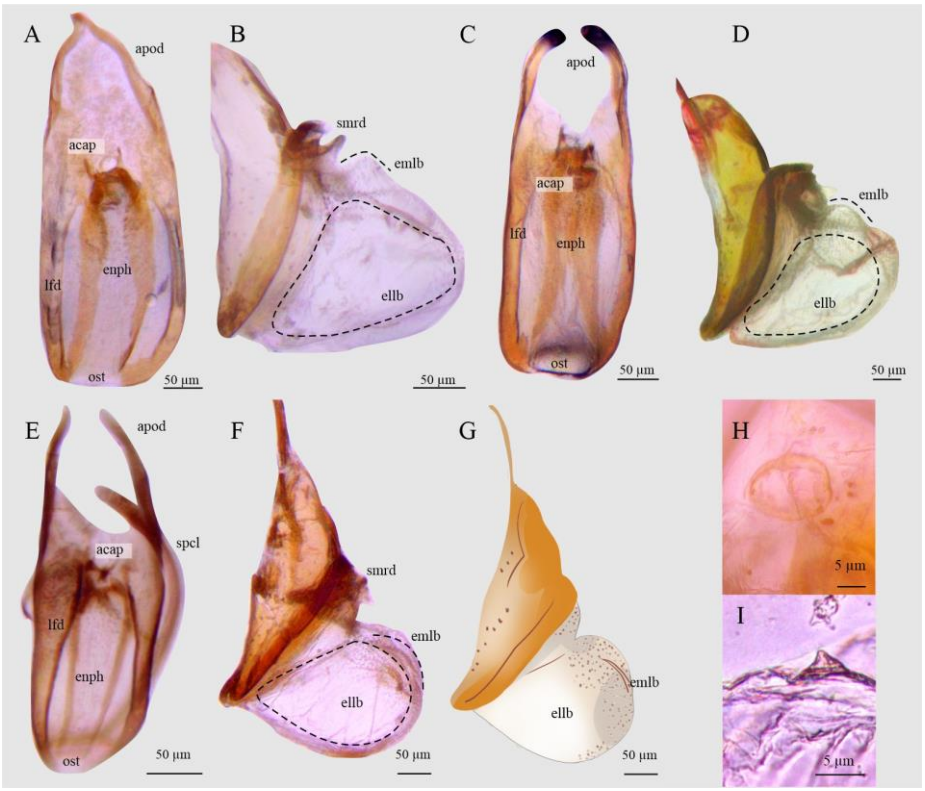

Figure 19

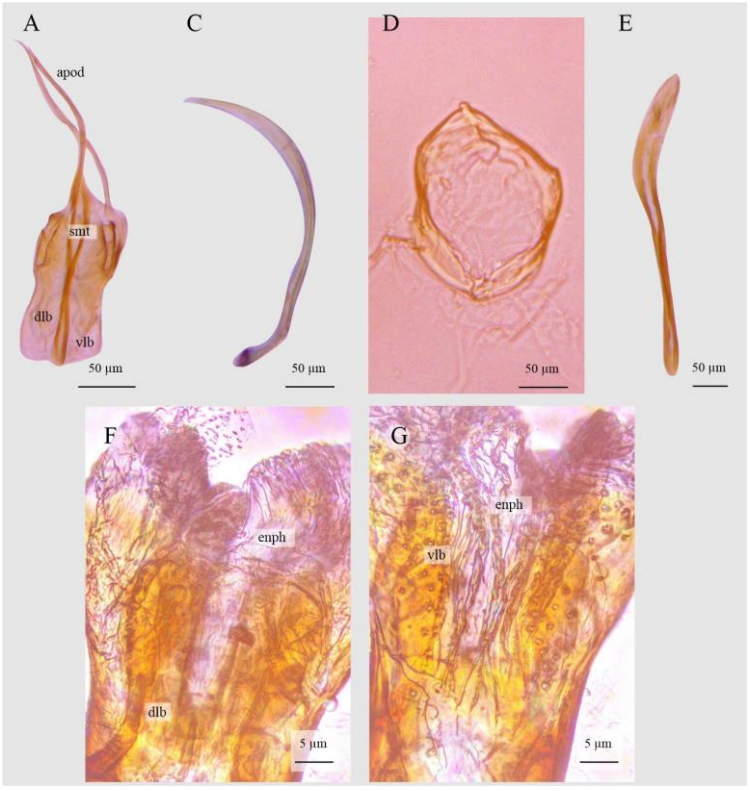

Figure 20

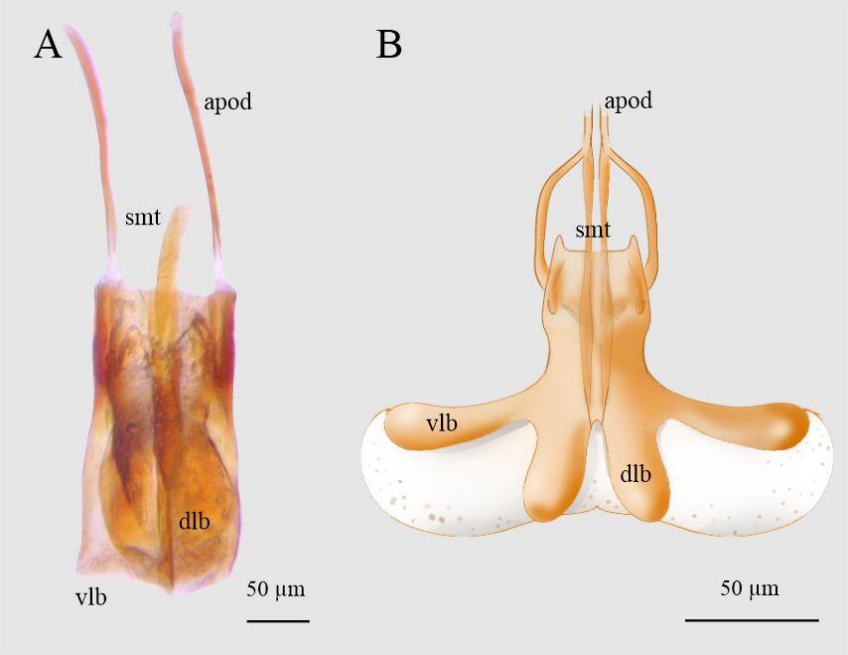
A
apod
smt
dlb
vlb
50 µm
B
apod
smt
vlb
dlb
50 µm

Figure 21

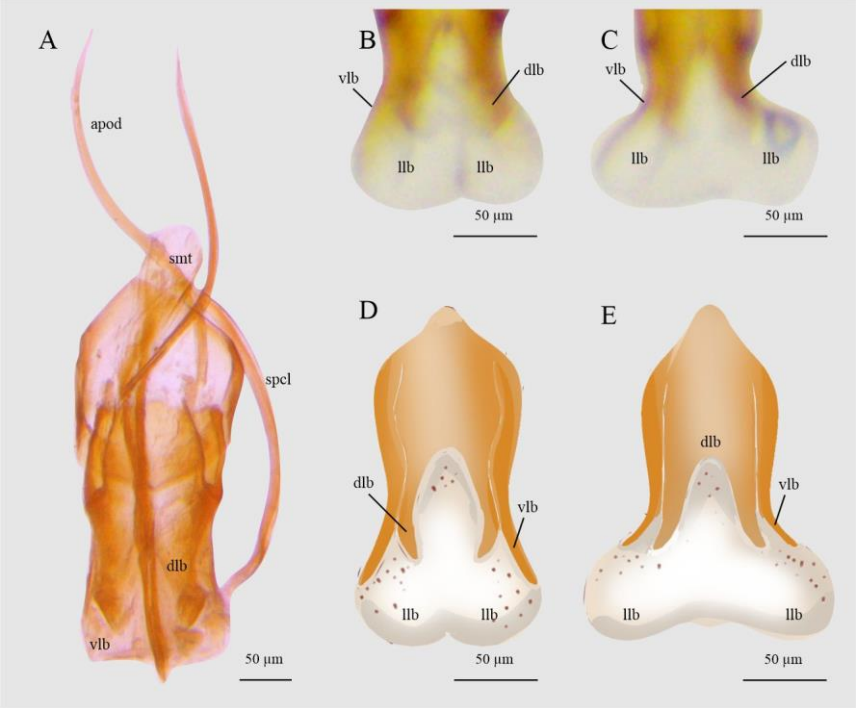
A
apod
smt
spcl
dlb
vlb
50 µm
B
vlb
dlb
llb
llb
50 µm
C
vlb
dlb
llb
llb
50 µm
D
dlb
vlb
llb
llb
50 µm
E
dlb
vlb
llb
llb
50 µm